River Bifurcations

Walter Bertoldi

UNIVERSITÀ DEGLI STUDI DI TRENTO

2004

Doctoral thesis in **Environmental Engineering** (XVI cycle)
Faculty of Engineering, **University of Trento**
Year: **2004**
Supervisor: **Prof. Marco Tubino**
Cotutor: **Guido Zolezzi**

Università degli Studi di Trento
Trento, Italy
2004

Where the world ceases to be the scene of our personal hopes and wishes,
where we face it as free beings admiring,
asking and observing,
there we enter the realm of Art and Science.

Albert Einstein

Acknowledgements

I’m grateful to my supervisor, prof. Marco Tubino, for the constant support during my PhD study and for the enthusiasm in the research that he has transmitted to me.

Thanks to Guido, for the scientific support and most of all for the friendship and for the sharing of joy and trouble of the research world.

I wish also to thank prof. Peter Ashmore for the period I spent at UWO and all the ’Sunwapta international group’ for the wonderful summer and the important experience I lived in Canada.

A special thank to all the ’Bonuti group’, Gianluca, Gianluca, Giuliano, Ilaria, Marco, Marco, Stefano, friends before colleagues, with whom I shared these years, and in particular to my flatmate GianDuca and GianLinux.

I’m grateful to all the students I worked with: Guido, Kilian, Anita, Edi, Igor, Tommaso, Stefano, Stefania, Rossella (thanks for the precise analysis of the Ridanna data and for the ’last minute’ plots!), Lisa, Luca, Alessio, Emanuele for their fundamental help in the laboratory and field activities and to the large group of people that helped me in the field work on the Ridanna Creek.

Thanks to my family for the constant support, to the friends of Ingegneria senza Frontiere and all the friends I lived with and that made unforgettable these years. A special thank to Mica for our wonderful friendship and for reading parts of this thesis!

Abstract

Bifurcation is one of the fundamental building blocks of a braided network; it is the process that determines the distribution of flow and sediments along the downstream branches. Braiding is a complex and highly dynamical system, whose evolution is at present predictable only on a short time scale; in this context bifurcations are the crucial process that control the adjustment of braiding intensity, being one of the main causes of the system continuous evolution. A complete description of river bifurcations is still lacking in the literature, though their importance for the onset of braiding is clearly recognized. Moreover, the physical quantitative description of river bifurcation appears as one of the main limitation of the most effective predictive models available at present, i.e. the branches or object-based models.

In the first part of the work the attention has been focused on the quantitative description of the evolution of a single laterally unconstrained channel until the occurrence of the first bifurcation. The analysis has been carried out performing four different sets of experimental runs with both uniform and graded sediments. An objective criterion for the occurrence of the bifurcation has been established, using the data provided by the Fourier analysis of the evolving bank profiles; the procedure enabled to characterise the morphodynamic sequence leading to flow and channel bifurcation and to point out the importance of the mutual interactions between the bed deformation and the planimetric configuration of the channel.

Along with the characterisation of the onset of bifurcations, it is crucial to investigate their further evolution, that has been pursued starting from the theoretical findings of Bolla Pittaluga et al. (2003), concerning their possible equilibrium configurations. Two sets of experiments has been carried out on a "Y-shaped" symmetrical configuration, in which the upstream channel diverge into two branches. The experimental results show the existence of an unbalanced configuration, when the Shields stress reaches relatively low values and the width to depth ratio is large enough. This asymmetrical configuration is characterised by different values of water and sediment discharges in the downstream branches and by a different bed elevation at their inlet, the channel carrying the lowest discharge showing a higher elevation. Experimental runs characterised by the presence of migrating alternate bars displayed an oscillating behaviour, generally leading to a more unbalanced configuration and, in some cases, to the abandonment of one of the branches. Experimental

findings can be interpreted in the light of the morphodynamic influence theory (Zolezzi & Seminara (2001)): the distance of the flow from the resonant value of the aspect ratio seems to be a good parameter to represent such phenomenon.

The dynamics of river bifurcation were also analysed in the field. Two field campaign were performed on the Ridanna Creek, Italy and on the Sunwapta River, Canada, joining an international research group. The detailed and repeated measurements allowed to point out the common features showed by the bifurcations, namely the unbalanced water distribution, the difference in bed elevation and the lateral shift of the main flow toward the external bank of the main downstream channel. The monitoring activity on the Ridanna Creek provided also the description of the planimetric and altimetric configurations of the study reach, employing both traditional survey techniques and digital photogrammetry together with the complete characterisation of morphological and hydraulic patterns. Moreover, the analysis of the long term evolution of the network pointed out the existence of three regions in the braided reach, with different morphological features and highlighted the crucial role of bifurcations in controlling braiding evolution.

Theoretical analysis, laboratory and field investigations have allowed a much deeper insight in the bifurcation process, giving a quantitative detailed description of the phenomenon. The investigation now provides a suitable description of the bifurcation process that can readily be implemented in predictive models for braiding evolution, for which the adoption of physically based nodal point conditions would be highly desirable and represent the main sought outcome of the present analysis.

Contents

List of Figures

List of Tables

1 Introduction

Rivers are an important resource that can be managed at best only considering a broad range of factors (morphological, biological, social, human, ...) in an integrated view. River training and management reflect the needs of a particular society at a certain stage of its evolution; in recent years local conditions, which allow for cost-effective solutions and sustainable strategies have become more and more important. Further river management activities are required to achieve traditional aims such as flood protection, maintenance of bank stability, prevention of efficiency of water intakes. In addition, one has also to consider the restoration of all the functions of the river system and the maintenance of instream and floodplain habitats. In this context, the concept of *leaving room* for the rivers is one of the key points of refurbishment projects, leading to nature and landscape restoration (de Vriend, 2002). Also the issue of vertical and lateral connectivity within the fluvial system has gained an increasing relevance, because of its influence on groundwater resources and on pollutant dispersion and its interaction with ecological aspects and biota.

This approach can also guarantee the extra benefit of a more successful prevention system of flood damages. In fact, the continuous rising of the main levees does not seem to be the best solution: high magnitude flood events in the last decade (Mississippi, 1993 and Rhine, 2002) showed that an absolute safety cannot be warranted, even in very regulated rivers. On the contrary, confinement between embankments implies a higher unit stream power leading to disastrous

Figure 1.1: Panoramic view of the Tagliamento River, Italy. (Flow is from left to right).

consequences when embankments fail, hence increasing flood damages (Gilvear, 1999). Novel approaches are currently under investigation, like the enhancement of water storage in more upstream part of the river basin, the removal of some bank protections, the re-opening or creation of secondary channels along the main branch (Klaassen et al., 2002).

In this process, fluvial geomorphology can decisively improve river engineering techniques in order to minimize flood damage and, at the same time, to reduce environmental degradation, restoring ecologically valuable and aesthetically pleasing water courses (Larson, 1996). In particular, a geomorphological approach can be relevant to highlight how river systems respond to water and sediment inputs from the upstream catchment and to point out the sensitivity of geomorphic systems to environmental disturbances and change (Gilvear, 1999).

1.1 Braiding phenomena

Braiding is one of the natural river patterns that appears over a wide range of scales, from small proglacial gravel-bed streams to large fluvial systems as the Brahmaputra River; it can be easily described as a network of channels, splitting and rejoining around islands and bars (Figure 1.1 and 1.2). Murray & Paola (1994) defined the braided pattern as *"the fundamental instability of laterally unconstrained free-surface flow over cohesionless beds"*. Braiding is a complex system of channels interconnected by nodes (namely, confluences and bifurcations), acting on a wide range of spatial scales, from the single chute and lobe unit till the whole braided belt.

At present, few examples of fully braided reaches can be find in Europe, where in the past the high land demand and the flood protection strategies led to river confinement and restricted the planimetric evolution of fluvial belts. In Italy some piedmont rivers, like the Piave River, experienced incision and narrowing processes in the last decades (Surian & Rinaldi, 2003); in this context the Tagliamento River, North-East Italy, is one of the latest large braided streams in Europe

Figure 1.2: A braided reach of the Sunwapta River, Canada. (Flow is from left to right).

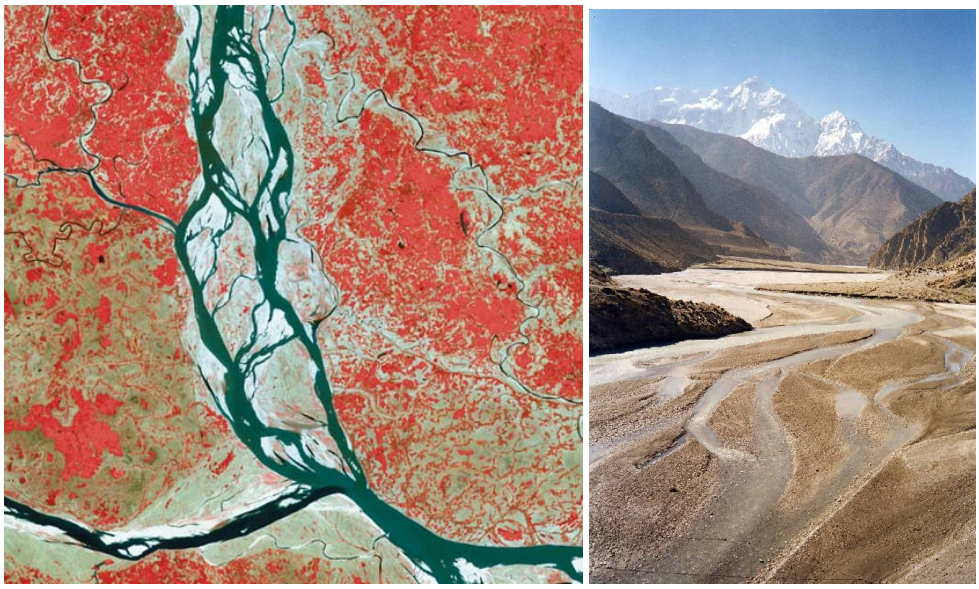

Figure 1.3: The Brahmaputra-Jamuna River, Bangladesh (on the left) and the Kali Gandaki River, Nepal.

and it is considered a fluvial corridor with a great ecological and environmental relevance (Figure 1.1). Braiding is more common in regions characterised by a lower human pressure, like Canada and New Zealand, and in the developing countries (in Figure 1.3 two examples are shown: the Brahmaputra-Jamuna River in Banghladesh, on the left, and the Kali Gandaki River in Nepal); in this case their management is quite problematic, due to the high bank erosion rate and the highly dynamic behaviour; hence the challenge is to develop sustainable techniques that meet local needs.

According to the new perspectives of river management presented above, braiding can be seen as one of the target patterns of recent river engineering projects, with the aim of promoting the restoration of the river functions. An attempt has been recently pursued with the re-opening of the secondary branches on the Rhine River. For these reasons the issue of predicting the planimetric and altimetric evolution of a channel network has gained a greater relevance in the last decades. Indeed, the present knowledge on river dynamics allows to predict the evolution of a single thread meandering channel, even on relatively long time scales, with sufficient accuracy and to interpret many unit processes acting in rivers. However, understanding and predicting braiding phenomena is still an ongoing task (Jagers, 2003).

Two different approaches have been recently pursued: the first, termed 'reductionism' according to Paola (2001), is founded on the classical mechanical approach and comprises both numerical models that solve the flow and sediment governing equations and the analysis of single unit processes, recursively repeating in the network. The second, termed 'synthesism', is essentially based

on the idea of 'emergent' phenomena: it considers that in a multi-scale system the behaviour at a given level may be controlled by only few crucial aspects of the next level below in the hierarchy of scales; this implies that such a model may become simpler, in spite of the system complexity. In this approach the attention is mainly focused on the general properties of the system, looking for spatial and temporal structures.

A first question to tackle when analysing a braided network is to determine *how much* braided it is. The most common quantification of braiding intensity, based on the number or length of the channels within the reach, can be represented by the *braiding index*, given in terms of the average number of anabranches across the river (Bridge, 1993) or by the total sinuosity, defined as the intrinsic length of channel per unit length of river. Recently, Ashmore (2001) pointed out that the *active* braiding intensity can actually be very low, with only 1 or 2 channels simultaneously active. In an experimental study Stojic et al. (1998) investigated the time evolution of a braided network through the analysis of a series of DEMs of bed topography, acquired using digital photogrammetry. The authors showed that, on a short time span, deposition and erosion occur only in few channels, thus implying that the evolution of the braided pattern can be interpreted as the history of channel shifting more than the result of the interaction of simultaneously active channels. As a result, the distinguishing features of braiding compared with single thread channels are the rapid channel shifting and the high rates and frequencies of changes in bed topography, with the tendency of radical readjustment of the channel pattern (Ashmore, 2001).

Sediment transport reflects this highly dynamical evolution: as widely reported (Hoey & Sutherland, 1991; Hoey, 1992), the dynamics of braided rivers is characterised by rapid spatial and temporal variations of the bed material transport rate, over a broad range of frequencies. As an example, the sediment transport rate measured at the downstream end of a laboratory model is reported in Figure 1.4 (Warburton & Davies, 1994). These fluctuations have been related to single dynamical processes, like the migration of bars (on the meso-scale) and to the reshaping of the network configuration through channel migration, creation and obliteration of channels and nodes (on the macro-scale). It has been observed (Ashmore, 1988) that a higher stream power could enhance more frequent breakdown of the morphology, thus increasing the fluctuations of the bedload.

Paola (2001), tackling this aspect from an alternative point of view, based on the results of the cellular model of Murray & Paola (1994), highlighted how the non linear response of sediment transport to variation in water flux is essential in developing a braided pattern. More specifically, the 'over-response' of sediment flux to acceleration in the confluences and deceleration in the diffluence areas promote continuous bed scouring and deposition of bars, so that *'bed and flow chase one another forever around the braid plain'*.

Topological properties of braided network have been widely analysed, starting from the work

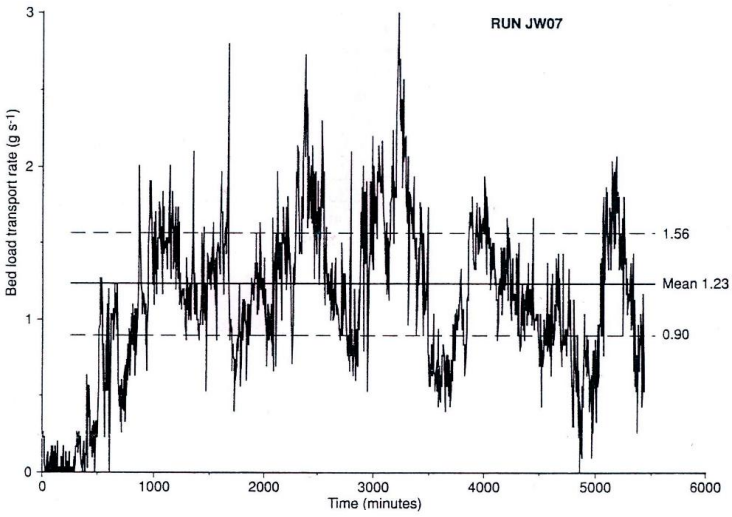

Figure 1.4: Bedload transport rate fluctuations in a braided laboratory model. Plot reported in Warburton & Davies (1994).

of Howard et al. (1970). A research line on braiding deals with the investigation of internal geometric similarity: it has been found that braided rivers show scale invariance, i.e. they display similar statistical properties independently of the spatial scale, if they are not subject to external controls. More precisely, Sapozhnikov & Foufoula-Georgiou (1996) demonstrated that braiding can be considered a self-affine object, since it has a preferential direction (that of the mean downstream flow). This maight imply that the underlying mechanisms responsible for the formation of braiding are the same at all scales.

Indeed, the characteristic scales of braided rivers and their relationship with morphological parameters as water discharge, mean valley slope and grain size are still not completely understood. Braided channel width can be considered as the sum of the width of the single anabranches or represented by the width of the braid belt. The width of a single gravel bed channel can be evaluated following rational regime theories (Parker, 1978), but the present state of knowledge does not allow to determine the functional controls on braided width (Warburton, 1996). Field and laboratory data show that total width can also be a function of the braiding intensity. Ashmore (2001) recently pointed out the existence of a characteristic length scale of braiding related to the total discharge of the river. Similarly to the relations for meander wavelength, the mean braid length is determined by the wavelength of individual pool-bar units which control the confluences and bifurcations spacing.

1.2 Prediction of braided rivers evolution

At present, the prediction of braided rivers planform evolution is possible with enough accuracy only on a short time scale. Braiding is a deterministic system characterised by a somehow chaotic behaviour, as it apparently shows unpredictable features (Paola & Foufoula-Georgiou, 2001). Time evolution of the channel network is affected by rapid changes, due to the rearrangement of the branches and nodes and, in particular, caused by the modification of the flow and sediment distribution at the bifurcations. The standard approach that solves the governing equations for the fluid and solid phases (Enggrob & Tjerry, 1999; McArdell & Faeh, 2001) encounters various difficulties arising from the complexity of the system. Such a model has to deal with a continuously changing domain and requires the full coupling between bed and bank evolution. Moreover, secondary flows, sorting effects and local turbulence disequilibrium have to be accounted for. Furthermore, braided rivers are characterised by several complicating features that must be taken into account by theoretical modelling. Principally:

- Strong non-linearities: the planimetric and altimetric evolution of the branches is affected by the interaction between the free bed-response of the system and the forced bed-response due to planform non-uniformities.

- Unsteadiness: flow field and sediment transport rate are typically unsteady and the system never reaches a steady equilibrium configuration.

- Finite length and amplitude effects: the relatively short length of single anabranches implies that the condition of infinite longitudinal domain, which is often introduced in theoretical models, can be hardly met in nature; as a consequence, upstream and downstream morphodynamic influence may crucially affect the evolution of single branches. Moreover, bar structures generally undergo a finite amplitude development, thus limiting the applicability of linear theories.

- Partially transporting cross sections and gravitational effects: braided rivers are generally characterised by low sediment mobility, near the threshold value for particle motion, which implies that sediment transport may occur only on a limited part of the cross section. Moreover, gravitationally effects on sediment transport are likely to be relevant due to the fairly large bed gradients associated with local depositions and scours.

To overcome the above complications other alternative models for braiding have been recently developed. Murray & Paola (1994) have shown that a simple cellular model, which includes only few relevant elements (namely the topographic effect of expansions and contractions and a non linear sediment transport law) is able to reproduce many features of braided networks (in Figure 1.5

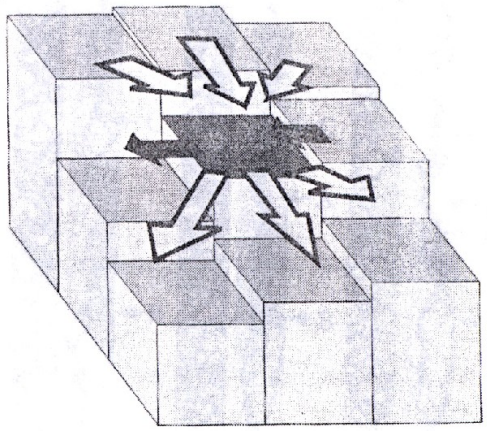

Figure 1.5: Cellular routing scheme of the Murray & Paola (1994) model.

the cellular routing scheme is reported). Though the above model was not designed to predict the actual planform changes, it is able to recognise some fundamental aspects of braided systems. Following a similar approach, Thomas & Nicholas (2002) have recently proposed an improved version of the cellular routing scheme, which has been tested with field data and compared with a more detailed 2D hydraulic model.

Jagers (2003) has tackled the problem of modelling planform changes in braided rivers. He has implemented two different models, a neural network and a branches model, testing their accuracy with observed data from the Brahmaputra-Jamuna River (Figure 1.6).

The branches model is based on a schematisation of the braided river as a network of channels, joining at the nodes (confluences and bifurcations). Each individual 'object' evolves according to four processes, namely width variation, mid-channel bar formation (and therefore creation of a new channel), lateral migration or channel abandonment. The spatial distribution of erosion and deposition probabilities is then computed from the results of a Monte Carlo simulation. Such a model seems to be very promising in predicting medium and long term evolution of a braided system. The main limitation is due to the difficulty in setting the correct values of parameters underlying the single evolution processes. For example, the creation of new channels is only accounted for through the mid-bar formation mechanism, provided a threshold value of the width to depth ratio of the channel is exceeded.

According to Paola (2001) a mixed model that combines both the reductionist and the syntesist point of view could be envisaged; such a model, essentially a 'two layers' model, could include both the ability of the cellular model to reproduce the effect of topography on the local flow path and the capability of channel based algorithms to account for non-local effects.

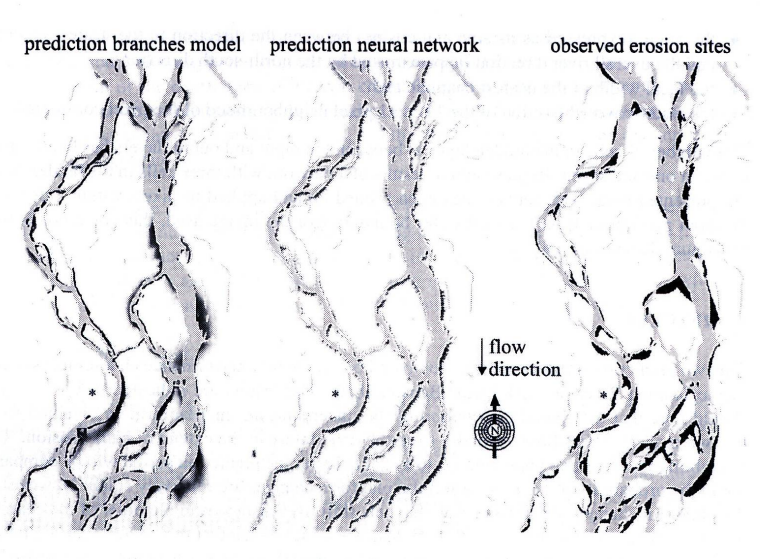

Figure 1.6: Comparison between the predictions obtained through the branches model, the neural network and the observed erosion sites on the Jamuna River. (From Jagers, 2001).

1.3 The unit process of bifurcation

Braiding is generated and maintained through the mechanism of flow bifurcation (see Figure 1.7 and the cover picture, taken from the Tagliamento River, Italy). Bifurcation is the process that determines the distribution of flow and sediments along the downstream branches and adds complexity to the system, thus reducing its predictability. Modelling a bifurcation is still a challenge for existing mathematical models, even in a simple configuration (Klaassen et al., 2002): hence, understanding river bifurcation is one of the open issues of fluvial research.

In order to model channel adjustment and to locate the preferential bank erosion areas and the probability of scour or deposition, the preliminary understanding of the mechanisms underlying the onset of the flow diffluence is required. Furthermore, the knowledge of the morphology and hydraulic conditions typical of a bifurcation allows one to know the water end sediment partition within the network. The availability of quantitative detailed description of the bifurcation process could ensure a decisive improvement in the ability of theoretical models to predict the planimetric and altimetric evolution of a braided river; moreover, such knowledge could be significant also in the context of other morphological pattern, as anastomosing and pseudo-meandering rivers.

A quantitative description of river bifurcation process is still lacking in the literature. The process has been firstly identified by Leopold & Wolman (1957) as the generating process of braiding; Ashmore (1991) describes in detail three possible mechanisms through which bifurcation may occur, as suggested by laboratory observations:

Figure 1.7: A bifurcation on the Sunwapta River, Canada. Flow is toward the camera.

- *Central bar mechanism and dissection of transverse unit bar.* This mechanism (also documented by Leopold & Wolman, 1957) imply the development of a central bar, displaying an avalanche faced downstream margin marked by the accumulation of the coarsest fractions. The bar forces the flow to diverge and is eventually exposed. A similar mechanism, with the dissection of a transverse unit bar may occur, when the channel is characterised by a higher sediment mobility.

- *Chute cutoff mechanism.* It is the most common bifurcation mechanism observed in the experiments; it is characterised by the modification of a an alternate bar structures in low-sinuosity channels. The bar is progressively transformed into a more complex bed form by lateral accretion, which determine more flow to be directed over the point bar. The steeper gradient near the head of the slough channel captures progressively larger volumes of water, leading to the bifurcation of the flow.

- *Multiple bars mechanism.* This mechanism applies only to channel with very high values of the width/depth ratio; it has been documented by Fujita & Muramoto (1988) and can be roughly explained in terms of the results of the linear stability analysis (Fredsøe, 1978). The multiple rows bars, which characterise the initial bed configuration, are gradually converted into fewer larger bars which concentrate the flow and lead to braiding.

The bifurcation process has been recently investigated also by Federici & Paola (2003) through experiments performed in divergent channels. They have found that stream lines diffluence invariably promotes the formation of a central deposition area, leading to the bifurcation of the current. According to their results two different configurations may exist, which mainly depends on the value of the Shields stress in the upstream channel. For relatively high values of the Shields stress

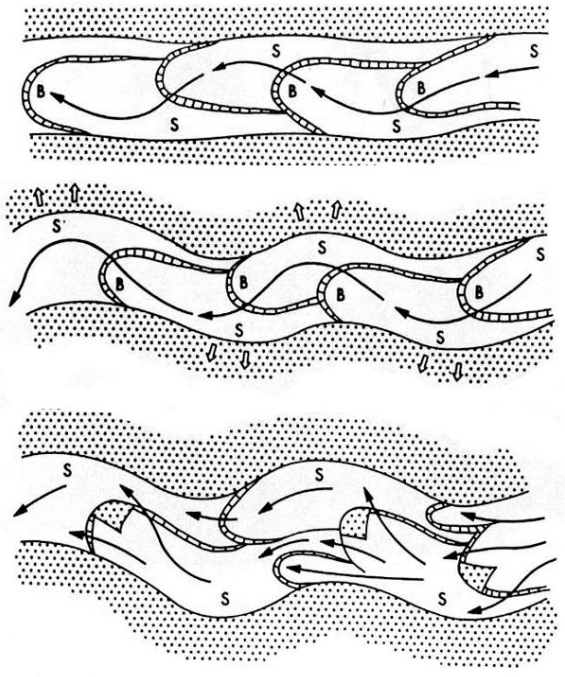

Figure 1.8: Alternating point bar chute cutoff mechanism, as reported by Ashmore (1982).

the bifurcation is stable, with both branches active; on the contrary, low sediment mobility leads to the closure of one of the branches. The authors notice that this 'switch' configuration is also triggered by the non uniformity of initial and boundary conditions: in fact, a flow perturbation can influence the stability of the bifurcation.

A predictive model for the equilibrium configuration of a simple 'Y-shaped' configuration in which an upstream channel divides into two branches has been proposed by Wang et al. (1995). The problem has been recently revisited by Bolla Pittaluga et al. (2003) through the introduction of a quasi-2D nodal condition that allows for transverse exchanges of water and sediment within the final reach of the upstream channel that feeds the bifurcation. The results of the model suggest the possibility of unbalanced equilibrium configurations, even in the case of perfectly symmetric geometry. The unbalanced solutions appear for low values of the sediment mobility and high values of the width to depth ratio; they are characterised by an unbalanced discharge ratio in the downstream branches and by a difference of bed elevation at the inlet of downstream branches. In spite of the simplified one-dimensional schematisation adopted by Bolla Pittaluga et al. (2003), their model seems to catch the fundamental features of the process and to replicate observed phenomena both in the laboratory and in the field.

Finally, it is worth noticing that understanding complex system like a braided network needs an integrated analysis, which allows one to deal with different spatial and temporal scales. Hence, it is highly recommended to join the information obtained through by theoretical analysis with data from laboratory and field investigations.

1.4 Outline of the thesis

In the present work the attention has been focused on the bifurcation process with the aim of describing quantitatively the flow conditions that lead to flow bifurcation and then determining its equilibrium configurations. The analysis is mainly based on experimentally and field observations: two different experimental works in the Hydraulic Laboratory of the University of Trento have been performed; further, two braided reach have been intensively monitored, paying particular attention to the analysis of bifurcations. Measured data have been integrated and interpreted with reference to theoretical results.

In summary, through the present work we have tried to address to the following questions:

- Which are the flow conditions that lead a laterally unconstrained channel to bifurcate?
- How can the chute cutoff mechanism be interpreted in the viewpoint of interaction and modification of bar structures?
- Is it possible to define a characteristic length scale of braiding based on bar analysis?
- Which are the main features characterising the equilibrium configuration of a bifurcation?
- Up to what extent such equilibrium configuration is affected by bar migration and/or upstream and downstream morphodynamic influence?
- What is the role played by bifurcations in controlling the planimetric evolution of a braided network?
- How is it possible to improve predictive models with a physical description of bifurcation process?

The thesis is organised as follows.

In Chapter 2 a brief review of the theoretical framework is reported, focusing the attention on single unit processes as bar formation and on the response of bed topography to planform non uniformities; a predictive model for channel bifurcation is also presented in Section 2.4. Chapter 3 is devoted to the experimental analysis of the bed and bank evolution of a single channel, until the onset of the bifurcation. Altimetric and planimetric configuration is analysed in detail to describe flow conditions at the moment of incipient bifurcation. In Chapter 4 the experimental investigation of a 'Y-shaped' configuration is reported; the results of two sets of runs allow to characterise the equilibrium configuration of a bifurcation and to highlight the role of the width to depth ratio on the degree of asymmetry of the discharge distribution. The field campaigns on the Ridanna Creek and on the Sunwapta River, the measurement techniques and the obtained data on bifurcations and planimetric evolution are described in Chapters 5 and 6. Finally, Chapter 7 is devoted to the comparison of the results and to some concluding remarks.

2 Theoretical framework

2.1 General formulation

Bed deformation in single thread channels may be due to spontaneously developing bedforms or to the forced pattern induced by planform non-uniformities. The subject has been widely investigated in the last decades (state of the art reviews can be found in Seminara, 1995; Tubino et al., 1999; Bolla Pittaluga et al., 2001). In particular, the 'mechanical' approach has been quite suitable for the understanding of the basic mechanisms characterising river morphodynamics, namely the formation of bars in straight channels, the bed deformation in meandering channels or in channels with variable width.

A suitable form of the governing equations for the liquid and solid phases can be obtained, introducing reasonable simplifying hypotheses which can be set once the relevant temporal and spatial scales have been identified. In the present work we focus our attention on processes scaling on the channel width (macro-scale bed forms); this enables us to use a two-dimensional form of the shallow water equations (the channel is generally assumed to be wide enough to neglect side boundary effects.)

Moreover, we assume that the temporal scale of bed evolution is much greater than the time scale of the flow; hence we ignore the time-derivatives in the momentum equation. A further quite restrictive hypothesis allows us to decouple the planimetric development and the altimetric evolution, provided the latter occurs on a much faster time scale. This approximation can be reasonable in the context of single thread meandering channels with cohesive banks, while it is not always justified in gravel bed rivers, where bed and banks may evolve at nearly the same time scale, particularly when a braided pattern establishes.

In a standard depth-averaged model the effect of secondary flows is neglected, because of the vanishing of the net contribution when averaged over the depth. Indeed, secondary flows are quite relevant to determine many of the features displayed by bed configurations. The decomposition originally proposed by Kalkwijk & De Vriend (1980) can be introduced to account for their effect within a depth-averaged model. Hence, the following structures for the longitudinal velocity u and the transverse component of the velocity v are assumed:

$$v = \nu_o v_o(\zeta, n, s) + V(n,s)\mathcal{F}_o(\zeta) \ , \tag{2.1}$$

$$u = \mathcal{F}_o(\zeta)U(n,s) \ , \tag{2.2}$$

where s is the longitudinal coordinate, defined along the channel axis, n is the transverse coordinate, $\nu_o = b/R_o$ is the curvature ratio, and reference is made to a channel whose width b remains nearly constant, while the curvature of channel axis may change arbitrarily, R_o denoting a typical (average or maximum) value of the radius of curvature.

Furthermore, ζ is a boundary fitted vertical coordinate

$$\zeta = \frac{z - \eta(s,n)}{D(n,s)} \ , \tag{2.3}$$

where η and D denote the local values of bed elevation and flow depth, respectively, and U and V are the depth-averaged components of velocity in longitudinal and transverse direction, respectively.

The decomposition 2.1 and 2.2 essentially implies that the effect of centrifugally induced secondary flow v_o, whose depth average vanishes, can be locally added to the depth averaged component, whose vertical structure $\mathcal{F}_o(\zeta)$ is assumed to coincide with the standard distribution of uniform flow evaluated in terms of the local flow characteristics.

Notice that a broader formulation which also accounts for the effect of the variable width has been recently proposed by Andreatta et al. (2004).

A suitable scaling can be introduced in the analysis, using the half channel width for the longitudinal and transverse coordinate and introducing reference values of velocity U_o and depth D_o as the values corresponding to a uniform flow, for given values of flow discharge, channel width, average bed slope and sediment size.

Once the above scaling is adopted, the following relevant dimensionless parameters arise:

- the width to depth ratio (or aspect ratio) of the channel

$$\beta = \frac{b}{2D_o} \ ; \tag{2.4}$$

- the Shields stress

$$\vartheta = \frac{\tau_o}{[(\rho_s - \rho)gD_s]} \ , \tag{2.5}$$

where τ_o is the average bottom shear stress, ρ_s and ρ are sediment and water density, respectively, g is gravity and D_s is a typical grain size;

- the relative roughness

$$d_s = \frac{D_s}{D} \, . \tag{2.6}$$

Referring to an orthogonal reference system (s,n,z) with s longitudinal coordinate, n transverse coordinate defined along a horizontal axis orthogonal to s and z coordinate of the axis orthogonal to s and n and pointing upwards, the governing equations of the two-dimensional model assume the following form:

$$\begin{aligned}
UU_{,s} + VU_{,n} + H_{,s} + \beta\frac{\tau_s}{D} &= \nu_o f_{11} + O(\nu_o^2) \, , && (2.7)\\
UV_{,s} + VV_{,n} + H_{,n} + \beta\frac{\tau_n}{D} &= \nu_o g_{11} + O(\nu_o^2) \, , && (2.8)\\
(DU)_{,s} + (DV)_{,n} &= \nu_o m_{11} \, , && (2.9)\\
(F_o^2 H - D)_{,t} + Q_o[q_{s,s} + q_{n,n}] &= \nu_o n_{11} \, , && (2.10)
\end{aligned}$$

where H is free surface elevation, Q_o is a dimensionless parameter defined as:

$$Q_o = \frac{\sqrt{(s-1)gD_s^3}}{(1-p)U_o D_o} \, , \tag{2.11}$$

where s is the relative density and p sediment porosity and F_o is the Froude number. Moreover τ_s and τ_n are the longitudinal and transverse components of the bottom stress vector, while q_s and q_n are the longitudinal and transverse components of the bedload transport; in the case of a slowly varying bed topography they can be evaluated through the semi empirical relationship (Shimizu et al., 1992):

$$\mathbf{q} = \frac{q_o(\vartheta)}{\tau}\{\tau_s[\cos(\alpha), \sin(\alpha)] + \tau_n[-\sin(\alpha), \cos(\alpha)]\}, \tag{2.12}$$

$$\tan(\alpha) = -\frac{r}{\beta\sqrt{\vartheta}}\frac{\partial \eta}{\partial y} \, , \tag{2.13}$$

where the angle α describes how gravity, acting on particles moving on a sloping surface, affects the direction and intensity of bedload motion, driving some deviation of the average particle trajectory from the direction of mean bottom stress. Furthermore, y is orthogonal to the local direction of bed stress and r is an empirical constant ranging between 0.3 and 0.6 (e.g. Talmon et al., 1995).

Finally, the quantities $f_{11,}$ g_{11}, m_{11} and n_{11} which appear in the right hand sides of equations

(2.7-2.10) account for the effect of centrifugally induced secondary flow and of dispersive terms related to its interaction with the topographically induced variations of the depth averaged flow.

2.2 Alternate bar formation

River bars are fundamental features which control the evolution of alluvial channels (Figure 2.1). Their formation has been conclusively explained in terms of an inherent instability of an erodible bed. The solution of system (2.7-2.10) in the case of a straight channel ($\nu_o = 0$) allows one to determine the occurrence conditions and the equilibrium configuration of migrating alternate bars. The problem has been tackled through linear and weakly non linear analytical approaches (Colombini et al., 1987; Tubino et al., 1999), fully non linear models (Colombini & Tubino, 1991; Schielen et al., 1993) and various experimental analyses (Jaeggi, 1984; Fujita & Muramoto, 1985; Garcia & Niño, 1993; Lanzoni & Tubino, 2000).

The results of the above investigations are presented and briefly summarized in the following. The theoretical plots presented herein are obtained using the Parker (1990) formula to compute the bed load function q_o appearing in 2.12, which allows one to obtain more accurate predictions at low values of Shields stress, typical of braided networks.

Field and experimental observations suggest that the longitudinal wave length of alternate bars fall in the range of 5-12 channel widths (Figure 2.2a). Furthermore, their equilibrium height, which is defined as the difference between the maximum and minimum bed elevation within a bar unit, increases as the width ratio of the channel increase, as shown in Figure 2.2b.

Figure 2.1: Alternate bar in a straight river, Tokachi River, Japan.

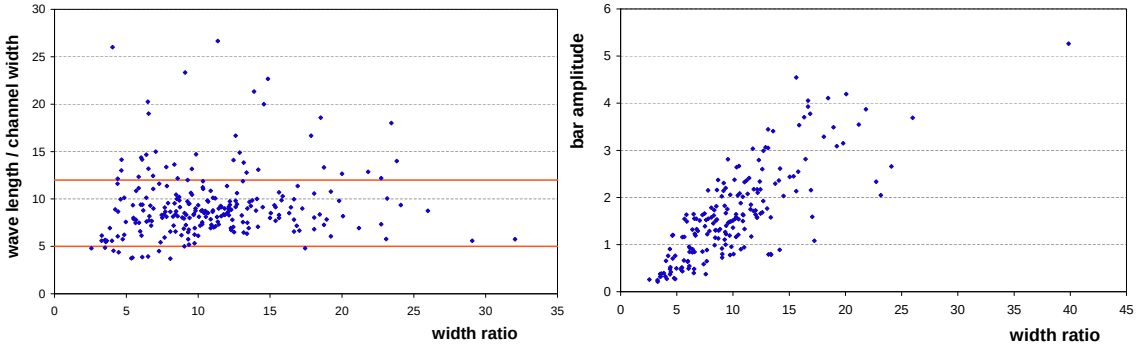

Figure 2.2: Observed values of the bar wave length (on the left) and of the bar height (on the right) as a function of the width ratio.

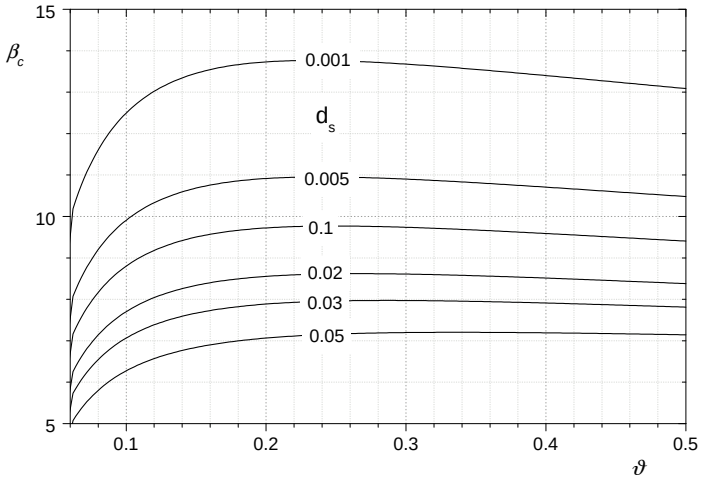

Figure 2.3: The critical value of width ratio β_c predicted by the linear model of Colombini et al. (1987) as a function of the Shields stress ϑ and the relative roughness d_s.

Indeed, linear studies suggest that the bifurcation parameter for bar instability is the width ratio: in Figure 2.3 the threshold value of the width ratio above which the occurrence of alternate bars is reported, as predicted by the linear model of Colombini et al. (1987).

Linear theories also show that the instability process is not strongly size-selective: the shape of marginal stability curves (Figure 2.4) suggests that different waves within the unstable range modes are characterised by almost similar growth rate.

On the contrary, the transverse mode selected by the instability process depends strongly on β; as a consequence, free bar instability generally displays an alternate pattern (mode 1), while central bars (mode 2) or multiple row bars (mode 3, 4, ...) can only form when the channel is fairly wide. As firstly pointed out by Fredsøe (1978), the critical condition for a given transverse mode m is given by $m\beta_c$, β_c being the threshold value for alternate bars (Figure 2.5).

Observed bar heights are of the order of mean channel depth. Provided the width ratio of the

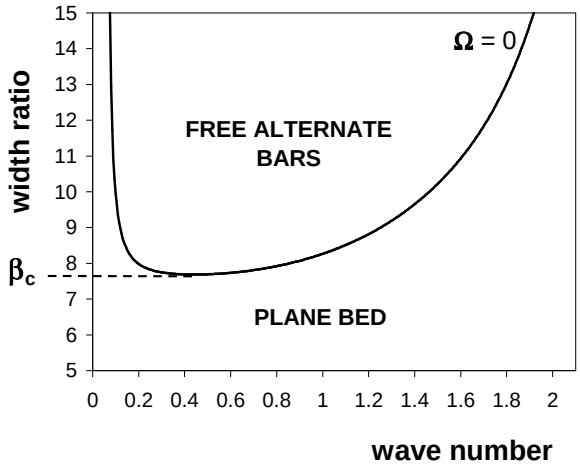

Figure 2.4: Marginal stability curve predicted by the linear theory (Shields stress = 0.07, relative roughness = 0.01).

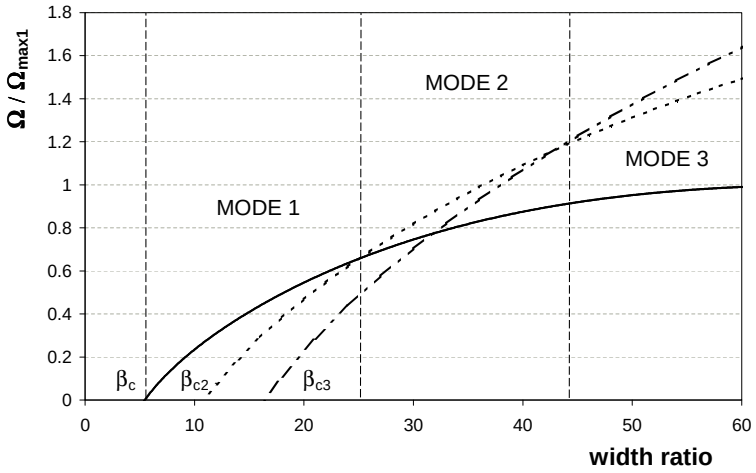

Figure 2.5: The growth rate Ω_{max} is plotted versus the width ratio for different transverse modes. (Shields stress = 0.07, relative roughness = 0.05).

channel falls in a neighborhood of β_c, the weakly non linear theory of Colombini et al. (1987) suggests that nonlinear interactions lead to periodic bar patterns migrating downstream, whose amplitude may asymptotically reach an equilibrium value. It is found that the equilibrium bar amplitude (H_{BM}), scaled by the average flow depth, is proportional to the square root of the excess of the width ratio relative to the threshold value β_c and can be expressed in the form:

$$H_{BM} = b_1 \varepsilon^{\frac{1}{2}} + b_2 \varepsilon \,, \qquad \varepsilon = \frac{\beta - \beta_c}{\beta_c} \,, \tag{2.14}$$

where b_1 and b_2 are functions of the Shields stress ϑ and the relative roughness d_s and are plotted in Figure 2.6.

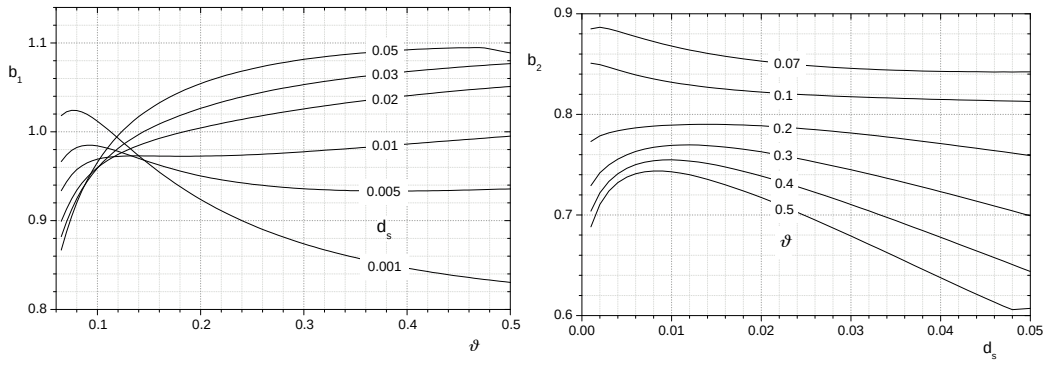

Figure 2.6: The functions b_1 and b_2 are plotted in terms of ϑ and d_s.

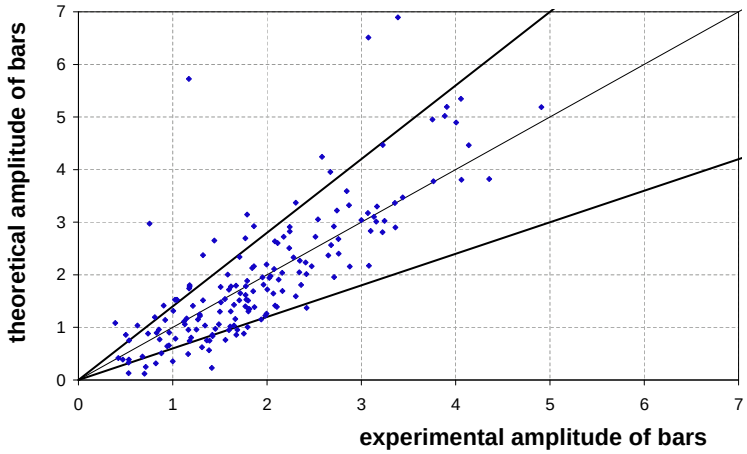

Figure 2.7: The maximum height of alternate bars as predicted by the weakly non linear theory of Colombini et al. (1987) is compared with experimental data of various authors.

Comparison of predicted bar height with flume data seems quite satisfactory, as reported in Figure 2.7.

2.3 Planimetric forcing

As pointed out in Section 2.1 the bed response of a natural channel is also determined by forcing effects induced by planform non uniformities, like the curvature of channel axis and width variations. The structure of the resulting bed pattern closely reflects that of the forcing effect. In particular bed topography displays a typical alternate pattern when the forcing is anti symmetrical, like in the case of periodic variation of channel curvature in meandering channels (Figure 2.8).

On the contrary, a 'symmetrical' forcing like that produced by a periodically varying width is likely to induce a sequence of central deposits whose longitudinal and transverse structure resemble that of central bars.

The forced bed pattern can in turn affects the process of bank erosion, thus enhancing the further development of channel non uniformities. Both the effects of variable curvature and of symmetrical width variations have been investigated in the last decades through experimental observations and theoretical models.

Kinoshita & Miwa (1974) and Tubino & Seminara (1990) investigated the interaction between free migrating bars and steady point bars induced by the variable curvature of channel axis, showing that a threshold value for channel curvature exists, above which free bars cease their migration and bed topography is characterised by steady patterns (see Figure 2.9).

Repetto & Tubino (1999) and Repetto et al. (2002) analysed both experimentally and theoretically the forcing effect of symmetrical, periodic width variations. Also in this case a threshold value of the amplitude of bank oscillation can be defined, above which alternate migrating bars are suppressed and the bed topography displays a steady central bar pattern. In Figure 2.10 the amplitude of width variations is expressed in a dimensionless form, where δ is the amplitude of

Figure 2.8: A meandering river, Alatna River, Alaska, USA.

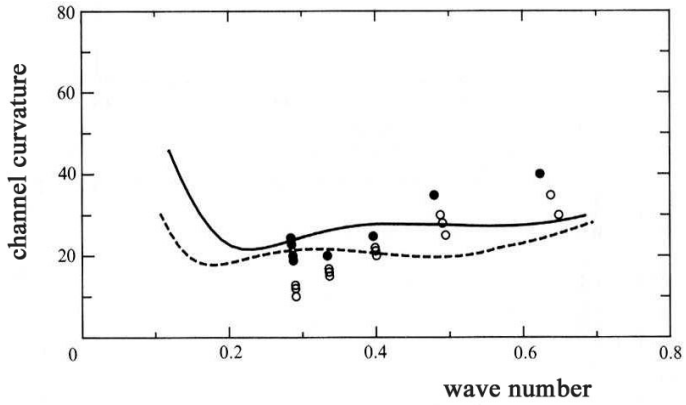

Figure 2.9: The critical values of the channel curvature, as determined by Tubino & Seminara (1990) compared with the experimental data of Kinoshita & Miwa (1974) (open symbols represent migrating bars, close symbols non-migrating bars).

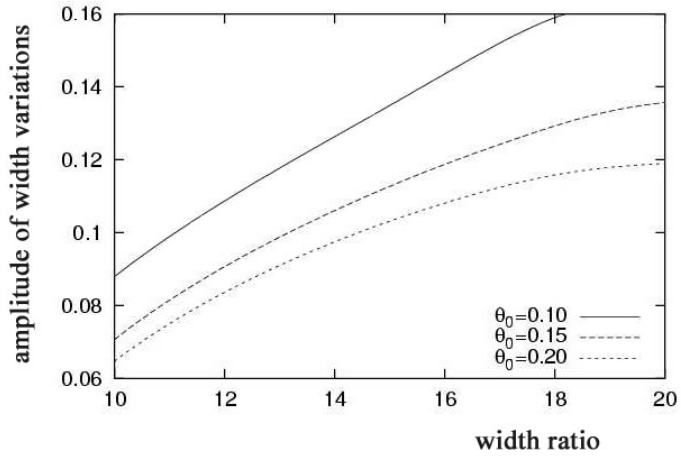

Figure 2.10: The critical values of the amplitude of width variations as a function of the width ratio and the Shields parameter (from Repetto & Tubino, 1999).

the bank oscillations divided by the mean channel width.

Repetto et al. (2002) also investigated the steady forced response of the system driven by periodic width variations. In this case, the bed topography is characterised by two leading components: the former (transverse mode 0) is a purely longitudinal bed deformation, with an associated deposition in the wide sections and scour in narrow sections, the latter (transverse mode 1) implies a transverse deformation in the form of a central bar deposit (Figure 2.11). The analysis with a complete three-dimensional model has shown that the secondary current induced by the stream

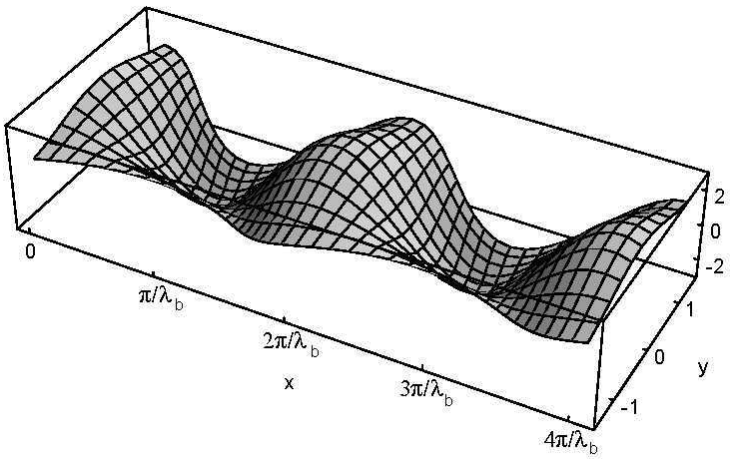

Figure 2.11: Equilibrium bed configuration of a channel with variable width. (from Repetto et al., 2002).

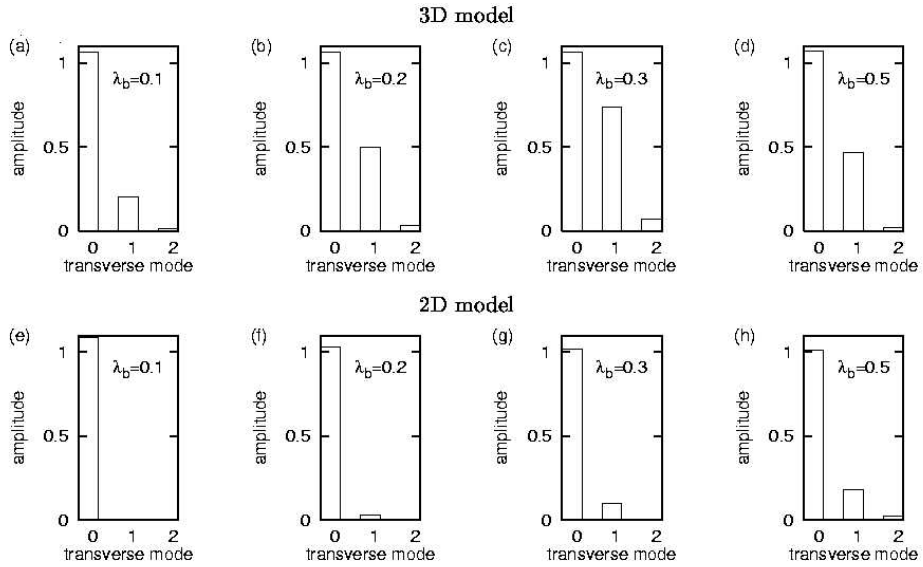

Figure 2.12: Amplitude of the leading transverse modes of the bed topography obtained with the three-dimensional model (a-d) and the two-dimensional model (e-h). (from Repetto & Tubino, 1999).

lines curvature are fundamental to determine the occurrence of the above central bar pattern. Results of the two-dimensional and the three-dimensional model are compared in Figure 2.12 in terms of the amplitude of the leading harmonics of the Fourier spectra. It is worth noticing that

a two-dimensional model, which is unable to account for secondary flows, can not reproduce a transverse bed deformation.

Furthermore, the formation of the central deposits is found to enhance the amplitude of the width variations, in particular for low values of the bottom shear stress and for high values of the width to depth ratio. As a result the planimetric configuration may be unstable and can lead to channel bifurcation.

2.4 Meander resonance and morphodynamic influence

In order to investigate the morphodynamics of a meandering channel the two-dimensional model presented above (Equations 2.7-2.10) can be solved through a linear approach, taking advantage of the fact that the curvature ratio ν_o is typically a small parameter; hence we can set:

$$(U,V,D,H) = (U_o,0,D_o,H_o) + \nu_o(u,v,d,h) + O(\nu_o^2) \; . \tag{2.15}$$

The above procedure has been widely used since the original work of Ikeda et al. (1981) (see also Blondeaux & Seminara, 1985; Johannesson & Parker, 1989; Seminara & Tubino, 1989; Seminara & Tubino, 1992).

The linearization of the mathematical problem allows one to obtain an analytical solution: it is worth noticing that the above solution exhibits resonant behaviour when the values of the width ratio β and meander wave number λ fall within a convenient neighborhood the resonant value β_r and λ_R. The above behaviour, which has been originally detected by Blondeaux & Seminara (1985), is displayed when the periodic variation of the curvature of the channel axis forces a non amplifying and non migrating free response of the bed configuration (Figure 2.13).

The linear system can be reworked to obtain a non-homogeneous ordinary differential equation with constant coefficients. The characteristic exponents λ_j for the first transverse mode are reported in Figure 2.14. One of the exponents is always real and positive, one real and negative, the other two are complex conjugate. The real part of the latter is negative, provided the width ratio is smaller than a threshold value, which, for the first mode, coincides with the resonant value β_R.

The main result of the analysis is that a two-dimensional perturbation of the bed topography is mainly felt upstream in super-resonant conditions ($\beta > \beta_R$) while it may dominantly influence the downstream bottom configuration in sub-resonant conditions ($\beta < \beta_R$) (Zolezzi & Seminara, 2001).

These theoretical findings may provide an explanation of the overdeepening phenomenon observed as a consequence of a local disturbance of channel planform, like that induced by a sudden variation of channel alignment or by the presence of a bifurcation. For example, the effect of a

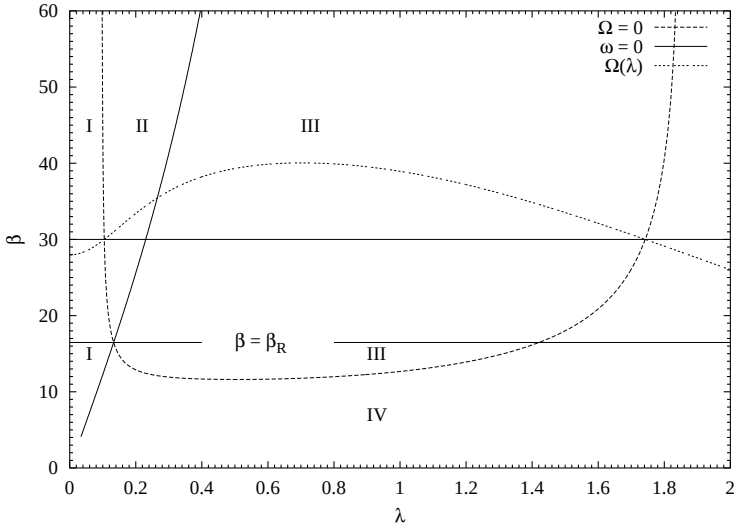

Figure 2.13: Neutral curves for two-dimensional free bars instability ($\Omega = 0$) and migration ($\omega = 0$). (from Zolezzi & Seminara, 2001)

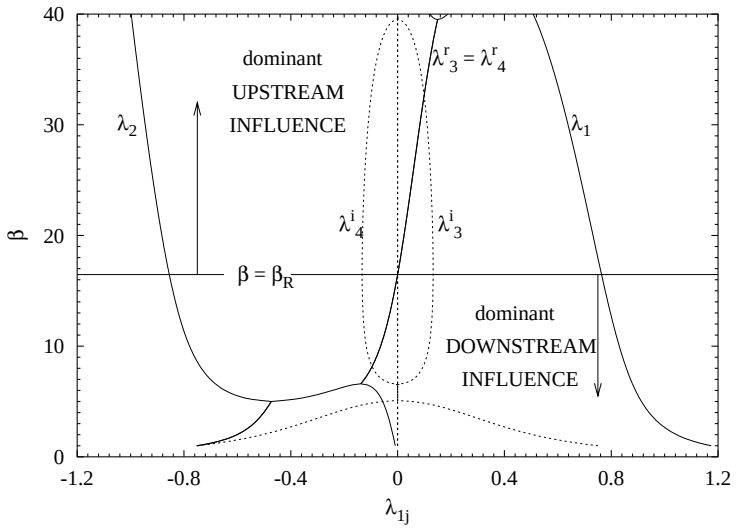

Figure 2.14: The four characteristic exponents λ_j as a function of the width/depth ratio. Solid lines denote the real parts of the exponents while dotted lines denote their imaginary parts. (from Zolezzi & Seminara, 2001)

sharp change in channel curvature (Figure 2.15) leads to the formation of a steady pattern of alternate bars in the upstream reach or in the downstream reach provided the flow is in super-resonant or sub-resonant condition, respectively. Experimental observations on a U-shaped channel by Zolezzi et al. (2004) confirm the above behaviour. A similar effect is determined by an unbalanced bifurcation: this is discussed in Chapter 4.

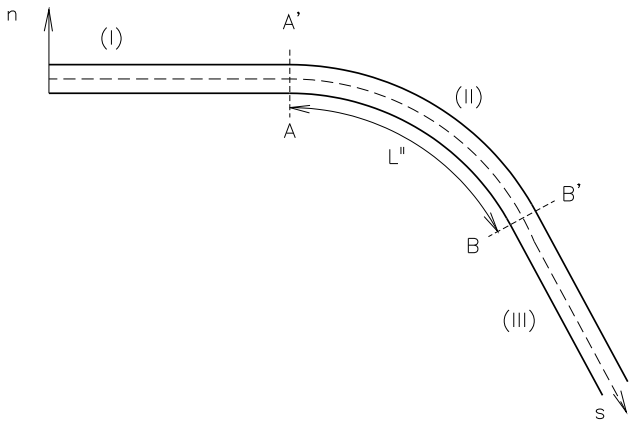

Figure 2.15: Overdeepening: sketch of the channel. (from Zolezzi & Seminara, 2001)

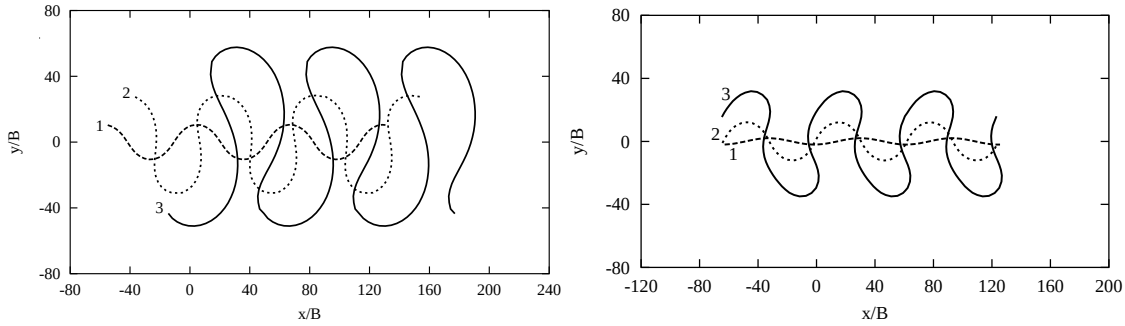

Figure 2.16: Sub-resonant (left) and super-resonant (right) evolution of periodic meanders. (from Seminara et al., 2001)

According to Seminara et al. (2001) sub-resonant and super-resonant conditions also affect the planimetric evolution of a meandering channel, as shown in Figure 2.16. In particular, the maximum erosion rate shifts from downstream to upstream of the bend apex, when crossing the resonant threshold, that is moving from sub-resonant to super-resonant conditions. As a consequence, a reversal of the channel skewness is observed.

2.5 A predictive model for channel bifurcation

The analysis of the equilibrium configuration and stability of a single bifurcation has been recently tackled by Wang et al. (1995) and Bolla Pittaluga et al. (2003) within the context of a one-dimensional model. They considered a simple geometry (see Figure 2.17) with one channel (labelled *a*) that bifurcates into two symmetrical branches (labelled *b* and *c*). All branches have constant width and slope and are in equilibrium with some given water discharge Q and sediment discharge Q_s.

Within the framework of a one-dimensional model with mobile bed, five nodal conditions are needed at the bifurcating point; in particular unlike in the case of confluences, a relationship is required, which governs water and sediment distribution in the downstream branches. Wang et al. (1995) introduced an empirical nodal points condition.

$$\frac{b_b\, q_{s,b}}{b_c\, q_{s,c}} = \left(\frac{Q_b}{Q_c}\right)^k \left(\frac{b_b}{b_c}\right)^{(1-k)} , \tag{2.16}$$

with q_s sediment transport rate, b channel width and Q water discharge in the downstream branches *b* and *c*.

The authors found two possible equilibrium configurations: in the first one both branches are open, in the second one of the downstream channels is closed. The stability of the two solution was found to be strongly affected by the empirical parameter *k*, whose determination is quite difficult, because it is neither related to the hydraulic conditions nor to the bifurcation geometry.

To overcome the above difficulties Bolla Pittaluga et al. (2003) proposed an alternative nodal point condition, based on a quasi two-dimensional approach. The authors divide the last reach of the upstream channel (for a length equal to αb_a, where b is the channel width) in two cells (Figure 2.18). The water and sediment discharges are considered uniformly distributed in the cross section; hence, the discharges into the two ending cells are proportional to their width. Lateral exchanges of both water and sediments are also possible. In particular, based on a generalised

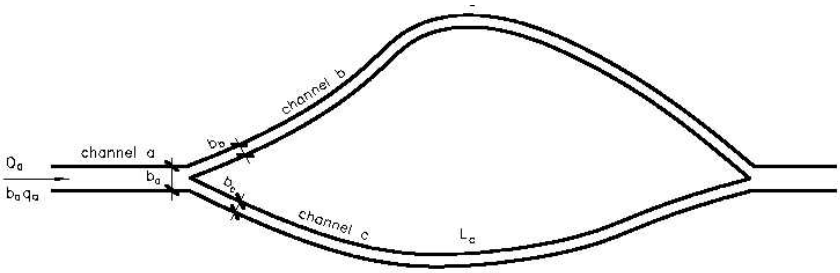

Figure 2.17: Sketch of the geometry of the bifurcation.

version of Equation 2.12, the transverse sediment discharge is evaluated as the sum of two contributions: the first is due to the fact that a transverse component of flow velocity may establish at the bifurcation due to bed deformation, which also implies a transverse exchange of sediments; the second contribution depends on the transverse bed slope; hence, the transverse exchange of sediment can be given in the following form:

$$q_y = q_a \left[\frac{Q_y D_a}{Q_a \alpha D_{abc}} - \frac{r}{\sqrt{\vartheta}} \frac{\partial \eta}{\partial y} \right] , \tag{2.17}$$

where

$$Q_y = \frac{1}{2} \left(Q_b - Q_c - Q_a \frac{b_b - b_c}{b_b + b_c} \right) , \tag{2.18}$$

$$D_{abc} = \frac{1}{2} \left(\frac{D_b + D_c}{2} + D_a \right) , \tag{2.19}$$

and q is the sediment discharge per unit width, D is flow depth, ϑ the Shields parameter, η the bed elevation and the subscripts a, b, c identify the channels. The length αb_a provides a measure of the upstream reach within which the effect of the bifurcation is felt; experimental findings by Bolla Pittaluga et al. (2003) suggest that α is an order-one parameter.

With such a nodal condition Bolla Pittaluga et al. (2003) investigated the possible equilibrium configurations of the bifurcation. The main results are reported in Figure 2.19. Here the equilibrium discharge ratio of the downstream branches is shown, as a function of the width to depth ratio of the upstream channel a for different values of the Shields parameter. A symmetrical solution invariably exists, whereby the same discharge flows within the downstream channels. For

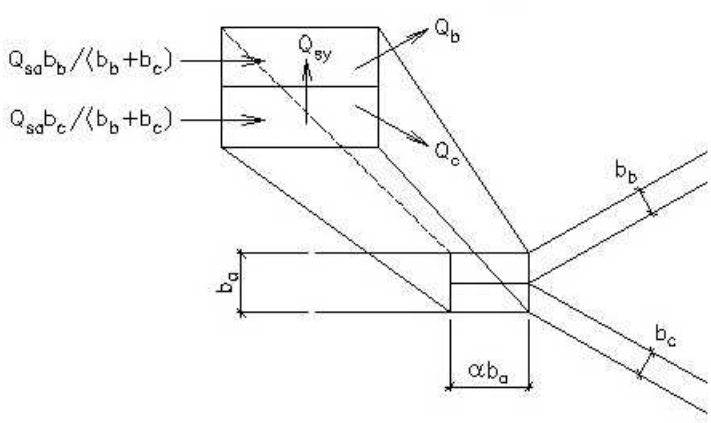

Figure 2.18: Scheme of the nodal point relationship proposed by Bolla Pittaluga et al. (2003).

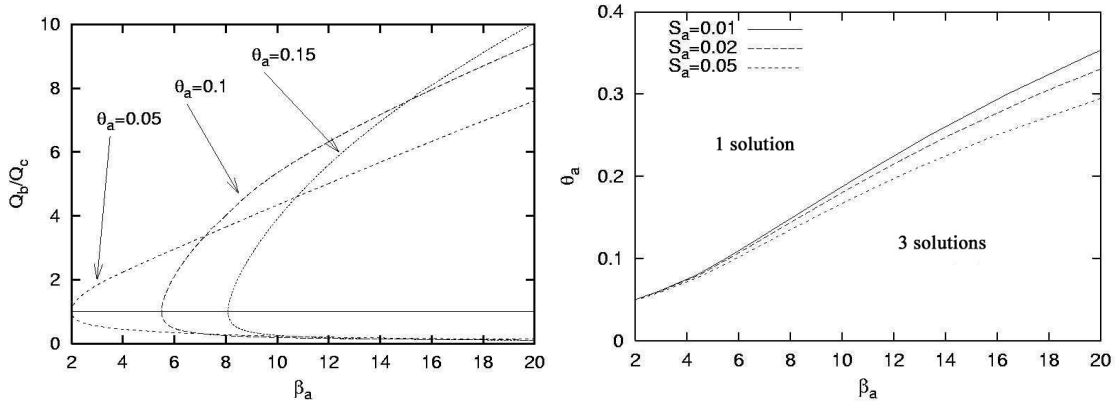

Figure 2.19: Equilibrium configurations of the bifurcation as determined by the model of Bolla Pittaluga et al. (2003). (a) Discharge ratio in the downstream branches as a function of the width to depth ratio of the upstream channel. (b) Separation lines between the region with one possible solution and three equilibrium configurations.

relatively high values of the width/depth ratio two further configurations occur, characterised by a strongly unbalanced water distribution. When a multiple solution exists, the symmetrical state is invariably unstable. Figure 2.19b shows that a unique balanced configuration can be obtained when the sediment mobility is high or when the width to depth ratio is quite small. The unbalanced configuration is also characterised by different bed elevations at the inlet of the downstream channels, the channel that carries more water showing a lower bed elevation. These results are in fairly good agreement with the results of the experimental investigation of Federici & Paola (2003), who found stable bifurcation in a divergent channel only when the Shields parameter attains relatively high values.

We may notice that field observations suggest that natural bifurcations generally exhibit an unbalanced configuration and, at the same time, different widths of the downstream branches (see Chapter 6). Hence, the theory should be extended in order to the case of self-formed channel, whose geometry may adjust to hydraulic conditions. An attempt in this direction has been recently pursued by Miori et al. (2004). Such analysis preliminarily requires the introduction of suitable 'regime' equations able to define an equilibrium channel width in terms of flow and sediment characteristics. Several empirical relationships of this kind have been proposed in the literature. Here the rational formula obtained by Griffiths (1981):

$$b = 5.28 Q S^{1.26} D_s^{-1.5}, \tag{2.20}$$

and the empirical formula proposed by Ashmore (2001) are reported:

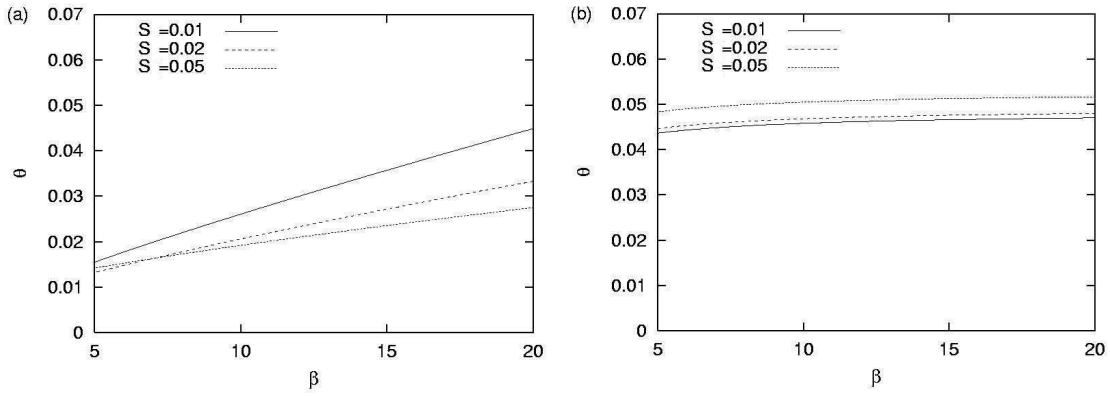

Figure 2.20: Relationship between the Shields stress and width/depth ratio as determined by the equation of Ashmore (2001) (a) and Griffiths (1981) (b) ($D_s = 0.05$ m).

$$b = 0.087\Omega^{0.559} D_s^{-0.445} \,, \tag{2.21}$$

where Q is the water discharge, D_s the mean grain size, S the average bed slope and Ω is the stream power.

The introduction of a 'regime' relationship in the model of Bolla Pittaluga et al. (2003) implies that the upstream values of Shield stress and width ratio are no longer independent and follow the regime relationships reported in Figure 2.20.

We notice that the proposed 'regime' relationships provide values of the Shields stress falling within a neighbor the threshold of the value for the incipient motion; as a consequence, bifurcations in self-formed channels are more likely to display an unbalanced configuration, falling in the region where the system admits of three solutions. The model results are reported in Figure 2.21, where the 'regime' equation proposed by Ashmore (2001) has been used.

The equilibrium configurations are similar to that obtained with fixed channel widths; for values of the width to depth ratio typical of gravel bed rivers, three solutions are possible and the two unbalanced configurations are stable. In Figure 2.21(b) the predicted ratio between the width of the downstream channels is reported: note that the width differences are less marked than that of flow discharges.

The model also reproduces the difference in bed elevation at the bifurcation, as shown in Figure 2.22 where $\Delta\eta$ is the difference of bed elevation at the inlet of downstream channels scaled by the depth of the upstream channel. The degree of asymmetry increases the more unbalanced is the discharge distribution, as also suggested by field and laboratory observations (see Chapter 4 and 6).

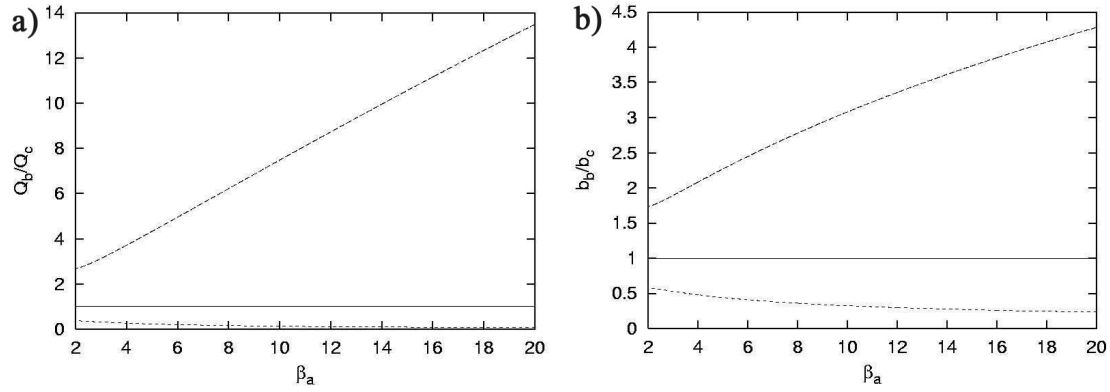

Figure 2.21: Equilibrium discharge ratio (a) and width ratio (b) in the downstream branches as a function of the width/depth ratio ($S = 0.01, D_s = 0.05m$)

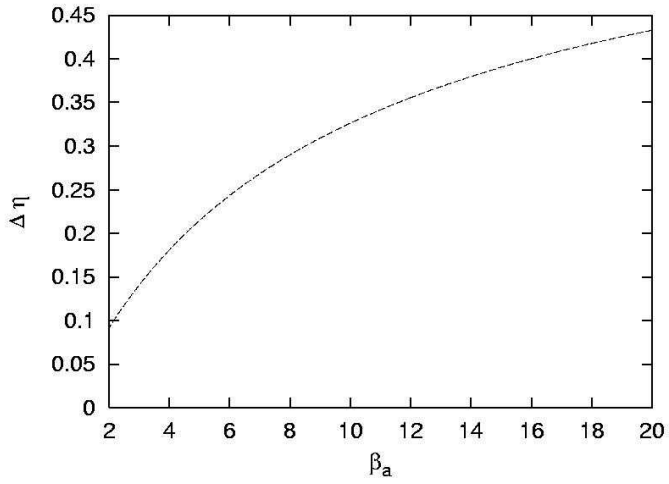

Figure 2.22: Equilibrium values of the parameter $\Delta\eta$ as a function of the width to depth ratio of the upstream channel. ($S = 0.01, D_s = 0.05m$)

3 Experimental study on bed and bank evolution in bifurcating channels

3.1 Introduction

The possibility of predicting the planimetric and altimetric evolution of natural rivers is still an ongoing debate and strongly depends at present on the type of river we are dealing with. While the essential processes characterising the dynamics of single thread meandering channels have been widely investigated in the last two decades (the subject has been recently reviewed by Seminara et al., 2001), effective modelling of channel adjustment in braided rivers can only be achieved over short prediction spans (e.g. Jagers, 2003).

The main reason for such difficulty must be sought in a crucial difference between single and multiple channel rivers, which essentially involves the time scales of bed and bank evolution. In river meanders bank erosion is mainly controlled by sediment cohesion and vegetation, which forces the planform to evolve on a much longer time scale with respect to the process of bed deformation. This implies that, as a first approximation, the corresponding mathematical problem can be decoupled, which provides a much simpler description compared with multiple thread channels. The peculiarity of braided rivers is that each channel can be considered, to a certain extent, as laterally unconstrained (Murray & Paola, 1994); hence, their dynamics depends strongly on the interaction between the altimetric patterns and the planimetric configuration. Both laboratory models and field studies suggest that under these conditions the planform of single channels is often unstable as bifurcations are promoted. This occurs preferentially through the mechanism of chute cutoff due to local flow acceleration (see Ashmore, 1991).

The above process is also common to other river morphologies. Striking evidence is offered by meandering channels, where the occurrence of chute cutoff gives rise to a cyclic reduction of channel sinuosity (Howard, 1996). Besides being common in meandering (Gay et al., 1998), pseudo-meandering (Bartholdy & Billi, 2002) and anastomosing rivers (Makaske, 1998), the process is quite frequent and ubiquitous in braided streams as witnessed by the weakly meandering character of each single branch.

Very few attempts have been made at present to explain the mechanics of chute cutoff (Klaassen & van Zanten, 1989; Slingerland and Smith, 1998; Jagers, 2003). Such knowledge appears even more relevant when considering that a braided pattern seems to reflect the history of few (say, one or two) active branches, though the number of wet channels can be quite large (Mosley, 1983; Ashmore, 2001). This suggests that the evolution of a braided network could be reconstructed in terms of the dynamics of single thread weakly meandering channels interacting at joining points, like confluences and bifurcations, provided bed and bank evolution processes are not decoupled. This 'synthetic' schematisation of braiding might provide a way to predict the time evolution of such complex systems over a relatively long time span: indeed, models in which the network development results from the interaction among single objects like channels and nodes (Murray & Paola, 1994; Jagers, 2001; Thomas & Nicholas, 2002) seem to produce more reliable results, particularly in the medium and long term, with respect to the classical approach that solves the governing equations for the fluid and solid phases.

The dynamics of channels and nodes is mutually dependent. Channel adjustment is largely controlled by the processes of node shifting, creation or annihilation; in turn, bifurcations often occur after a well defined sequence of in-channel events (Ashmore, 1991) which reflect the strong interaction between the planimetric and the altimetric response. All these processes have been independently investigated and understood in detail, particularly those related with the effect on the bed deformation of planimetric non-uniformities, such as channel curvature and width variations. The role of planimetric forcing on the equilibrium bed topography has been analysed in detail in Section 2.3. It has been pointed out also how symmetrical width variations causes the formation of a central steady bar, hence triggering the bifurcation of the stream. The above findings agree qualitatively with the results of the laboratory investigations of Ashworth (1996) on the evolution of a confluence - diffluence unit. The formation of a central bar downstream of the confluence induces the flow to diverge and to concentrate towards the banks, determining the instability of the planimetric configuration.

Notice however that most of the above results on bed dynamics mainly refer to fixed-bank channels; hence, a detailed knowledge of the simultaneous development of the bed and the banks of laterally unconstrained channels is presently not available. The above issue might be rephrased in terms of the following questions: how are free-forced bed interactions affected by the erodible character of the boundaries? How can the altimetric pattern modify the evolution of channel planform? Which conditions define the occurrence of channel bifurcations?

The attempt of providing a quantitative characterisation of bed and bank evolution of a laterally unconstrained channel until the occurrence of the first bifurcation is pursued in the present work. Four sets of experimental runs have performed, with both uniform and graded sediments, in order to highlight the interaction between planimetric and altimetric development and to ascertain the

combined role of free and forced altimetric bed responses. In each experimental run the following sequence of processes has been invariably detected: the initially straight channel first widens, then forms an alternate pattern of bars, which determines the occurrence of a regular sequence of erosional bumps along both banks. Therefore, a slightly meandering configuration establishes, displaying fairly large width oscillations. Under these conditions the pattern of previously formed bars appears highly reworked and soon leads to the occurrence of flow bifurcation through a chute cutoff mechanism.

Experimental findings on planform development suggest that a suitable criterion for channel bifurcation can be given, through the Fourier analysis of bank profiles, in terms of the relevant dimensionless parameters, namely the Shields stress and the width to depth ratio of the channel.

The Chapter is organised as follows: in Sections 3.2, 3.3 and 3.4 a description of the experimental setup and of the data analysis procedure is given. In Section 3.5 the results of the altimetric and planimetric evolution of the channel are presented and the bifurcation process is finally analysed. In Section 6 a summary of experimental results is included along with some concluding remarks.

3.2 Experimental set up

A laboratory model reproduces the main features of water and sediment motion of a gravel bed braided river provided it satisfies the Froude similarity and the flow is fully turbulent, hydraulically rough and the dominance of bed load transport is ensured (Yalin, 1971). A laboratory flume that meets the above criteria reproduces the behaviour and the processes of a gravel bed stream in general (Ashmore, 1982). The main advantages in physical model investigations are the direct control of specific variables and the possibility to observe and to measure the development of planimetric and altimetric patterns, even if all the characteristics of a prototype stream can not be modelled in the correct way (Young & Warburton, 1996).

The experiments were carried out in a laboratory flume, 12 m long and 0.6 m wide, in the Hydraulic Laboratory of the University of Trento (Figure 3.1). A constant water discharge, measured through an electromagnetic meter on the delivery pipe, and a constant sediment rate were supplied into the channel. The sand was fed through a volumetric sand feeder and dropped into the channel via a diffuser, in order to avoid local disturbances. The appropriate sediment discharge in equilibrium with the values of water discharge and channel slope for each experimental run was fed into the channel, in order to achieve an overall equilibrium, i.e. to avoid, on the average, bed degradation or aggradation. At the channel inlet a system of metallic meshes regularised the incoming flow and at the downstream end of the flume a tailgate was constructed to maintain the outlet elevation. Along both sides of the channel a 0.3 m high rail supported a carriage used for

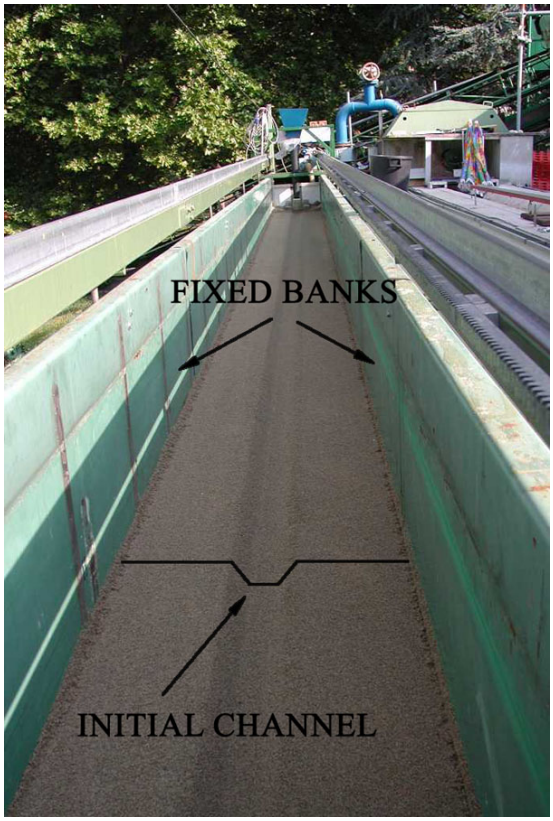

Figure 3.1: The initial configuration of the channel.

levelling the bed and measuring bottom topography and the channel planimetric evolution. The rail slope could be adjusted to the prescribed value.

The experiments involved different values of water discharge (Q), sediment rate (Qs) and initial slope (S), which were chosen to obtain values of dimensionless parameters typical of gravel bed rivers (Table 3.1). The above initial values were calculated under the assumption of uniform flow with reference to the initial trapezoidal section. In Table 3.1 the following notation is employed: Ds is the mean grain diameter, σ is the geometric standard deviation of the grain size distribution, while the dimensionless parameters ϑ, β, ds are the Shields stress, the width ratio of the channel and the relative roughness, respectively, which are defined as follows:

$$\vartheta_o = \frac{\tau_o}{(\rho_s - \rho) g D_s}, \qquad \beta_o = \frac{b_o}{D_o}, \qquad d_s = \frac{D_s}{D_o}, \tag{3.1}$$

where b is the half free surface width, D is the reach averaged value of water depth, ρ_s and ρ are the sediment and water density, g is gravity and τ is the average bed shear stress. The subscript $_o$ denotes the initial (reference) values of parameters and variables.

RUN	D_s [mm]	σ	S [%]	$Q \cdot 10^{-3}$ [m³/s]	Q_s [g/s]	β_o	ϑ_o	d_{so}
A1-10	0.5	1	1	0.167	0.567	4.74	0.086	0.059
A1-15	0.5	1	1	0.250	0.833	4.03	0.104	0.047
A1-20	0.5	1	1	0.333	1.517	3.61	0.118	0.040
A1.5-7	0.5	1	1.5	0.117	0.267	6.03	0.099	0.081
A1.5-10	0.5	1	1.5	0.167	0.767	5.16	0.117	0.066
A1.5-15	0.5	1	1.5	0.250	1.600	4.36	0.142	0.053
A1.5-20	0.5	1	1.5	0.333	2.333	3.90	0.162	0.045
B1.5-20	1.3	1	1.5	0.333	0.583	3.58	0.069	0.103
B1.5-25	1.3	1	1.5	0.417	1.350	3.31	0.076	0.091
B1.5-30	1.3	1	1.5	0.500	1.517	3.12	0.082	0.083
B2-15	1.3	1	2	0.250	0.467	4.20	0.076	0.130
B2-20	1.3	1	2	0.333	1.050	3.77	0.086	0.111
B2-25	1.3	1	2	0.417	1.650	3.48	0.095	0.099
B2-30	1.3	1	2	0.500	1.900	3.27	0.103	0.090
MB1.5-7	0.8	1.7	1.5	0.117	0.350	5.71	0.066	0.120
MB1.5-10	0.8	1.7	1.5	0.167	0.450	4.91	0.077	0.099
MB1.5-15	0.8	1.7	1.5	0.250	0.783	4.17	0.093	0.079
MB1.2-10	0.8	1.7	1.2	0.167	0.400	4.69	0.065	0.093
MB1.2-15	0.8	1.7	1.2	0.250	0.700	4.00	0.078	0.075
MC1.5-15	1.04	2.1	1.5	0.250	0.783	4.07	0.074	0.099
MC1.5-20	1.04	2.1	1.5	0.333	1.717	3.65	0.084	0.085
MC1.5-25	1.04	2.1	1.5	0.417	2.133	3.38	0.092	0.075
MC2-12	1.04	2.1	2	0.200	1.283	4.70	0.083	0.121
MC2-15	1.04	2.1	2	0.250	2.000	4.30	0.092	0.107
MC2-17	1.04	2.1	2	0.283	2.283	4.10	0.098	0.100
MC2-22	1.04	2.1	2	0.367	3.000	3.72	0.109	0.087

Table 3.1: Experimental conditions of the performed runs.

The experimental investigation consisted of four sets of experiments. In the first two sets (denoted by "*A*" and "*B*" in the following) two different well sorted quartz sand distributions were used, with values of the mean diameter *Ds* of 0.5 mm and 1.3 mm, respectively. Note that the restriction to almost uniform sediments allows for a closer comparison between experimental data and existing theories, since most theoretical results have been derived with reference to uniform grain size.

The other two sets of runs were performed with two different bimodal mixtures, that are denoted by *MB* and *M*C in the following. *MB* was a weakly bimodal mixture, obtained with equal percentages of sands *A* and *B*, whereas *MC* was a strongly bimodal mixture, resulting from equal percentages of sand A and another uniform sand (C) whose diameter was 1.9 mm. The degree of bimodality of *MB* (*MC*) was chosen to be lower (higher) than the threshold value beyond which the critical shear stress for the incipient motion of each fraction becomes dependent on the size according to Wilcock (1993).

3.3 Experimental procedure

In each experiment the following procedure was adopted.

The bed was flattened to the prescribed slope using a wide scraper attached to a carriage that ran along the rails. At the same time a narrow channel of trapezoidal shape was cut into the cohesionless sloping surface, with base width of 6 cm and sloping banks such that the initial width of the free surface was 8-12 cm (see Figure 3.1). Then a very low discharge was passed over the bed to prepare a smoothly saturated surface.

During the runs, the planimetric development of the channel was continuously monitored and documented through series of pictures taken from a digital camera mounted on a carriage that ran along the longitudinal rails, every picture covering 1 m of the channel length. Dry bed topography was surveyed periodically, with a laser scanning device, on a regular grid spacing 10 cm in the longitudinal direction and 1 cm in the transverse direction.

Each experimental run followed same method and sequence of measurements, until finishing when channel bifurcation occurred. At first each run was performed without interruptions while continuously monitoring its planimetric evolution. Then the experimental run was repeated, starting from the same initial condition and settings, with a regular sequence of stops that were imposed in order to perform laser survey of the dry bed topography. The experiment was restarted after any intermediate stop and the effect of bar dissection induced by the withdrawal of the water was always found to be negligible. In a few runs the planimetric evolution of the system led the channel banks to reach the fixed walls of the flume before the occurrence of a bifurcation.

Additional measurements of surface flow velocity were made at fixed locations along the channel using a high-speed video camera and light particles as flow tracers. During the experiments the presence of bedforms was observed and their wavelength and migration speed estimated. The sediment discharge was collected periodically using a trap placed at the downstream end of the channel and compared with the sediment supply Qs at the inlet.

3.4 Data analysis

In order to characterise quantitatively the conditions that determine channel bifurcation, both planimetric and altimetric data, namely the evolution in time of channel width, bank profiles and bed elevation have been analysed.

As shown in Figure 3.2, prior to the occurrence of flow bifurcation the channel exhibited a fairly regular and periodic pattern, displaying a negligible longitudinal variation of the overall geometry within the measuring reach; this enabled to employ a Fourier Transform procedure to process the above data. The analysis of bank and bottom configuration was performed both on the

Figure 3.2: A step of the evolution of the channel: a slow meandering channel displaying regular width variations.

whole channel and per single wavelength. No significant differences were detected in the computed results. The Fourier analysis allowed to determine the wave number λ_w and the amplitude δ of bank oscillations, defined in terms of the length L and amplitude A of the leading component of the Fourier representation of bank profile. In the dimensionless form they read:

$$\lambda_w = \frac{2\pi}{L/b_o}, \qquad \delta = \frac{A_w}{2b_o}. \tag{3.2}$$

A suitable procedure was devised to inspect the length of the record looking for the condition which maximized the amplitude of the leading component of the spectrum. It is worth noticing that in all cases such component was clearly distinguishable as shown in Figure 3.3. This fact is closely related to the control exerted on the planimetric bank profile by the development of free bars in the channel.

The bed topography elevation was analysed through a 2D Fourier procedure in order to recognise the contribution of different bar patterns to the overall bed morphology. In the following the "1^{st} transverse mode" denotes the alternate bar pattern and the "2^{nd} transverse mode" denote a central bar structure. The geometrical characteristics of such modes are given in terms of the

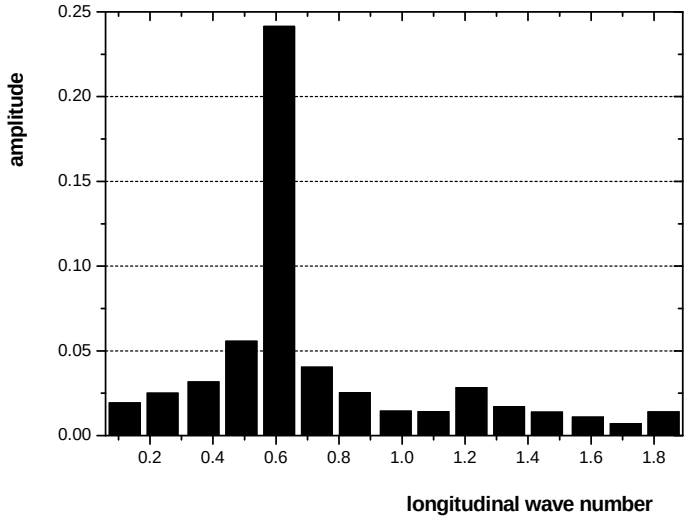

Figure 3.3: A typical Fourier spectrum of the longitudinal bank profile (run B2-20).

dimensionless values of bar wave number λ_b (scaled with the reach averaged value of half channel width b) and of the corresponding amplitude A_b (scaled with the initial depth of the flow D_o).

The major problem encountered in the analysis of topographical data is the definition of suitable reach averaged values of the relevant dimensionless parameters, namely the Shields stress ϑ and the width ratio β. In fact, their evaluation for a given channel configuration would also require the direct measure of flow depth or velocity. In the absence of local measures of such variables a possible way to determine the average depth is to refer to the uniform flow that would occur in a rectangular channel with the same average width and for the same values of water discharge and longitudinal slope. The latter was not found to vary appreciably during the experimental run with respect to the initial prescribed value. Note that the above procedure does not take into account the actual geometry of channel cross sections and the consequent non uniform lateral distribution of bottom stress; at low values of Shields stress this may imply a strong underestimate of the average shear stress, as also pointed out in a recent contribution by Ferguson (2003). This is shown in Figure 3.4 where predicted values of the sediment discharge obtained with the above simplified procedure are compared with observed values (open symbols).

To overcome this difficulty an alternative procedure was adopted whereby the measured bottom topography was used to define a transverse partition of the cross section into narrow strips in order to compute the sediment rate as the sum of the contributions associated with the local values of flow depth. A suitable reach averaged value of ϑ was then defined as the value corresponding to the computed solid discharge in a rectangular channel with the same width. In this way more realistic values of ϑ, and hence of Qs can be obtained, as shown in Figure 3.4 (closed symbols). It is worth noticing that the agreement with the observed data also depends on the sediment

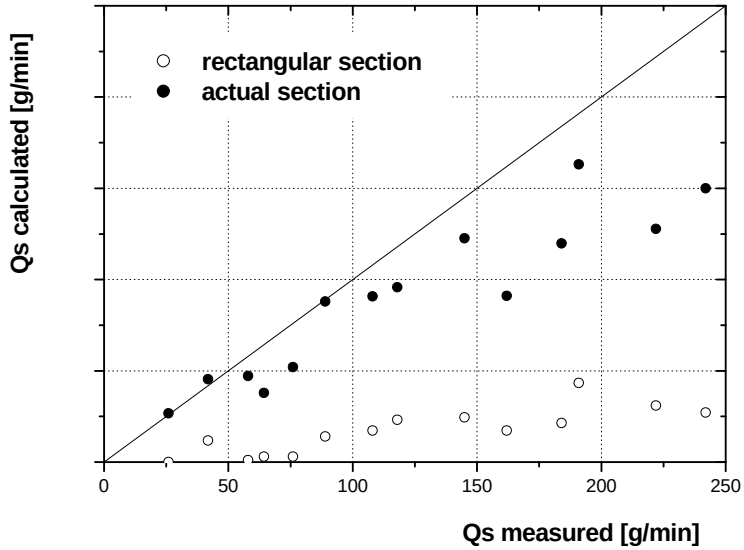

Figure 3.4: Comparison between the measured solid discharge and that calculated according to two different estimates of the Shields stress.

transport formula adopted in the computation. Results reported in Figure 3.4 are obtained using Parker (1990) relationship, which performs better at relatively low values of Shields stress, which are more relevant for present analysis. The use of a bedload transport formula of Meyer-Peter & Müller type, which includes a threshold value, would cause overestimates of measured sediment discharge. The same procedure was adopted to compute the reach averaged value of the width ratio β.

3.5 Results

In this Section a quantitative description of the observed channel dynamics is presented, focusing the attention on the interaction between bar structures and planimetric patterns. Experimental data are also compared with theoretical results on both bar and channel planform evolution in straight and weakly meandering channels (Colombini et al., 1987; Tubino & Seminara, 1990). The discussion of experimental results also comprises further information concerning the configuration displayed at channel bifurcations, namely the angle between the two downstream channels and the relationship among the relevant flow parameters at the onset of bifurcation.

3.5.1 Altimetric evolution

Since the initial width of the channel was not in equilibrium with the imposed flow discharge, an initial, almost uniform widening of the straight channel occurred. The width of the channel at the beginning of each experiment was set such as the value of the width ratio β_o was lower than the threshold value β_c for the formation of free alternate bars (Colombini et al., 1987), which implies a stable plane bed configuration.

The formation of regular trains of migrating alternate bars was then observed as channel widening and the consequent reduction of the average water depth caused the width ratio β to exceed the threshold value (see Figure 3.5).

Bar amplitude and wave number were determined processing the output of the laser bed survey through a Fourier transform procedure. In the first two series of the runs (*A* and *B*) the bars were fairly regular, with dimensionless wave number λ_b ranging between 0.35 and 0.45, which roughly corresponds to the typical range of values of free alternate bars in channels with fixed banks and uniform sand (Tubino et al., 1999).

A slightly different behaviour was observed in the two series of runs with bimodal mixtures. In

Figure 3.5: Formation of alternate bars in the early stage of channel development.

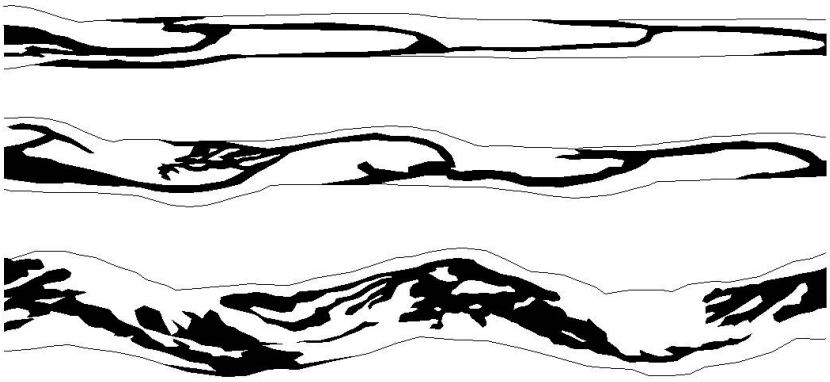

Figure 3.6: Example of sorting pattern for three stages of channel development in bimodal sediment. Dark regions denote the accumulation of coarse particles.

this case bar morphology was less regular, especially in the *MC* runs (Table 3.1) characterised by a higher degree of bimodality where the lengths of single bar units were different and the migration speed was considerably reduced. The dimensionless wave number was on the average lower compared with uniform sediments, ranging between 0.25 and 0.3. Moreover, the presence of graded sediment caused the formation of regular sorting patterns, characterised by the selective deposition of coarse particles on the bar fronts (Figure 3.6). These findings agree with the theoretical and experimental results of Lanzoni & Tubino (1999) and Lanzoni (2000), who highlighted the role played by sediment non uniformity on the formation and equilibrium configuration of alternate bars in straight channels.

The observed morphological features of bars have been also compared with those predicted by the weakly non linear theory of Colombini et al. (1987) (Figure 3.7). The theoretical results refer to a sequence of alternate bars that have reached an equilibrium amplitude in straight channel with fixed banks. This configuration differs from that of present experiments, where the channel banks are subject to lateral erosion. In the latter case the role of the forcing effects of planform non uniformities, such as channel curvature and width variations, may prevent the achievement of an equilibrium amplitude and cause modification of bar structures through non linear interaction (Tubino & Seminara, 1990; Repetto & Tubino, 1999).

Note that, in the early stage of channel evolution, when the amplitude of such planimetric forcing remains relatively small, bars may undergo a finite amplitude development such that their amplitude is quite well predicted by the theory, at least within the weakly non linear regime, $(\beta < 2\beta_c)$, in which the theory is applicable.

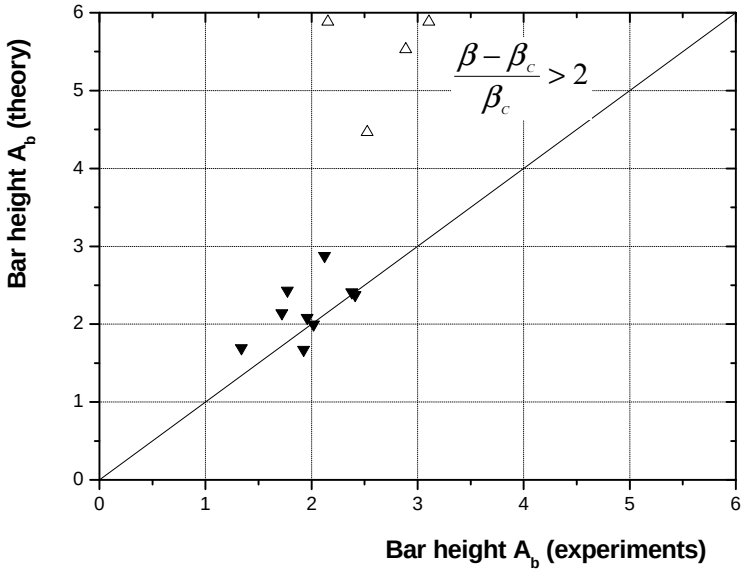

Figure 3.7: Comparison between the measured values of bar hight and theoretical predictions of Colombini et al. (1987).

As the experimental run proceeds, the adjustment of the flow field to the presence of alternate bars determines the lateral shift of the main flow close to the banks and the formation of a regular sequence of indentations along the bank profiles, (Figure 3.2), whose length scale coincides with that of the alternate bars. The resulting planimetric configuration is a weakly meandering channel that also exhibits regular width variations. As pointed out in the Introduction these planimetric non uniformities may strongly affect bed topography, as they promote the transition from the migrating free response (alternate bars) to a steady forced bed deformation. Bar structures then progressively become fixed with respect to the planimetric configuration; this enhances local bank erosion which, in turn, implies a further increase of the planimetric forcing effects.

Due to the above processes, only do the bars stop migrating, but also their morphology is strongly modified. The analysis of the Fourier spectra of bed topography (Figure 3.8) reveals a tendency for bed topography to evolve from alternate to central bar patterns as a run proceeds. Figures 3.9 and 3.10 summarise the results of the whole set of experiments for the amplitude of the leading components of bed topography measured at the initial stage and at the final stage of the experimental runs, respectively (notice that in the plots the cumulative effect of higher orders transverse modes, 2^{nd} and 3^{rd}, is reported). Figures 3.8-3.10 show that a similar tendency was displayed in almost all the experiments, with a decrease of the amplitude of the alternate bar component (1^{st} mode) and the simultaneous increase of the amplitude of higher order transverse modes (2^{nd} and 3^{rd}). This embodies the fundamental mechanism leading to channel bifurcation: the resulting topography, forced by planimetric non uniformities, progressively leads to the process

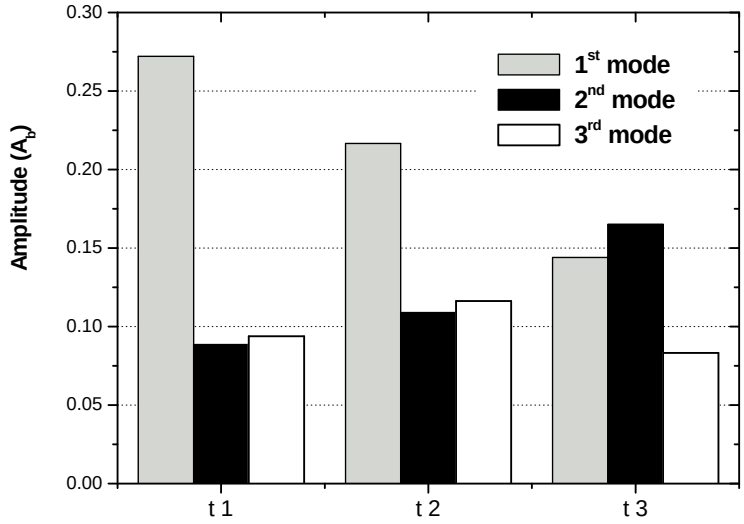

Figure 3.8: The amplitude of leading components of the Fourier spectrum of bed topography measured at three subsequent stages (t1, t2, t3) during the experimental run A1.5-10.

of chute cutoff of the alternate bars formed in the initial stage of the experiment.

One might be tempted to explain the above process in terms of the standard approach based on linear theories, the so-called "bar theory of river meandering" (Fredsœ, 1978; Kuroki and Kishi, 1985) according to which the onset of braiding is related to the amplification of higher order modes. As shown in Figure 3.11 this typically occurs for relatively large values of the width ratio β, provided it exceeds a threshold value. Indeed the observed values of flow parameters at the onset of bifurcation (in particular the width ratio) fall within the range of amplification of higher order modes. Furthermore, the value of the dimensionless longitudinal wave number of bars λ_b was found to invariably increase during the experiments since the length of bars was almost fixed and equal to the "initial length", while the channel width increased (Equation 3.2). According to linear theories this also promotes the instability of higher order transverse modes (Tubino et al., 1999). However, the present experimental findings suggest that the modification of previously formed bars and the transition to a central bar pattern occur when alternate bars have already undergone a finite amplitude development, as shown in Figure 3.7, which implies that linear theories no longer applies. Moreover, the experimental results show that the modification of bar structures is mainly associated with the forcing effects of planform, which are not included in linear theories.

It is possible to observe that the Fourier spectrum reported in Figure 3.8 shows that the 3^{rd} transverse mode can attain a relatively high amplitude. Its role can be related to the asymmetry of the planimetric configuration and to the history of the bed evolution. In fact, due to channel curvature lateral erosion is alternatively shifted towards the left and right bank; hence, width variations are not symmetrically displaced with respect to the channel axis. The presence of third harmonics

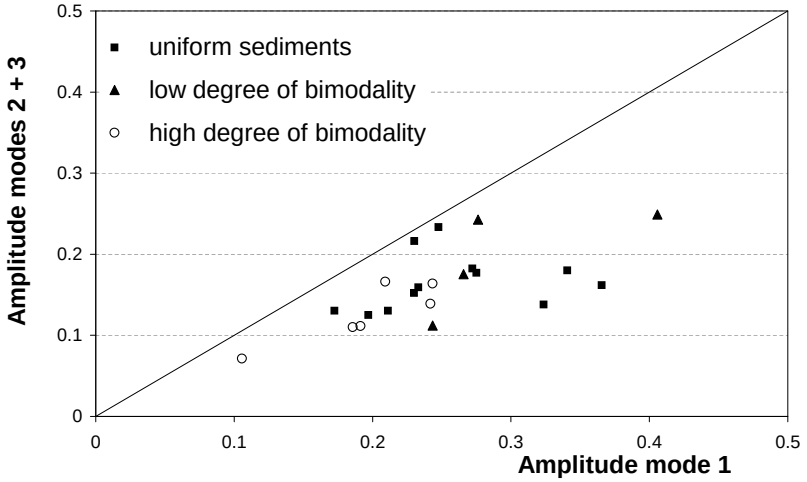

Figure 3.9: Comparison between the amplitude of alternate bars and that of transverse modes 2 + 3 in the initial stage of experimental runs.

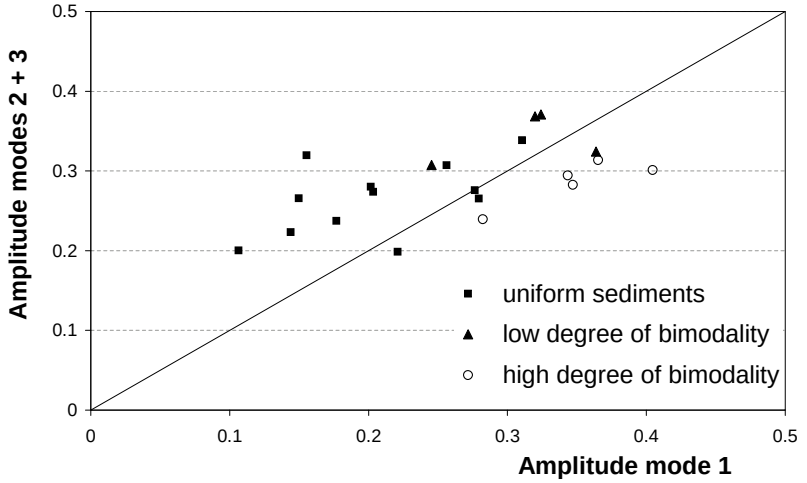

Figure 3.10: Comparison between the amplitude of alternate bars and that of transverse modes 2 + 3 at the onset of the bifurcation.

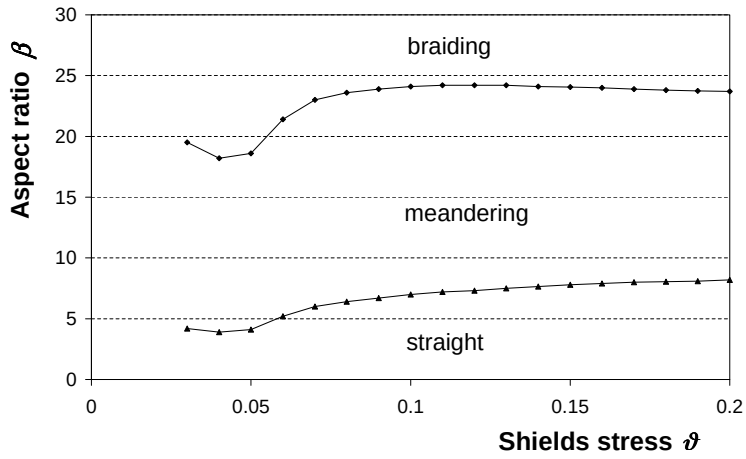

Figure 3.11: Threshold values of the width ratio for the occurrence of different river regimes according to linear stability analysis.

has then to be considered in the light of the overall channel evolution, the final configuration being the result of the gradual drifting of alternate bars towards the channel axis.

Finally, it is worth mentioning that in the runs with graded sediments the evolution of bed topography was slightly different. In particular, the development of higher order modes was less prominent, the alternate bar mode being invariably dominant until the onset of the bifurcation (Figure 3.10). This was mainly related to the deposition of coarse particles on bar fronts (Figure 3.6) which caused a local decrease of Shields stress, thus slowing down the evolution of the bed configuration.

3.5.2 Planimetric evolution

In all the experiments the overall channel alignment was found to continuously adapt to macro-scale perturbations of bed topography. As a result, the evolution of channel planform was crucially controlled by the migration speed of alternate bars. Indeed, two different evolutionary scenarios were detected that are closely related to the ratio between the migration speed of bars and the bank erosion rate. In the case of cohesionless banks the latter process is mainly controlled by the intensity of local erosion induced by migrating bars. Hence, both effects contributing to the above ratio are related to the topographic expression of bars. The above ratio is a key parameter that affects the subsequent development of the channel. Bars that migrate quite fast are unable to produce high localised bank erosion in which case the amplitude of planform non uniformities (width variations, curvature) can not reach a value high enough to suppress bar migration and to enhance the development of a central pattern. The slowing down of bars is mainly related to the continuous channel widening, with a consequent reduction of the averaged bed shear stress.

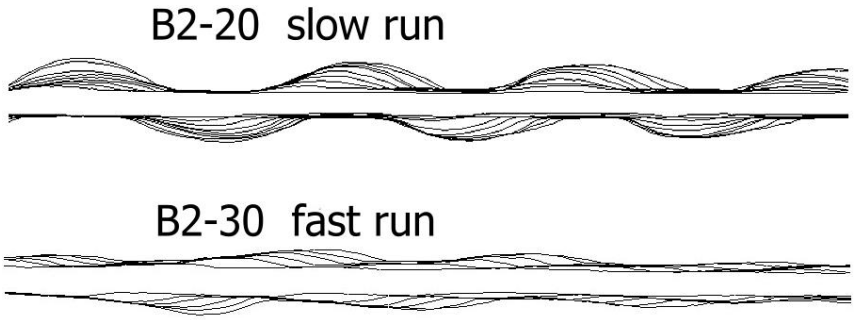

Figure 3.12: Examples of the planimetric development in a slow run and in a fast run.

The experimental runs can be divided into two groups, namely "slow" runs and "fast" runs (Figure 3.12). The above distinction also embodies a different mechanism of channel bifurcation. The slow runs are characterised by slowly migrating bars, so that bend amplification is much larger than channel migration, consequently width variations and channel curvature strongly affect bar patterns and bifurcation occurs through the mechanism of chute cutoff. On the contrary, fast runs are characterised by a much faster bar migration. In this case, bifurcation mainly occurs due to the different mobility of single bar units which may lead a bar front to merge into a scour hole left by the preceding bar. Most of the experiments displayed the characteristic of the "slow" runs, in particular those with bimodal sediments which were invariably characterised by lower bar migration speed due to the sorting effects (Lanzoni & Tubino, 1999).

The evolution of channel planform can be described through the Fourier analysis of bank profiles, which clearly shows the presence of a dominant harmonic: its amplitude increases in time and its length coincides with that of alternate bars (Figure 3.3).

The interrelation between altimetric and planimetric patterns is quantitatively revealed by the high correlation between the length of width variations and that of bars. This is shown in dimensionless form in Figure 3.13, where the values of the wave number of width variations λ_w and of bars λ_b, measured at the initial stage and at the onset of bifurcation, are compared. As pointed out before, the increase of the dimensionless value of the wave numbers is mainly related to channel widening, since λ is scaled through the actual width of the channel (Equation 2). On the contrary the physical length of bank oscillation remains almost constant and coincides with the length of bars that formed at the initial stage of the process.

The above findings may shed some light on the debated question of identifying typical length scales in braided networks (Ashmore, 2001). According to our observations the spacing between subsequent bifurcations is essentially related to the length of initially formed bars. Though this picture neglects the reworking effects which may arise from the interaction between different

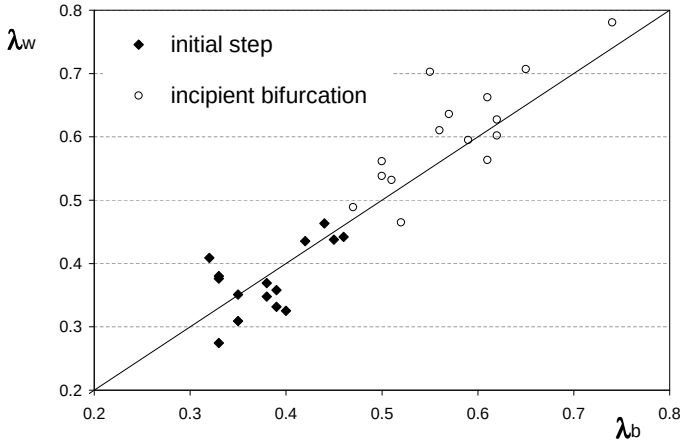

Figure 3.13: Comparison between the wave numbers of bars (λ_b) and of the bank profiles (λ_w).

Figure 3.14: The braided reach of the Sunwapta River: field campaign of Summer 2003.

branches, a strong indication is obtained on the role of bars on the definition of the link length. Figure 3.14 shows a braided pattern with a regular sequence of confluence-diffluence units.

The amplitude of the leading component of bank oscillations is plotted in Figure 3.15, versus the width ratio, i.e. for increasing times. It is worth noticing that all the "slow" runs show a similar behaviour, characterised by an initial growth, until a peak value is reached, followed by a stage of slow decay. The occurrence of this maximum is of crucial importance as it may provide an objective criterion to set the onset of the bifurcation. In fact, on the rising limb, bank oscillations increase their amplitude as the main flow is shifted toward the bank by the presence of the alternate bar. When the channel bifurcates, the flow erodes also the opposite banks, the location of maximum bank erosion shifts along the channel, leading to a more irregular bank line. The process is depicted in Figure 3.16. As a consequence the amplitude of width variations starts decreasing immediately after the occurrence of flow bifurcation.

The maximum values of the amplitude of bank oscillations are plotted in Figure 3.17, for

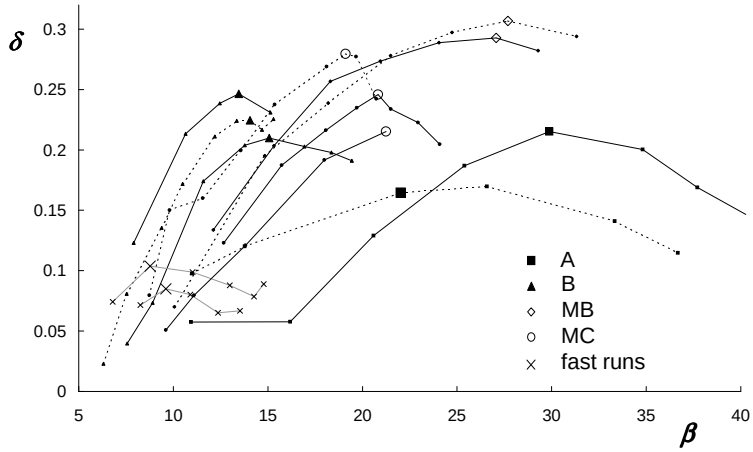

Figure 3.15: Evolution of the dimensionless amplitude of bank oscillations as a function of the width ratio.

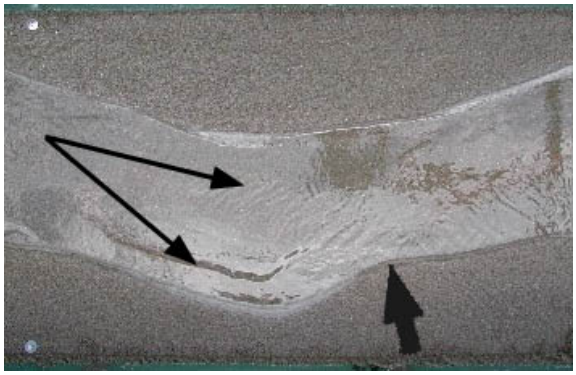

Figure 3.16: The onset of flow bifurcation.

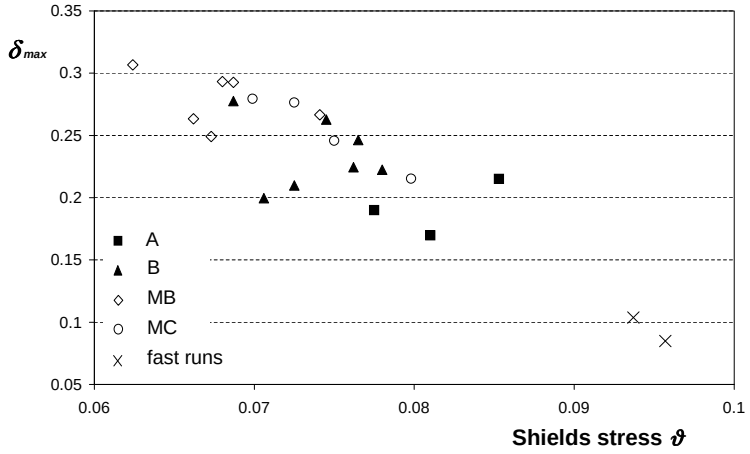

Figure 3.17: Peak values of the dimensionless amplitude of bank oscillations as a function of Shields stress.

all of the experiments. These values are greater than the threshold values above which migrating alternate bars are suppressed in variable width channels as predicted by Repetto & Tubino (1999). Furthermore, present experimental results agree qualitatively with the above theoretical analysis, which predicts that the threshold amplitude of width variations that marks the transition from migrating alternate bars to steady central bars is a decreasing function of the Shields stress ϑ. Also note that the two "fast" runs show a different behaviour, reaching a maximum value of approximately 0.1. In this case width variations are unable to stop the migration of the bars. The maximum amplitude of bank oscillations attains, on the average, higher values in the runs with graded sediments, which may be seen as a further indirect effect of the reduced mobility of bars in this case. As a result, the bifurcation occurs at higher values of the width ratio and consequently at lower values of the Shields stress.

3.5.3 Flow parameters at incipient bifurcation

Once an objective criterion for the occurrence of the bifurcation has been established, as discussed in the preceding Subsection, it is then possible to describe channel geometry and characterise channel and flow at the onset of flow bifurcation.

The angles between the streamlines of the two main branches were measured, analysing the planimetric configuration. The observed values range between 35 and 55 degrees, displaying a weakly positive dependence on the width ratio of the channel. In the runs with graded sediments, the formation of a central wedge shaped deposit of coarse particles was invariably observed (as shown in Figure 3.18). The characteristic angles of this sorting pattern was slightly greater than the streamline angles, ranging between 40 and 60 degrees, (see Figure 3.19). These findings are

Figure 3.18: The central, wedge shaped deposit of coarse particles.

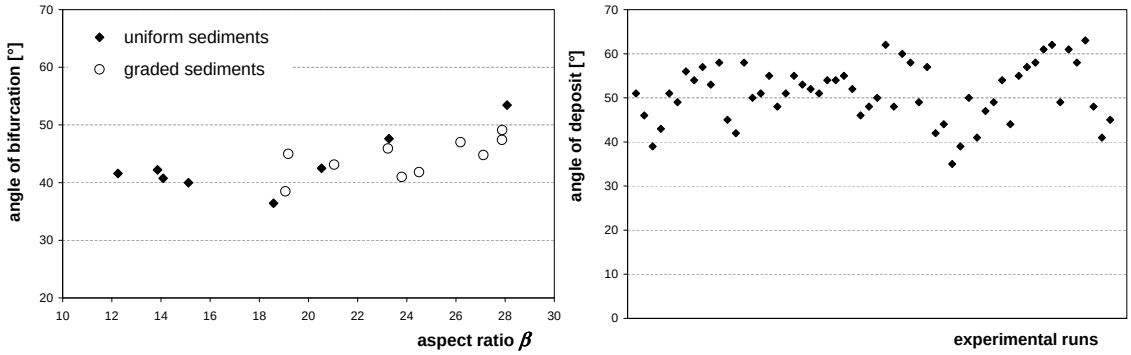

Figure 3.19: Angles of bifurcations measured by the planimetric configuration (left) and angles of the central deposit (right).

in fairly good agreement with other experimental and field observations. In particular, Federici & Paola (2003), investigating the occurrence of bifurcations in diverging channels, found that the angle between the two branches was typically about 50 degrees, with a larger value of the angle formed by the central bar deposit.

Finally, in Figure 3.20 the path of each experimental run in the $\vartheta - \beta$ plane is traced. The plot describes the instantaneous reach-averaged hydraulic conditions. Each run is represented in this plane by a decreasing curve, the last point of which roughly corresponds to the flow conditions at the onset of flow bifurcation. The experimental runs in which bifurcation did not occur before the channel reached the fixed flume banks are plotted in Figure 3.20 with dashed lines.

It appears that the values of the Shields stress and of the width ratio at the onset of bifurcation can be somehow related, at least for the runs with uniform sediments. The points sit along a critical curve, whereby larger values of the Shields stress are associated with larger values of the width ratio. The diameter of the sediments does not seem to affect this relationship, in that series *A* and

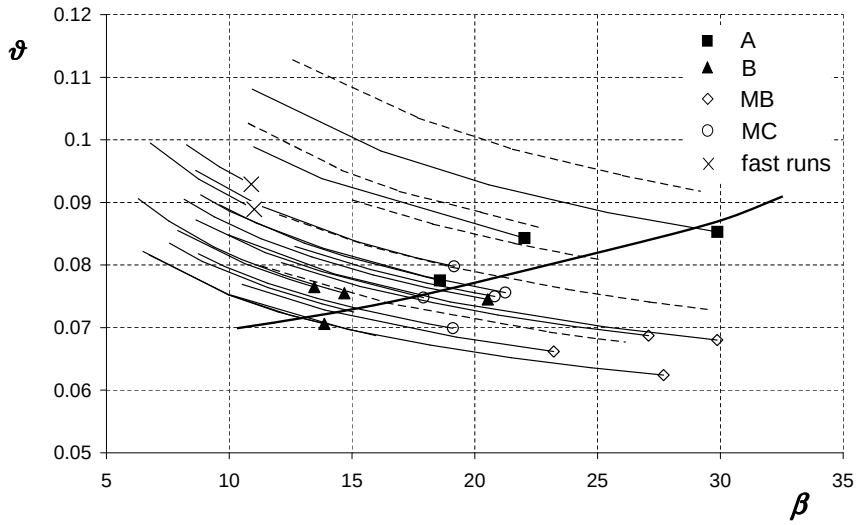

Figure 3.20: Bifurcation points on the plane Shields stress - width ratio.

B display a similar behaviour.

It must be pointed out that results obtained with graded sediments do not conform to the above behaviour. The paths on the $\vartheta - \beta$ plane show a similar trend, but the bifurcation points are more scattered and correspond to lower values of Shields stress and higher values of width ratio. Finally, it is worth noticing that the two "fast" runs display a different behaviour and bifurcate at lower values of the width ratio, which confirms a different bifurcation mechanism.

3.6 Discussion

In this work the attention has been focused on the interaction between bed and bank processes which characterised the evolution of laterally unconstrained channels.

The following outcomes are significant:

- in a laterally unconstrained planform the development of forcing effects, which are mainly related to width variations, lead to a strong modification of the bar structures, driving the transition from spontaneously developing migrating bars to fixed steady bars;

- the main effect of bars on the planimetric pattern is the generation of channel curvature and width variations through local bank erosion. Bar migration speed is a crucial parameter which controls the subsequent development of the channel, in that channel dynamics may be strongly or weakly conditioned by planimetric forcing depending on the ratio of bar migration speed to lateral bank erosion rate (this sensitive dependence on the migration

properties of bars may result in a severe restriction on the applicability of numerical models to predict channel changes with cohesionless boundaries);

- the analysis of the development of the planimetric configuration allowed to define an objective criterion for the occurrence of channel bifurcation; in particular the amplitude of width variations and channel sinuosity increases until the onset of bifurcation and then decreases as the concentration of the main flow is shifted towards bank lines that were previously undisturbed;
- the planimetrically driven modification of bar structures is responsible for flow and channel bifurcation, occurring mainly through the mechanisms of chute cutoff and of bar dissection;
- experimental findings suggest that the length of bars developing in the channel strongly influences the longitudinal spacing of bifurcation points, which implies a bar control on the scale of link length in braided rivers.

The experimental investigation also allowed to characterise the flow and channel geometry at the onset of bifurcation: the configuration was described in terms of both geometrical properties, as the angle between the two main flow directions downstream, and by hydrodynamical parameters, like the average Shields stress and channel width ratio. This characterisation provides useful data and possible rules to be implemented in predictive models of channel changes in braided systems (e.g. Murray & Paola, 1994; Jagers, 2003), with the aim of ensuring a more physical base to the prescribed rules. Indeed, understanding and predicting the occurrence of channel bifurcations is a crucial step to improve morphological predictions in braided networks, as chute cutoffs control the position of the main flow, therefore channel adjustment and the location of bank erosion.

4 Experimental study on the equilibrium configurations of river bifurcations

4.1 Introduction

The bifurcation is a crucial building block of braided networks: it causes braiding initiation and it determines flow division in the downstream branches (Figure 4.1). In spite of its importance, few quantitative investigations have been carried out and there is a major lack of information on flow and sediment distribution in the downstream channels, on the bed configuration close to the bifurcation region and on the existence and stability of equilibrium configurations.

It is now useful to summarise the most relevant experimental studies on river bifurcations.

Bifurcations in braided streams are often found to arise in the context of a confluence-diffluence unit, as examined by Ferguson et al. (1992); the effect of channel divergence has been investigated experimentally by Federici & Paola (2003), who showed that in this configuration a central deposition is likely to occur, due to flow divergence that determines stream bifurcation into two branches. Federici & Paola (2003) pointed out that two different configurations may exist, depending mainly on the value of the Shields stress in the upstream channel. For relatively high values of the Shields

Figure 4.1: Bifurcation in a braided river (Sunwapta River, Canada).

stress the bifurcation was found to show a stable configuration, with both branches open, while a low sediment rate eventually leads to close one of the branches. The authors notice that this 'switch' configuration is triggered also by the non uniformity of initially and boundary conditions: the bifurcation stability might be significantly affected by a slight flow upstream perturbation.

As indicated by de Heer & Mosselman (2004) the bifurcation angle may be a crucial ingredient to determine a proper physically-based nodal point relation, as it strongly affects flow structure and the division of bedload transport rates in an alluvial diversion with fixed walls.

Hirose et al. (2003) investigated the role of alternate bars on the equilibrium configuration of a 'Y' shaped configuration. They highlighted how the migration of free bed forms alternately shifts the main flow in the upstream channel and consequently induces a fluctuation of the water and sediment discharge in the two downstream branches.

In the present Chapter the outcomes of an experimental study on equilibrium configurations of channel bifurcations are presented. This study is the first systematic attempt to quantitatively describe the equilibrium configuration of a bifurcation, both in terms of bed topography and of flow distribution. The experiments have been carefully designed in order to test the validity of the theoretical predictive model presented by Bolla Pittaluga et al. (2003) and discussed in Section 2.5. The aim of the experimental work is to verify the existence of asymmetrical equilibrium configurations, with both branches open, for an imposed planimetrically symmetrical configuration. Such unbalance is actually predicted theoretically for low values of the Shields stress and high values of the width ratio in the upstream channel by Bolla Pittaluga et al. (2003). The attention is focused on the ratio between the discharges in the two downstream branches and on the differences in bed elevation at the bifurcation.

In the experimental study the influence of bar formation and migration on equilibrium and stability has been also analysed. The presence of large scale bedforms in the upstream channel enhances two-dimensional effects on flow division, that may alter the stability conditions identified in a purely one-dimensional context. Moreover bedforms migration can promote morphodynamic unsteadiness, shifting the observed configuration to a more oscillating pattern.

Finally, the results are analysed referring to the theoretical framework of two-dimensional morphodynamic influence (Section 2.4). In this context, the transverse slope induced by an unbalanced bifurcation plays a similar role to the forcing effect of channel curvature in a sequence of straight reaches connected with bends of constant curvature, that typically produces the well known overdeepening phenomenon. The morphodynamic influence of bifurcation is investigated relating the observations, namely the upstream and downstream channel topography and the flow pattern, to the preferential conditions characterising the 'free' response of the system, represented by the 'resonant' value of the width ratio (Blondeaux & Seminara, 1985).

4.2 Experimental set up

A new laboratory flume was constructed in the Hydraulic Laboratory of the University of Trento, in order to model large scale river morphodynamics with a special focus on the investigation of the planimetric and altimetric evolution of a braided network. The flume, with concrete walls, is 25 m long and 2.90 m wide (Figure 4.2). Its peculiar external width, 3.14 m, suggested the name π.

The water discharge is supplied by a pump, regulated with an inverter, that allows to set discharge values from 0.5 to 20 liters per minute. At the upstream end of the flume, the first meter is devoted to dissipate the kinetic energy of the incoming flow. At the downstream end a tailgate is placed in order to fix the bed elevation. A chute conveys the flow in a submerged tank, held up by four load cells, that measure the weight of the transported sediments at 1-minute intervals.

The sediment input is provided by an open circuit, made up by a volumetric sand feeder with three screws that convey the sand into the flume through a diffuser. Only dry sand is fed, in order to ensure a constant and well defined input, particularly for relatively low sediment rates.

Two different sets of rails have been mounted: the inner one supports a carriage for levelling the bed at the prescribed slope. The outer one has been positioned with high accuracy as it supports a carriage driven by a motor, whereby the measuring instruments can move along the longitudinal, transversal and vertical directions. At present the monitoring instrumentation includes a laser profiler and a water gauge (Figure 4.3), but the flume is planned to be equipped with a profile indicator, that will allow to monitor the time evolution of bed topography and with a digital camera

Figure 4.2: Picture of the π flume.

Figure 4.3: The high precision automated carriage with the monitoring equipment.

in order to produce digital photogrammetric images of the evolving patterns. The flume has been designed also with the aim of reproducing the typical unsteadiness that characterise hydrological inputs to natural braided rivers: water and sediment rates can be adjusted with a software and automatically adjusted to the desired sequence.

For the present experiments a 'Y' shaped configuration has been built inside the flume, consisting in three channels with fixed walls and rectangular cross section, as shown in Figure 4.4. The upstream channel is 5 m long and 0.36 m wide. The two downstream channels are 0.24 m wide and the bifurcation angle has been set to 30 degrees. The width of the channels has been chosen in order to reproduce typical configuration observed on natural bifurcations: rational regime theories predict a non-linear relationship between the flow discharge and the channel width, implying a ratio of 1.3 between the total width of the downstream channels and the upstream width, in the case of a symmetrical configuration (Ashmore, 2001). In order to measure the water discharge in each channel, the flow has been conveyed in two different tanks, where the flow depth is measured through a triangular mill weir. The flume was filled with a well-sorted quartz sand, with mean diameter of 0.63 mm.

4.3 Experimental procedures

The main goal of the experiments was to investigate the equilibrium configuration of the bifurcation, examining both flow distribution and bed topography. A second objective was to assess how the presence of bedforms, namely alternate migrating bars, could affect equilibrium and its

Figure 4.4: Upstream view of the 'Y' shaped configuration.

stability.

Two sets of experiments were performed: the first, with a longitudinal bed slope of 0.3%, was characterised by lower values of the aspect ratio and the formation of bar was inhibited. The second series, with a higher slope (0.7%), was characterised by the occurrence of free bars, in almost all the runs.

The influence of flow parameters, namely the width ratio β and the Shields stress ϑ, on the equilibrium configuration was analysed by changing the values of water discharge and longitudinal slope.

The relevant dimensionless parameters fell in the following ranges of values:

$$4 < \beta < 25 \text{ and } 0.045 < \vartheta < 0.11,$$

reproducing typical values that are found in natural braided networks. The flow parameters characterising the incoming flow for all the runs are reported in Table 4.1, where S is the final bed slope, Q is water discharge, D the average depth; rQ and $\Delta\eta$ are defined in the following Section.

run	s	Q [liters/s]	D [m]	β	ϑ	ds	rQ	$\Delta\eta$
F3-18	0.0031	1.8	0.0167	10.77	0.0459	0.038	0.294	0.694
F3-20	0.0026	2	0.0189	9.55	0.0425	0.033	0.466	0.594
F3-21	0.0027	2.1	0.0191	9.45	0.0453	0.033	0.56	0.514
F3-23	0.0031	2.3	0.0194	9.26	0.0524	0.032	0.730	0.365
F3-25	0.0026	2.5	0.0215	8.38	0.0487	0.029	0.65	0.312
F3-29	0.0031	2.9	0.0223	8.08	0.0599	0.028	0.8	0.153
F3-37	0.0033	3.7	0.0254	7.09	0.0721	0.025	0.91	0.043
F3-45	0.0037	4.5	0.0277	6.50	0.0873	0.023	0.99	0.022
F3-61	0.0029	6.1	0.0363	4.95	0.0855	0.017	0.97	0.019
F7-06	0.0065	0.6	0.0068	26.30	0.0420	0.092	0	1.307
F7-07	0.0066	0.7	0.0075	23.91	0.0462	0.084	0	1.370
F7-08	0.0077	0.8	0.0077	23.30	0.0559	0.082	0	1.726
F7-09	0.0078	0.9	0.0083	21.66	0.0606	0.076	0.25	1.318
F7-10	0.0067	1	0.0093	19.38	0.0574	0.068	0.05	1.228
F7-12	0.0070	1.2	0.0102	17.71	0.0655	0.062	0.45	0.821
F7-13	0.0076	1.3	0.0105	17.21	0.0734	0.060	0.5	0.773
F7-15	0.0076	1.5	0.0113	15.88	0.0787	0.056	0.5	0.397
F7-17	0.0068	1.7	0.0126	14.28	0.0784	0.050	0.45	0.722
F7-20	0.0078	2	0.0134	13.45	0.0943	0.047	1	0.485
F7-24	0.0072	2.4	0.0153	11.73	0.0985	0.041	1	0.198

Table 4.1: Relevant parameters for the π flume experiments.

In each experimental run the following procedure was adopted.

First the bed was flattened to the prescribed value, saturated with a very low water discharge in order to have a smooth surface and then surveyed with the laser profile to check the initial conditions.

Water discharge was then set to the prescribed value. The free surface level was surveyed with the water gauge on ten locations along the 'Y' configuration.

During the run the water discharge flowing in the two downstream channels was periodically measured, gauging the water elevation in the downstream tanks. In addition a pressure sensor device automatically measured water depth in the right tank at 2-minutes intervals.

When flow configuration and bed topography reached an equilibrium configuration the run was stopped. Just before, the free surface level was gauged again and the sediments were collected in two different basins for each channel.

Finally bed topography was surveyed with the laser profiler, on a grid spacing 10 cm in the longitudinal direction and 1 cm in the transverse direction.

The runs characterised by the occurrence of free migrating bars behaved differently from those where bedforms did not generate. Indeed, the system did not reach an equilibrium configuration, as both flow distribution and bed topography showed an oscillating trend. The response of the system could either fluctuate around the symmetrical configuration or lead to the closure of one of

the two downstream branches.

The topography of the two downstream channels was analysed in order to highlight the difference in bed elevation at the upstream end, that invariably was detected when an asymmetrical equilibrium configuration was reached. Data concerning bottom elevation were analysed through a Fourier Transform procedure, in order to point out the presence of alternate bars and to assess the downstream and upstream influence that bifurcation exerts on the channel morphology.

4.4 Experimental results

4.4.1 Bifurcations configuration

The configuration of a 'Y' shaped bifurcation can be described referring to flow and sediment distribution and to the morphology of the two downstream branches. In the following this notation will be used: rQ is the ratio of the water discharges in the downstream channels (always defined such that $0 < rQ < 1$), rQs is the corresponding ratio of the sediment discharges, rs is the ratio between the slopes of the two branches and $\Delta\eta$ is the difference in bed elevation at the upstream end of the two downstream branches scaled with the mean flow depth of the incoming stream (referred to as 'inlet step' in the following).

The first set of runs clearly highlighted the existence of an unbalanced equilibrium configuration in which the flow distribution into the two downstream branches became fairly asymmetric. An example is reported in Figure 4.5 referring to run F3-21, in which the discharge ratio decreases from the initial balanced solution towards the asymptotic value of 0.56, reached after about 12 hours.

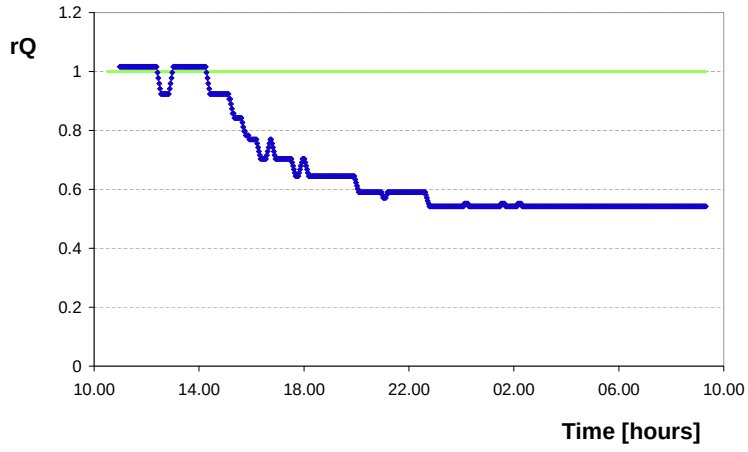

Figure 4.5: Run F3-21: time evolution of the discharge ratio rQ, as measured by the pressure sensor device.

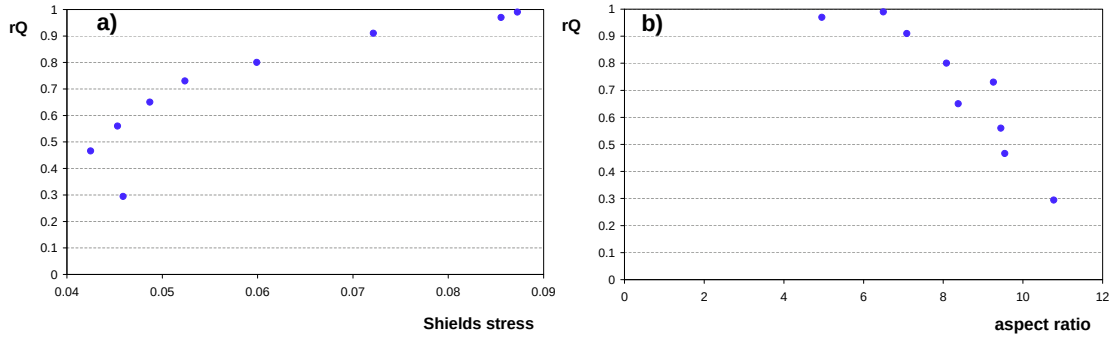

Figure 4.6: Discharge ratio *rQ* versus Shields stress (a) and width ratio (b) for the runs with bed slope equal to 0.003.

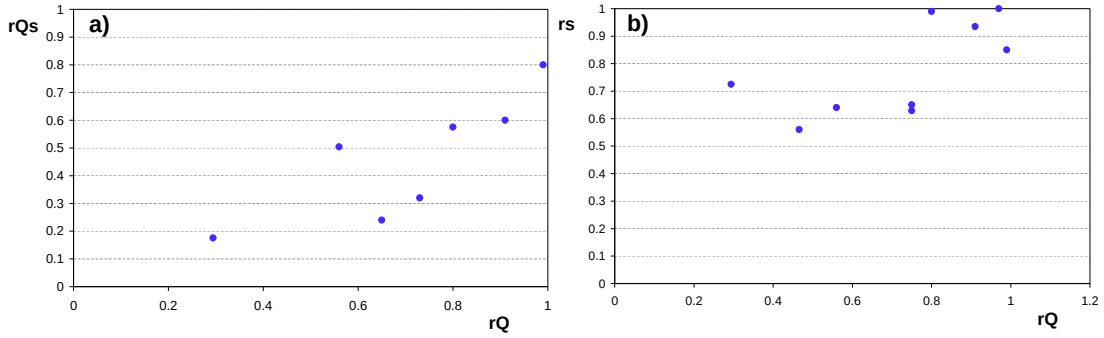

Figure 4.7: Sediment discharge ratio *rQs* (a) and slope ratio *rs* (b) as functions of *rQ* at equilibrium.

In Figure 4.6 the discharge ratio *rQ* is reported as a function of the Shields stress (a) and of the aspect ratio (b) for the runs characterised by a 0.3% slope. Note that *rQ* is in close relationship with the parameters of the incoming channel. For low values of the Shields stress and for high values of the aspect ratio, the symmetrical configuration has been found to be invariably unstable. One of the two downstream channels became deeper and carried a larger part of the total water and sediment discharge, even if the other one continued to be open and active.

A similar behaviour can be detected examining the ratio between the sediment transport rates. Figure 4.7 (a) shows the values of *rQs* as function of the equilibrium discharge ratio *rQ*: sediment discharges appear to be more unbalanced compared with flow distribution, due to the non linearity of the relationship between water and sediment discharges.

The analysis of the bed topography in the downstream channels also showed a difference in the slopes (Figure 4.7 b). In an unbalanced configuration the channel that carries a lower water discharge is generally characterised by a milder slope, while the other is steeper, so that the ratio between the slopes could reach values around 0.5 - 0.6 in the more unbalanced runs.

The description of the typical unbalanced equilibrium bifurcation is completed with the analy-

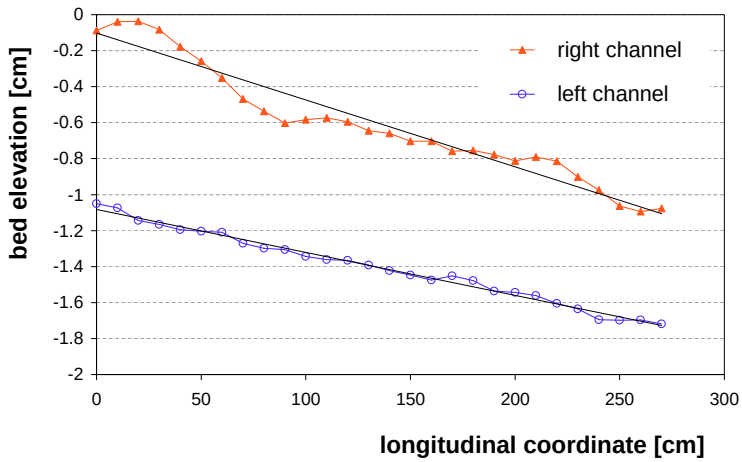

Figure 4.8: Sample longitudinal profiles of the downstream branches (run F3-21).

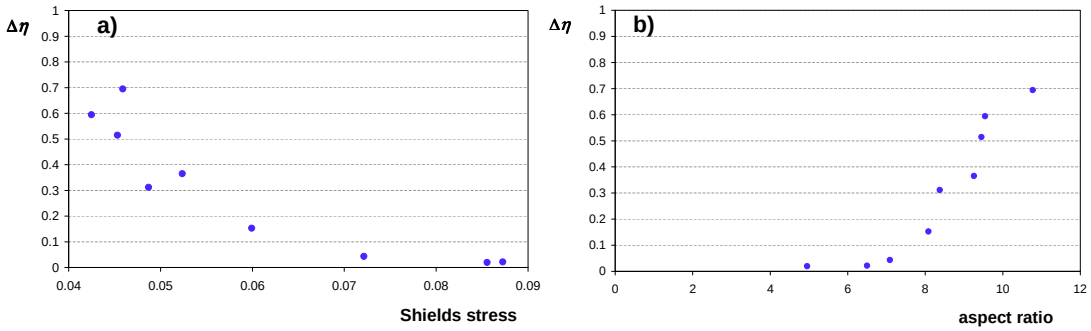

Figure 4.9: The dimensionless 'inlet step' Δη as a function of Shields stress (a) and width ratio (b).

sis of the difference in the bed elevation at the inlets of the two downstream branches: the channel carrying the highest water discharge is invariably the deepest at its upstream end. In Figure 4.8 the longitudinal bed profiles of the downstream channels for run F3-21 are reported; here the water was carried mostly by the left channel, with rQ reaching 0.56 at equilibrium. Two different methods have been used to determine the inlet step, that lead to closer results. In the first case Δη was determined as the average difference of the channels' bed elevations in a reach located immediately downstream of the bifurcation whose length has been chosen as about two times the downstream channel width. In the second procedure the longitudinal profiles of the downstream channels have been linearly interpolated and then Δη has been computed as the relative distance of these two lines at the bifurcation section.

All the morphodynamical properties defining bifurcation asymmetry has been found to be related with the flow parameters of the upstream channel. Namely, higher values of Δη correspond to lower values of the Shields stress and to higher values of the aspect ratio (Figure 4.9). Moreover it is worth pointing out that the relationship between the discharge ratio and the inlet step was found

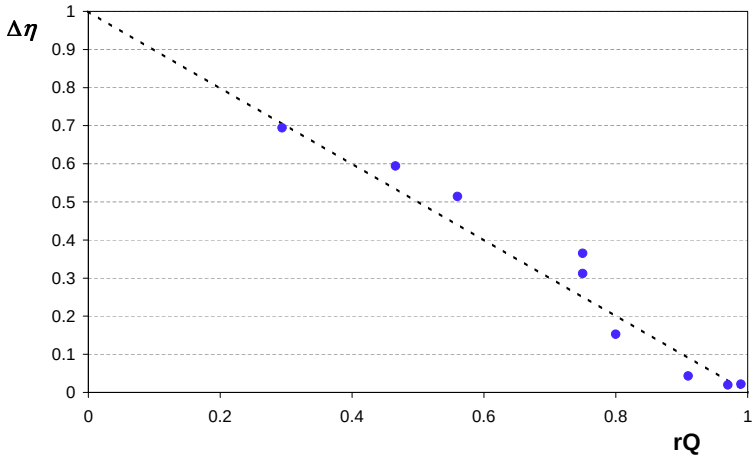

Figure 4.10: Relationship between the discharge ratio rQ and the inlet step $\Delta\eta$.

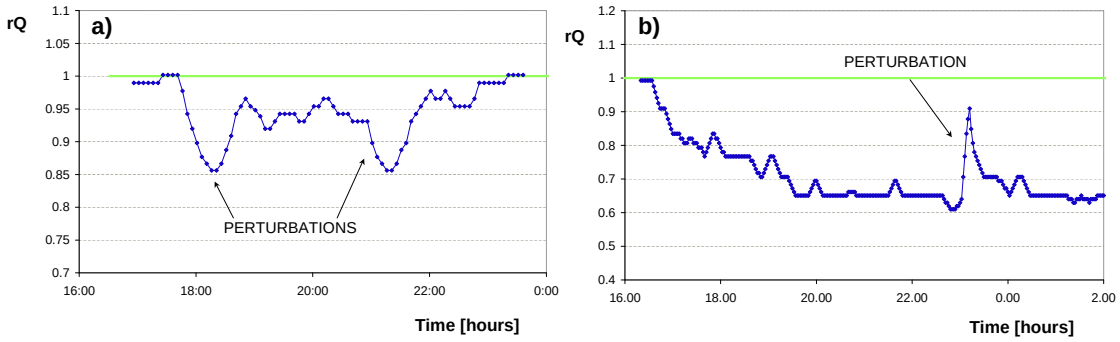

Figure 4.11: Two examples of a perturbation of the equilibrium in the case of symmetrical (a) and asymmetrical (b) configuration.

to be almost linear and well represented by the following simple relationship

$$\Delta\eta = 1 - rQ, \tag{4.1}$$

as shown in Figure 4.10.

To assess the stability of the reached equilibrium configurations both the flow and bed topography were modified by imposing an artificial perturbation. A fixed amount of sand was positioned at the inlet of one of the two branches, just downstream of the bifurcation, in order to partially close the channel. The sand accumulation suddenly modified the morphodynamic configuration of the system, but, as indicated by the behaviour of the discharge ratio (Figure 4.11), such variations were only temporary and after a short time lag, the system came back to the previous equilibrium stage.

4.4.2 The effect of bar migration on bifurcations configuration

The second set of experiments was characterised by a higher value of the longitudinal slope (0.007); hence, the same values of the Shields stress correspond to higher values of the width ratio. The threshold for the formation of free alternate bars was exceeded in all the runs and the development of regular trains of migrating bars was observed at the beginning of each run (Figure 4.12a). The presence of alternate sequences of scour and deposition caused a regular lateral oscillation of the main flow towards the left or the right bank, thus alternatively forcing unbalanced configurations of the bifurcation. This was associated with a regular fluctuation of the discharge ratio around equilibrium.

In Figure 4.13 two examples are reported: the first one shows a run with a high value of the Shields stress (F7-24), characterised by small oscillations around the equilibrium value of rQ. The discharge distribution keeps almost balanced and the presence of bar affects slightly the bifurcation configuration.

The second example (run F7-08, Figure 4.13b) shows an unbalanced run. The runs with lower values of the Shields stress and higher values of the aspect ratio were characterised by two different evolution time scales: the first one is related to the bar migration and it initially dominates; the second one represent the time requested by the system to reach the equilibrium configuration, characterised by the development of the inlet step. The presence of migrating, alternate bars further complicates the above scenario, causing a sudden instability of the bifurcation, especially for the

Figure 4.12: Pictures and bed topography maps of the upstream channel. Initially free migrating bars (a) and steady longer bars caused by the bifurcation (b).

runs characterised by unbalanced configurations. Due to bedforms migration the flow suddenly switch from one channel to the other, determining the closure and re-opening of the downstream branches.

As observed in the case of a bend of constant curvature connected with two straight reaches (Zolezzi et al., 2004), the lateral bed gradient due to the inlet step induced, for relatively high values of the width ratio, an upstream influence (see Section 2.4), that displayed itself with the formation of steady bars, whose wave length was equal to 1.5 - 2 times the length of the initial free migrating bars. Their presence was invariably observed associated with the migration of small, irregular fronts (Figure 4.12b).

The continuous interaction among free and forced bars prevented the system from reaching an equilibrium configuration. The amplitude of the fluctuations depends on the governing parameters and the bifurcation could be either characterised by an asymptotic value of the discharge ratio or switch continuously.

The choice of equilibrium parameters is less obvious in this continuously unsteady framework. Referring to the discharge ratio rQ the observation of the different evolution patterns suggested to choose unity as the equilibrium value for balanced runs (as F7-24 in Figure 4.13a) and to employ its minimum value when the bifurcation evolves asymmetrically (as in run F7-24 in Figure 4.13b). In this case the sudden switch between to unbalanced states induced by bar migration often corresponds to mirror solutions whereby the discharge ratio shifts between two reciprocal values.

The inlet step is both affected by the presence of migrating bars and by the upstream influence of the bifurcation. The computation of $\Delta\eta$ has been carried out both from the bed topography of the downstream branches (as reported in the previous section) and from the analysis of the cross sections located just upstream the bifurcation in the main channel. The amplitude of the steady bar in the upstream channel can represent a good measure of the inlet step, which has been calculated as the difference of the average level of the left and right sides of the above cross sections and

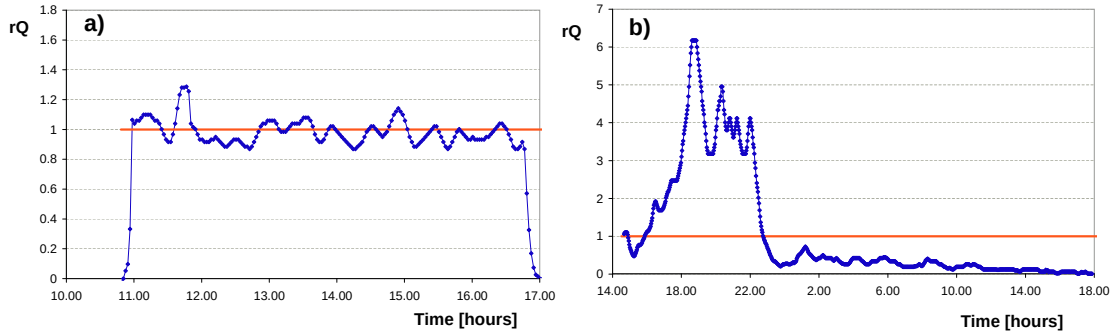

Figure 4.13: Two examples of runs affected by bar migration: (a) balanced run F7-24, (b) unbalanced run F7-08.

quantified through a Fourier analysis of each section as the amplitude of the first harmonic. The two methods showed similar results.

The best quantification of the inlet step has been chosen as the maximum between the results of the two methods. As expected from the theory on two-dimensional morphodynamic influence, the location of the maximum inlet step height moves upstream as the width ratio increases.

In Figures 4.14 and 4.15 the values of the discharge ratio rQ and of the inlet step $\Delta\eta$ for all the runs of the series with migrating bars are reported.

As observed in the first set of runs, a close relationship between the bifurcation configuration (described by rQ and $\Delta\eta$) and the flow parameters (Shields stress and width ratio) has been found. The trend looks less regular due to the presence of alternate bars and to the increased complexity in the choice of the significant values characterising the bifurcation. Two main differences between these runs and the first series are worth to be pointed out:

1. the combined effect of higher width ratios and of bar migration caused the closure of one downstream branch when the Shields stress fell below 0.06;

2. the amplitude of the inlet step has been found to be higher in the presence of bars, also exceeding unity.

The above observations could be explained considering that the presence of alternate bars enhances the asymmetry of bed configuration at the scale of bar migration even when the flow distribution at the bifurcation is balanced.

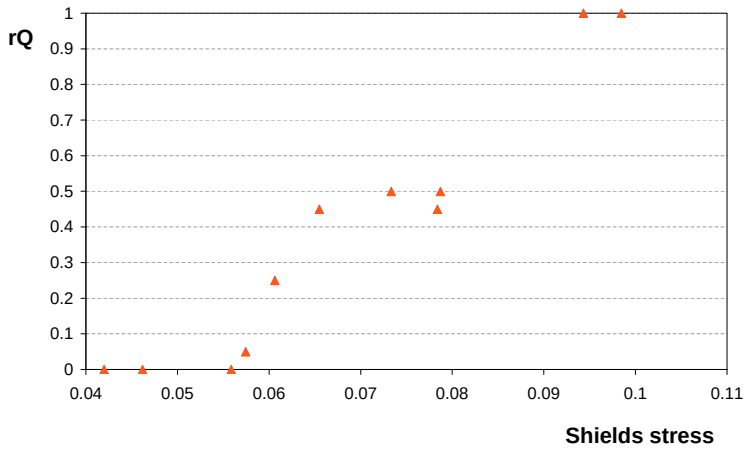

Figure 4.14: Discharge ratio in the downstream branches rQ as a function of Shields stress.

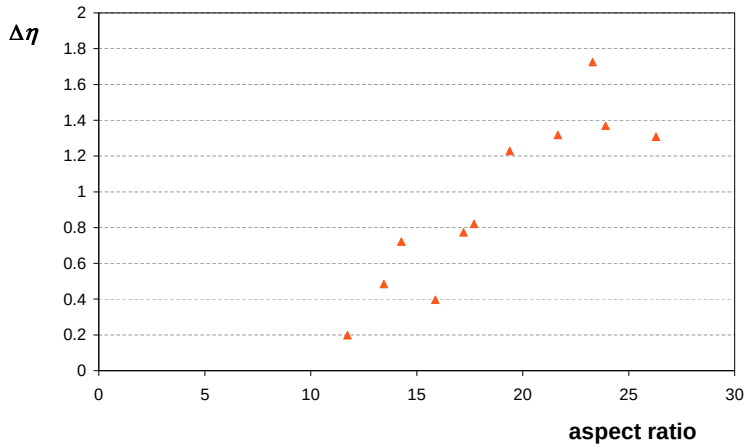

Figure 4.15: Difference in bed elevation $\Delta\eta$ as a function of the aspect ratio.

4.5 Discussion

The one-dimensional theory proposed by Bolla Pittaluga et al. (2003) invariably predicted the existence of unbalanced bifurcations for low Shields stress and high width ratio. The present experiments (see Chapter 7 for a comparison) confirm the existence of the proposed solution and definitely indicate how the equilibrium configurations depend on the relevant parameters of the upstream flow. While the one-dimensional model of Bolla Pittaluga et al. (2003) has the great advantage of predicting the equilibrium configuration of a Y-shaped bifurcation, more insight in the process can be gained from the view point of two-dimensional morphodynamic influence, whose theoretical framework provides possible explanations for the relevant physical mechanisms.

The experimental runs have been classified in sub and super-resonant, depending on the value of the width ratio of the incoming flow falling below or above the *resonant* value (β_R), originally discovered by Blondeaux & Seminara (1985).

In Figures 4.16 and 4.17 the discharge ratio rQ and the inlet step $\Delta\eta$ are reported as a function of the relative distance between the upstream flow and the resonant conditions. It appears that the sub-resonant runs generally correspond to balanced configurations, whereas super-resonant bifurcations are increasingly asymmetric.

An even more interesting fact is that the points of the two series merge in a unique curve. This implies that the relative distance from resonant conditions, $(\beta_R - \beta)/\beta_R$ is a suitable unified parameter to describe the dependence of bifurcation morphodynamics from the average parameters of the upstream channel.

Upstream influence occurring under super-resonant conditions is likely to enhance an initial asymmetry, hence consolidating an unbalanced configuration. The formation of a steady alternate bar upstream the bifurcation permanently deviates the main flow into one of the downstream

branches.

Similarly, a sub-resonant run is characterised on the average by a flat transverse bed in the upstream channel and therefore the bifurcation tends to keep balanced.

The present experiments suggest that further theoretical work is required in order to investigate how a perturbation of the initial symmetrical state is enhanced under super-resonant conditions and how this mechanism reinforces bifurcation asymmetry.

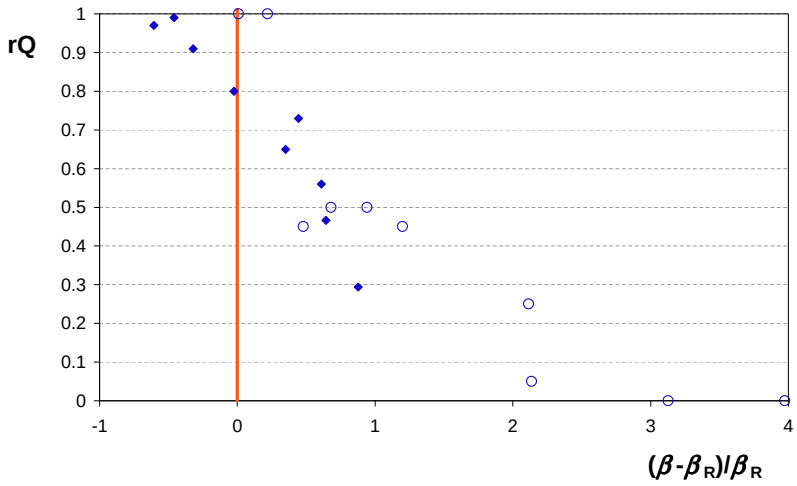

Figure 4.16: Discharge ratio in the downstream branches rQ as a function of the relative distance from resonant conditions.

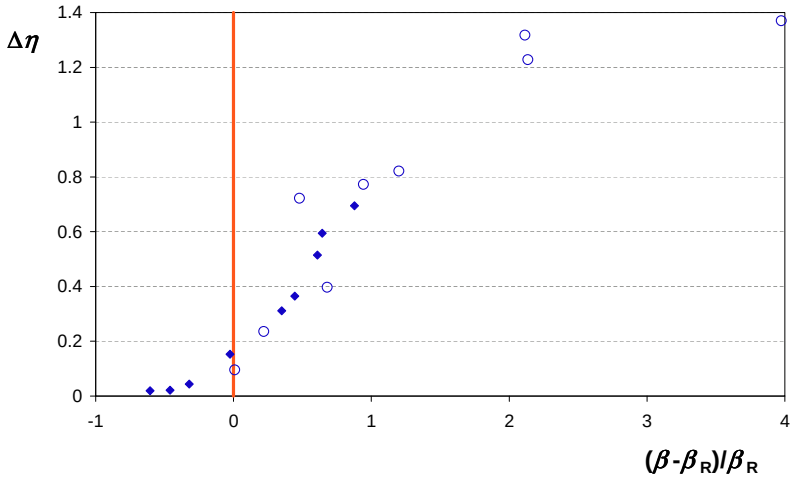

Figure 4.17: The inlet step $\Delta\eta$ as a function of the relative distance from resonant conditions.

5 Field measurements

5.1 Introduction

The dynamics of braided networks is characterised by strong fluctuations and interactions which occur at different spatial and temporal scales and lead to a continuous production and destruction of bar-channel complexes (Ashworth & Ferguson, 1986; Ashmore, 1991; Ferguson et al., 1992; Warburton, 1994). Both the altimetric and the planimetric pattern of braided streams may display frequent and fast changes. The dynamics of braided rivers is much more complex than the evolution of single channel streams, basically because braiding is determined by the interaction of several channel evolving laterally at a much more faster scale due to the almost cohesionless character of their banks (e.g. Figure 5.1). Field data and laboratory investigations suggest that both the number of channels and their position in the floodplain may vary over a timescale of the order of hours or days of the competent flow (Hoey & Sutherland, 1991; Warburton, 1996; Ashmore, 2001).

Understanding the morphological changes of such complex systems and their relationships with flow and sediment transport fluctuations preliminary requires the availability of detailed data from actual networks. The recent development of numerical models, in particular those physically based, claims distributed and detailed boundary conditions to be used either as input data or to

Figure 5.1: A proglacial braided river, Val Martello, South Tyrol, Italy.

validate the predictions of the models themselves. Moreover, specific field surveying is needed to validate theoretical and experimental results which have been recently obtained in the analysis of single unit processes, like bifurcations and bar-channel interactions, which can be seen as building blocks of braided networks (examples are reported in Chapters 2, 3, 4) (e.g. Repetto & Tubino, 1999; Bolla Pittaluga et al., 2001; Repetto et al., 2002; Bolla Pittaluga et al., 2003; Federici & Paola, 2003).

For these reasons, fluvial geomorphologists and engineers interested in the evolution of river networks must face the need of field data collection, that is often onerous. Data from the field commonly need to cover bed topography, grain size distribution, flow dynamics, water discharge and sediment load. Collecting such integrated data set on the relevant morphodynamical changes and describing in detail the dynamics of different branches require numerous teams that work for long periods of time. Additional difficulties arise also from the choice of the appropriate field site, that must combine a good accessibility and a morphodynamical scenario that has evolved under the least possible anthropic effects. Moreover, research in this field has been mostly carried out by scientific teams belonging to western and developed countries, where the number of naturally evolving rivers has been strongly reduced by the impact of river regulation works; the desired conditions are often met in regions located quite far from the usual working place.

In the last decades field activities have taken advantage from relevant innovations in monitoring techniques and in particular from the development of digital photogrammetry, remote sensing and flow measurements based on Doppler effect (Klaassen et al., 2002). Recently it has been demonstrated (Chandler et al., 2002) that high resolution terrestrial digital imagery combined with automated digital photogrammetry is able to supply terrain data with density unattainable by the traditional survey techniques. Difficulties posed by the long periods of time and numerous team required to collect integrated data sets have been reduced and the completeness of high quality field data is gradually increasing.

There are few field data on the bifurcation process in literature: Ferguson et al. (1992) reported the evolution of a *chute and lobe* unit of the Sunwapta River, Canada and showed how a sediment wave could affect the bed topography, inducing a modification of the water distribution in the two downstream branches. On a much larger spatial scale, but in a similar context, Richardson & Thorne (2001) described the flow field in newly formed bifurcations on the Jamuna River, Bangladesh. They pointed out that flow instability can generate a multi thread current and therefore it can trigger the bifurcation process.

The present Chapter describes some field activities that have been planned and carried out with the objective to monitor braided river reaches and to collect quantitative data on their morphology, both on a static and dynamic point of view. A specific aim has been the quantitative characterisation of channel bifurcations, describing both the flow field and the bed topography, in order to test

how theoretical predictions and the laboratory observations presented in Section 2.5 and Chapter 4 perform when applied to natural configurations.

Two field campaign were carried out in two different braided rivers.

1. The braided reach of the Ridanna Creek at Aglsboden, a small river in the North-East of Italy, that has been monitored in these years for the first time. The field activity involved the whole River Morphodynamics Research team of the Civil and Environmental Engineering Department to carry out the feasibility, preparation, planning, management and implementation phases of the field survey. The goal of the field campaign has been the morphodynamic characterisation of the whole network, together with a more detailed study of the configurations of channel bifurcations.

2. The Sunwapta River, Jasper National Park, Canada. The reach monitored in the summer 2003 has been already surveyed in the past years. The activity was carried out in the framework of an international research group directed by Peter Ashmore. This co-operation allowed a fruitful sharing of knowledge, field techniques and research activities developed in the different groups, as well as resources optimisation. Also in this case, the specific aim was to investigate the dynamics of bifurcations.

A braided system is characterised by multiple spatial scales, from the size of grains that represent the scale of many sorting patterns typical of gravel bed rivers up to the width of the whole braided belt, of the order of tenth single channel widths. This wide range increases the complexity of the field monitoring: a detailed survey is needed in order to capture local processes and morphological variations. Moreover the time scale of the morphological evolution could be very fast, with consistent planimetric and altimetric modification occurring in few hours. To collect a complete and up-to-date data set covering the wide range of relevant scales for a braided river is often a great challenge that becomes impossible if the largest spatial scale is of the order of kilometres as on the Jamuna River (Jagers, 2003).

A small network, as the braided reach of the Ridanna Creek at Aglsboden gives the possibility of performing a complete survey of the network, covering topography and flow field on a time scale compatible with the evolution time of the reach. From this point of view such a network can be viewed as a laboratory model at a natural scale.

In this Chapter the objectives, field sites and monitoring techniques of the field activities on the Ridanna Creek and the Sunwapta River are described. The analysis of the collected data are presented in Chapter 6 where the outcomes concerning both the morphodynamics of bifurcations and the description of the channel adjustment on the Ridanna Creek are discussed.

5.2 The Ridanna Creek

5.2.1 Study location

The Ridanna Creek is a pro-glacial gravel bed river in South Tyrol, North East Italy. The study reach lies in a glacial excavation plane (Aglsboden) placed at a medium elevation of 1750 m above sea level. It is located approximately 4 km downstream of the snouts of the Malavalle and Vedretta Pendente glaciers, immediately downstream of a steep reach, characterised by the presence of a series of falls. (Figure 5.2).

The braided reach is approximately 700 m long and the maximum width is around 300 m. At the upstream end of the study reach the river is confined to a single channel; braiding intensity increases along the reach. At the downstream end the stream is constrained by the morphology of the valley flanks and converges again into a single channel. The study reach could be divided into three main regions (see Figure 5.3).

- In the upstream portion (Region A) the river is almost confined to a single channel: bifurcations and consequent opening of new channels have occurred in the past only on a time scale of the order of ten years.

- The central region (B) is located immediately downstream, after a narrow transition zone in which a main bifurcation sets a sharp increase of the braiding index. Here the morphological activity is much more frequent and takes place every one or two years.

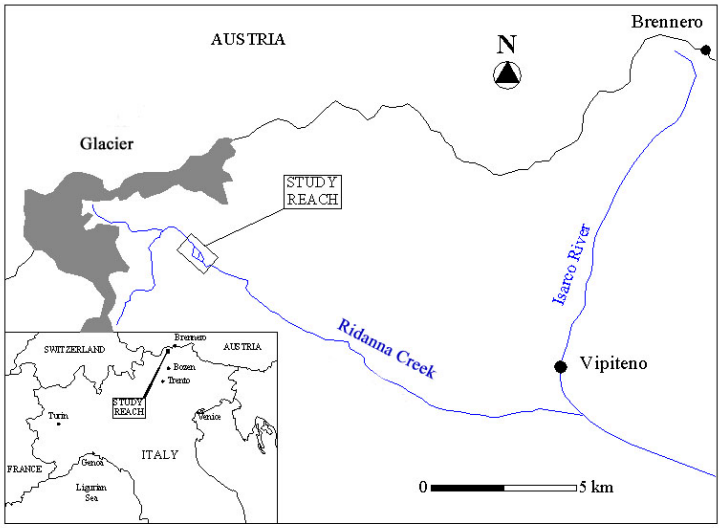

Figure 5.2: Study location map showing the field site on the Ridanna Creek.

- The third region (C) is close to the downstream end where the stream is constrained by the morphology of the valley flanks and it converges again into a single channel. This area can be also affected by the presence of a small dam that causes the formation of a basin when the discharge exceeds the threshold value of approximately 12 m^3/s.

At the study area the valley gradient is approximately constant and equals 2.2%. The bed material is mainly of gravel size, with cobbles and pebbles. The reach shows a significant decrease in surface bed material size in spite of the absence of relevant lateral tributaries and of the quasi constancy of valley slope. The above behaviour, which has been also detected in previous field measurements (Chew & Ashmore, 2001), can be related to the increase of stream width and braiding intensity along the reach. The mean diameter of the bed material ranges from 0.05 to 0.25 m, depending on the location along the reach and on the presence of finer depositional areas on the top of the bars.

The Ridanna Creek at Aglsboden is primarily fed by melt water coming from the Malavalle and Vedretta Pendente glaciers. Peak annual flows at Aglsboden occur from July to September, which may range up to $20 \div 25$ m^3/s. During this period flow discharge follows a daily cycle driven by solar radiation, with similar and predictable behaviour. Low flows occur in the period November to April due to the quasi absence of incoming flow from the glacier upstream: in this period the free surface is often frozen.

Basically this site has been chosen because it represent a rare combination of easy accessibility, low anthropic effects on river dynamics and good predictability of morphological movement. Moreover it offers the additional advantage of being surrounded by high cliffs, a condition that enables one to easily acquire remote sensing digital images with an inclination that is high enough to guarantee an accuracy of the order of the average grain size.

5.2.2 Description of the field measurements

In order to completely characterise the braided reach of the Ridanna Creek both from a static and a dynamic point of view, we decided to undertake a monitoring activity on a medium-long time span. Moreover recent survey techniques, as digital photogrammetry and remote sensing with thermal infrared data acquisition were tested. The rapidity and non-predictability of the morphological variations was faced with the installation of a continuously monitoring system consisting of an automatic digital camera and a pressure sensor device.

We have monitored the evolution of the Ridanna Creek at Aglsboden along two periods of potential morphological activity, from June to September 2002 and 2003. No relevant channel adjustment has occurred from August 2001 and July 2003, due to the weak snow precipitation in winter 2002 and the fairly low temperature in summer 2002. This relatively long period of

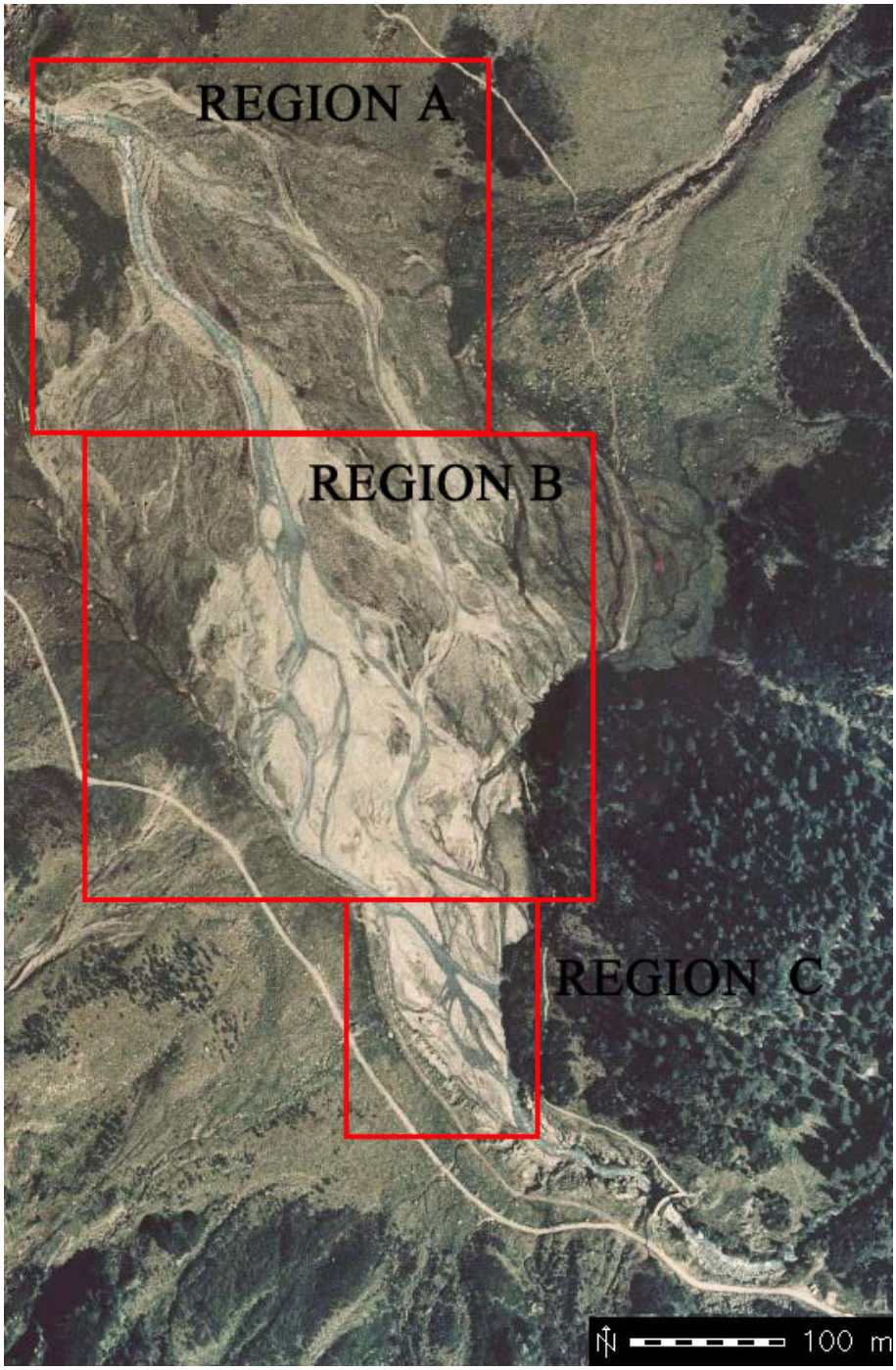

Figure 5.3: The braided reach of the Ridanna Creek at Aglsboden, with the three main morphological regions. (Aerial orthoimage referring to year 2000; courtesy of Bolzano local River Authority).

inactivity has been exploited to carefully characterise the *static* morphology of the braided reach.

The field campaign during summer 2002 was devoted mainly to the implementation of the monitoring techniques and to a initial network characterisation. In June 2003 a more specifically oriented activity has been carried out, lasting a whole week of measurements which required a group of 20 people. Besides the characterisation of the whole braided reach, the main bifurcations were surveyed in detail, in order to collect quantitative data on this unit process.

On July 28^{th} and August 29^{th} two intense rainstorms added a significant contribution to glacier meltwater triggering morphological changes in the central part of the study reach. In these conditions the water discharge was estimated to peak around 20 m^3/s. The main channel shifted laterally with bank erosion of several meters and the process determined the modification of bar structures in the central region of the braided reach (Figure 5.3).

The detailed analysis of the collected data is reported in the next Chapter. In the following the monitoring techniques are described and their strengths and weaknesses are pointed out.

- **Determination of a flow rating curve**

  A relatively stable cross section has been chosen to set a gauging station at the upstream end of the study reach where a pressure sensor device was placed to obtain a continuous measurement of the free surface level. The acquisition time step was set equal to 5 minutes. In the same section a flow rating curve has been obtained by means of direct discharge measurements through the salt dilution method. The salt concentration was measured using conductivity hand-held meters from both bank sides (Figure 5.4). Fitting the collected data held the following expression for the rating curve (reported also in Figure 5.5):

  $$h = 0.3129 Q^{0.39}, \tag{5.1}$$

  with h free surface elevation and Q water discharge.

  This relationship, coupled with free surface elevation data, has allowed to accurately reconstruct the time sequence of water discharge at the study site (Figure 5.6). Daily fluctuations with fairly regular trend were observed in the sunny days in both years, according to a cycle driven by solar radiation. Summer 2003 was characterised by an initial cold period with daily level fluctuations of about 0.1 m, corresponding to a discharge variations of about 3 m^3/s, while from late July to the end of August the amplitude of diurnal flow rate oscillations could reach even 10 m^3/s.

  Discharge measurements in a braided river is not a straightforward task. Difficulties arise from the high velocity of the flow that hinder direct velocity measurements with flow meters and from the presence of a multi channel pattern. The salt dilution method allows accurate

discharge measurements provided the transversal mixing of the salt is complete, i.e. the concentration is the same at both banks (see Figure 5.7). It is worth noticing that in our case this condition was achieved only thanks to the presence of a sequence of falls just upstream the study reach, that ensured a complete dispersion of the salt concentration cloud.

- **Discharge measurements at bifurcations**

  The hydrodynamics of bifurcations was characterised through discharge measurements in each channel of the single 'Y' configuration, in order to obtain the water distribution as a function of the free surface level. Three different techniques were employed:

  - the salt dilution method, when channel length was enough to ensure transverse mixing;

Figure 5.4: The conductivity meter.

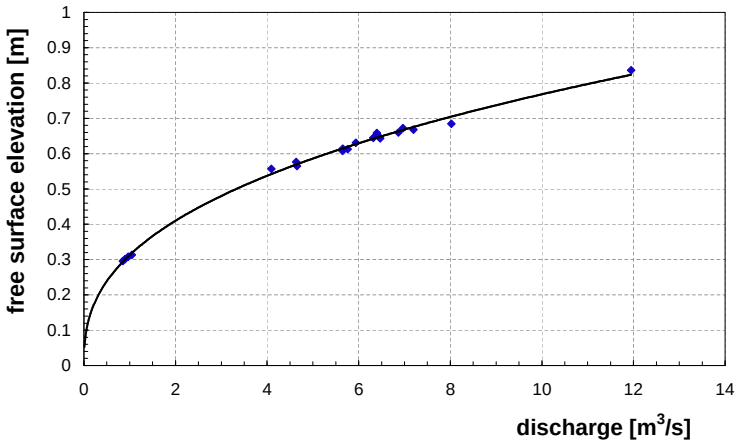

Figure 5.5: Flow rating curve of the Ridanna Creek at the gauging station located at the upstream end of the surveyed reach.

- velocity measurements with a 5 cm propeller current meter (Figure 5.8a);
- velocity measurements with an electromagnetic current meter (Figure 5.8b).

The velocity measurements were performed on a regular grid in each cross section, with a transverse spacing of 1 m. On the vertical direction the velocity was gauged at an elevation corresponding to 40% the water depth, when this was lower than 40 cm, or to 20%, 40% and 80% the water depth for deeper flows.

Data collected through the three methodologies showed a good agreement: measurements performed at the same time and location returned similar values of the total discharge and

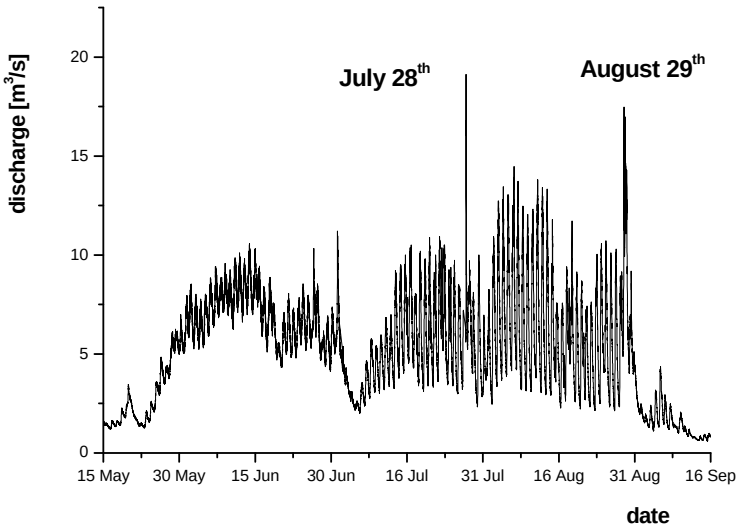

Figure 5.6: Recorded discharges during summer 2003.

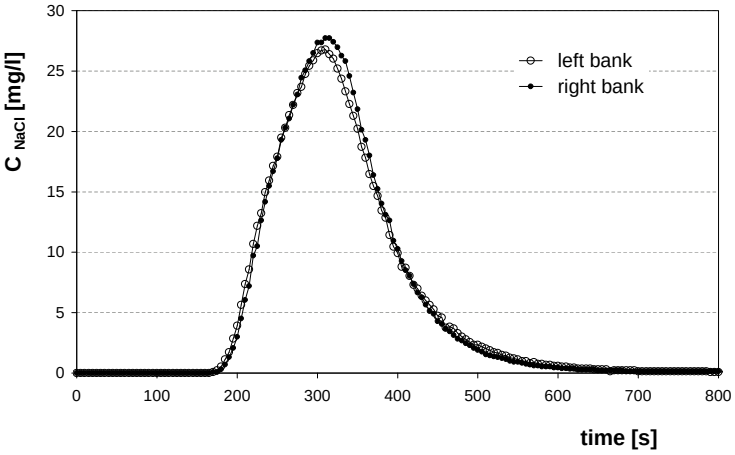

Figure 5.7: Concentration waves measured on the left and right banks. (Right downstream channel of bifurcation 2 in the Ridanna Creek, August 16^{th}. $Q = 0.22\ m^3/s$.

the sum of the downstream branches discharge well approximated to that of the upstream channel, with an error ranging between 1 and 10 percent. Velocity measurements in very shallow channels were less accurate, because of the presence of large pebbles which affect strongly the flow field and local velocity measures and due to local recirculations around larger grains; moreover a minimum depth is required by the instruments.

- **Grain size distribution measurements**

  Grain size measurements are needed to estimate the hydraulic roughness of the channel and to characterise the bed load sediment transport. The most used and suitable survey technique in gravel bed braided rivers is the Wolman Count (Wolman , 1954), a size-by-number method, with random sampling of surface particles. The particles were measured and classified through a standard *'gravelometer'*, as reported in Figure 5.9. Grain size sampling was carried out in different locations and revealed a strong non uniformity; besides an average

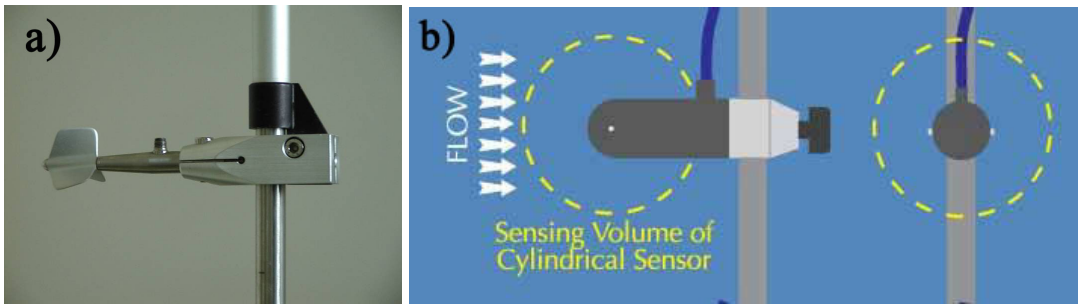

Figure 5.8: The propeller (a) and electromagnetic (b) current meters.

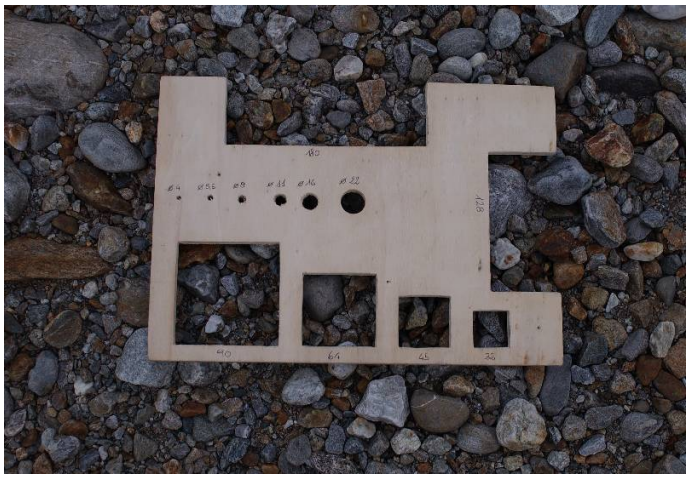

Figure 5.9: The *'gravelometer'*.

downstream fining the mean diameter of the bed material ranges from 0.25 to 0.05 m, depending on its location along the channel or banks regions and on the presence of sorting patterns driven by the morphology at different scales.

- **Digital images acquisition** A digital camera was placed on the cliff behind the study reach. The camera has been modified in order to automatically take pictures at prescribed hours during the day (every 4 hours in our case). In Figure 5.10 four examples with different values of water discharges are reported. The continuous acquisition of digital images allowed to reconstruct the planimetric evolution of the network and to relate channel adjustment to the hydraulic conditions. Moreover it is possible to analyse the relationships between relevant braiding parameters (as the total wet width and the braiding index) and the total discharge flowing in the network.

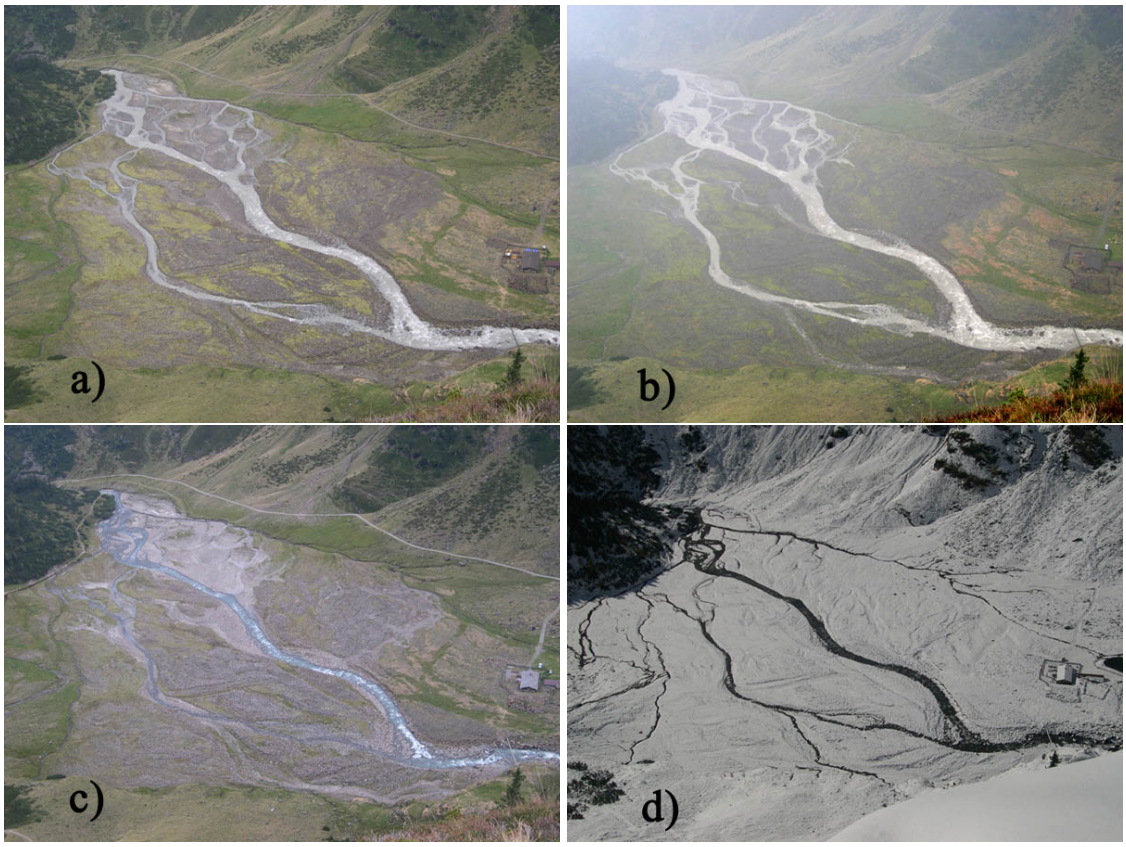

Figure 5.10: Images taken from the automatic digital camera. a) on August 14^{th} at 14.00, $Q = 8.0 m^3/s$; b) on August 29^{th} at 10.00, $Q = 10.4 m^3/s$; c) on September 2^{nd} at 18.00, $Q = 1.9 m^3/s$; d) on October 10^{th} at 12.00, $Q = 0.8 m^3/s$.

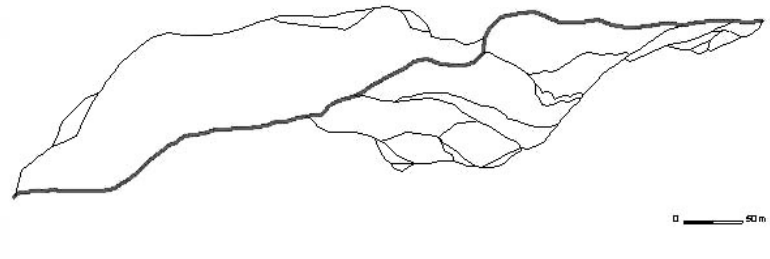

Figure 5.11: Planimetric configuration of the Ridanna Creek in June 2003.

- **Topographic survey**

  A complete map of the bed topography of the braided reach of Ridanna Creek was acquired during the field campaign, integrating traditional survey techniques with the automatism of digital photogrammetry. It is known that the application of digital photogrammetry to natural systems has opened new paths in the acquisition of geomorphic data. However, according to several contributions (Chandler, 1999; Chandler et al., 2002), traditional field survey methods are still required to provide surface data beneath the water surface and to guarantee accuracy checks for DEMs obtained with automated digital photogrammetry.

  Longitudinal channel bed profiles and cross sections were surveyed with a *Leica TPS 700* total station; in addition the free surface level along the network was surveyed. In Figure 5.11 the planimetric configuration of the network in June 2003 is reported. Traditional topographic measurements included 30 cross sections of the network located mainly in the central region; the longitudinal section spacing was 10 m. More accurate measurements were performed close to the selected bifurcations.

- **Photogrammetric measurements**

  Digital photogrammetry was used to automatically extract DEMs and digital orthophotographs (i.e. planimetrically true images) of the monitored reach. Digital images were acquired using a Nikon D1x digital camera equipped with 60 mm and 85 mm lens. Three camera stations were selected on the steep cliff on the right side of the braided reach, 150 m above the centreline of the main channel (Figure 5.12a). Every image captured with the 60 mm lens covered a 200x300 m surface; hence, it was possible to acquire the entire monitored reach with a strip made of two images from both the camera stations used. With the 85 meters lens 4 images were necessary, but a higher accuracy was achieved. This configuration provided appropriate stereo coverage for the desired site with a geometrical accuracy of 0.055 m.

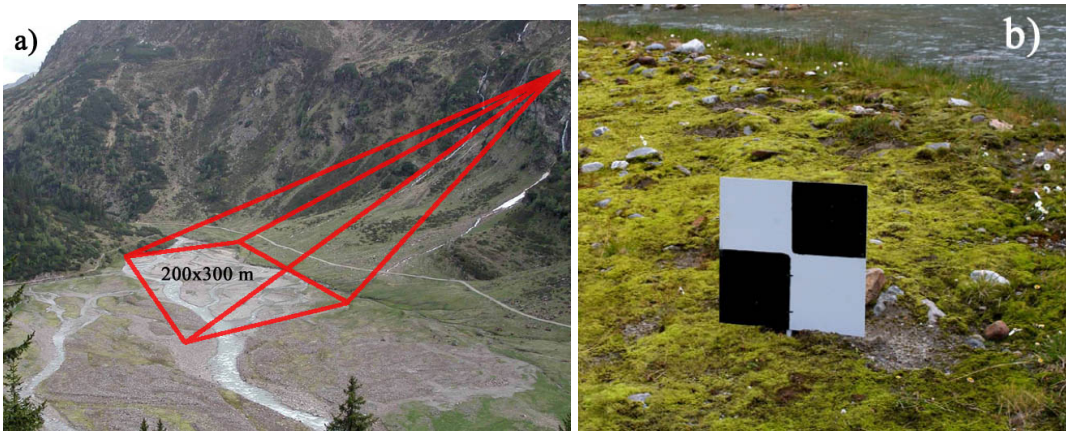

Figure 5.12: Location of the camera station and area covered by the photogrammetric survey (a) and control target (b).

Further bed monitoring has been carried out using the total station. It consisted of measuring 300 points disposed on a regular grid covering an area of 250x180 m. Eighty photo-control targets were disposed throughout the monitored reach to provide the required information for the orientation of digital images. They consisted of black and white painted boards with dimensions 0.5x0.5 m, attached to the stream bed surface through steel bars (Figure 5.12b). The ground coordinates of the photo-control targets were surveyed using the Leica Total Station. The accuracy of each control point was approximately $\pm$ 0.05 m.

To establish the interior and exterior orientation parameters of the acquired digital images the digital photogrammetric system ERDAS® IMAGINE OrthoBASE Pro^{TM} was used. The system provides these parameters for one or more images in a block using an approach denominated Self Calibrating Bundle Block Adjustment, with root mean square errors comparable with that of a tested independent self-calibrating approach (Chandler et al., 2003). Once the orientation parameters of a stereo-pair are established, OrthoBASE Pro^{TM} generates DEMs automatically. Two digital elevation models representing the braided dry reach of Ridanna Creek were generated at a ground resolution of 0.5 m and merged together using the Erdas IMAGINE® DataPrep.

The comparison with the independent data set collected via traditional surveying shows that root mean square accuracies of 0.25 m in elevations have been achieved: this may be seen as a satisfactory outcome considering that is comparable to the reach-averaged grain size. Finally, the photogrammetric DEM was merged with the ground survey data representing river bed topography. The final product is shown in Figure 5.13.

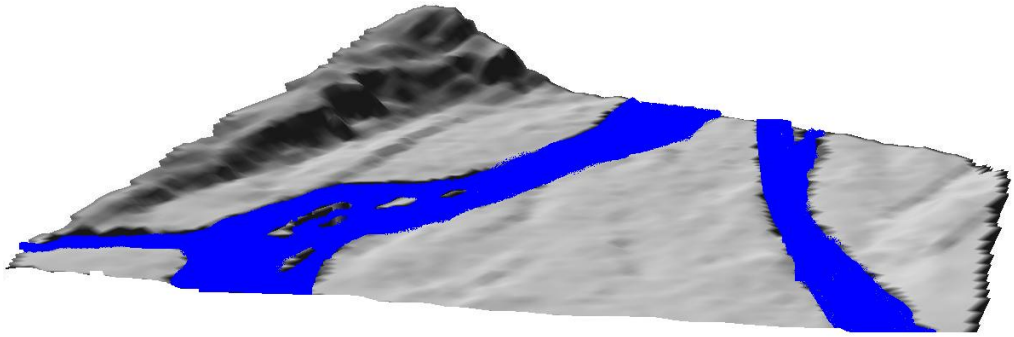

Figure 5.13: A three-dimensional view of the DEM obtained with the digital photogrammetry. Downstream region of the Ridanna Creek, summer 2003.

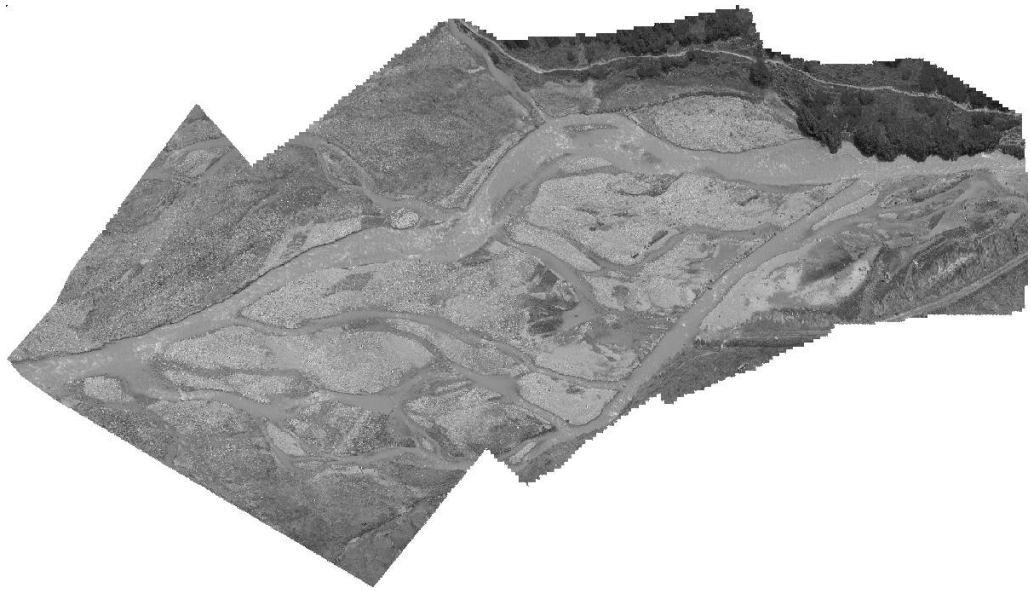

Figure 5.14: Orthoimage of the central region of the study reach.

Once the topographic relief was known, the geometric distortion inherent in imagery was removed using the Ortho Resampling process of OrthoBASE Pro^{TM}. Hence, a planimetrically-true image of the monitored braided reach was obtained, representing ground objects in their true, real-world X and Y positions (Figure 5.14). Such a map may help in monitoring the daily and seasonal planimetric evolution of the network and provides relevant morphological parameters of the network itself.

- **Thermal infrared image analysis**

  Groundwater flow is an important ingredient of braided rivers and paleo-river beds may be typically active under the ground surface due to their high permeability; their analysis can supply useful information on the long term planimetric evolution of the network. These gravel bed channels are not wet because they are filled by sedimentary particles or could be activated by higher discharges; their identification is possible with remote sensing techniques that capture mass properties, like temperature and thermal conductivity. The result is an immediate distinction between wet and dry areas that enables the determination of the groundwater flow pattern and a partial post rebuilding process of previous planimetric network configurations.

  The spectral ranges chosen for the survey were the visible and the thermal infrared band. They were acquired with a Kodak DC 290 digital camera and through a thermograph, respectively. The resulting thermographic image (Figure 5.15) shows many coherent patterns on the dry bed surface characterised by lower temperatures than the surroundings, which can be easily recognised as preferential flow patterns active under the ground surface that could be related with paleo-river beds or with channel active only for a higher discharge and presently characterised by subsurface flow. In Figure 5.15 regions characterised by lower temperature are represented with a darker gray tone; water is colder than the surrounding dry areas. In order to assess the effectiveness of the procedure a comparison was made between the estimated distribution of paleo-river beds obtained from the images taken during the field campaign (summer 2002) and that resulting from an image in the visible band taken in June 2001.

  The analysis of the texture and the radiance properties of the image pixels also enable to

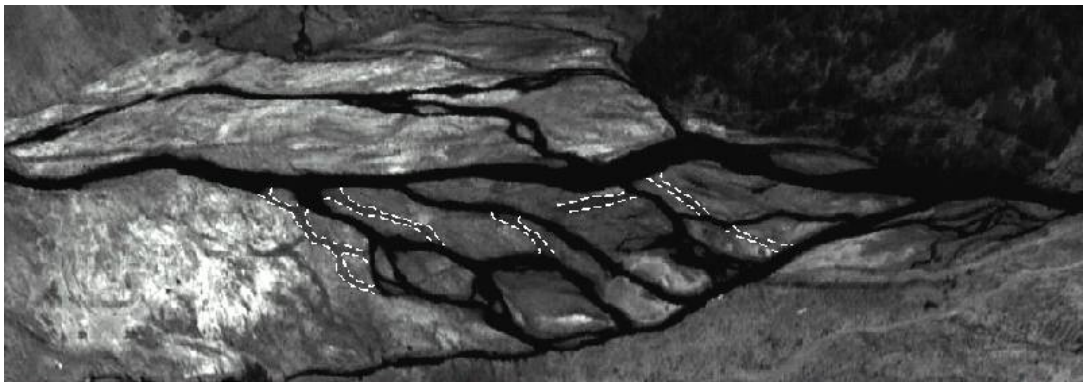

Figure 5.15: Planimetric configuration of the Ridanna Creek in July 2002, acquired with the thermograph. White dash lines represent the paleo-river beds.

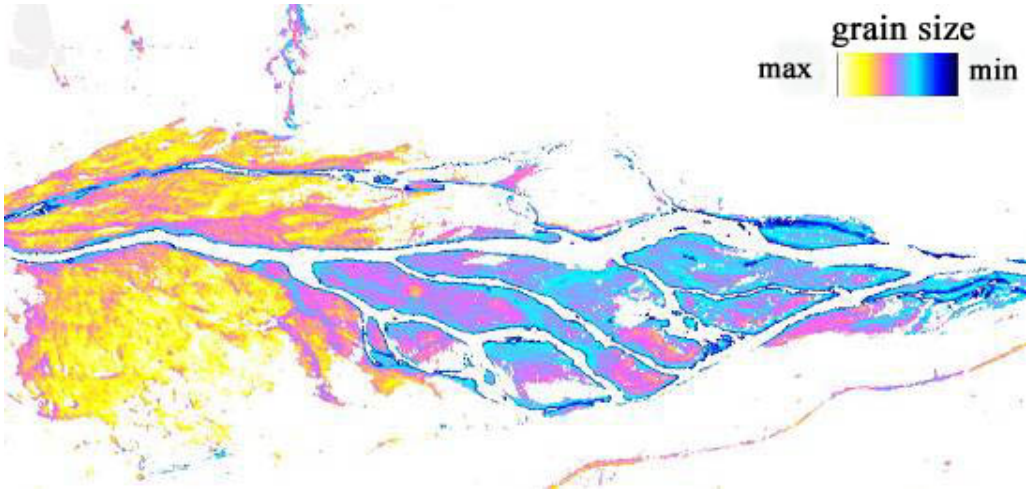

Figure 5.16: Map of the study reach in which the color scale is related with the grain size.

collect distributed information on the mean sediment grain size. Figure 5.16 reports a qualitative map in which the longitudinal sediment fining along the network is pointed out.

5.3 The Sunwapta River

5.3.1 Study location

The second field site was on the Sunwapta River, in the Jasper National Park, Alberta, Canada (see Figure 5.17). This river was subject to a series of studies and surveys in the past years, thanks to a particularly favourable combination of accessibility and good predictability of morphological changes during the summer melting period (Ferguson et al., 1992; Goff & Ashmore, 1994).

The Sunwapta River comes out from the Athabaska Glacier snout and immediately downstream forms the Sunwapta Lake, a proglacial lake originated in the early 40's due to the ice recession. In the first kilometre the river was channelised in a straight and incised bed, in order to rectify the Icefield Parkway; 1100 m downstream it is reached by the melt-water stream of the Dome Glacier and 250 m downstream it starts to braid. Historically the lack of coarse sediment accumulated in the lake and the rectification consequent to the highway construction affected the braiding index of this reach, determining a decrease in the upper part (due to the incision of the main channel) and an increase further downstream (Chew & Ashmore, 2001).

The study reach (Figure 5.18) is located approximately 3.5 km downstream from the glacier and has a longitudinal extension of about 150 m. The area shows an evident braided pattern, with a braid plane width of around $100 \div 150$ m and unvegetated bars in between the channels. The reach is characterised by a constant discharge (there are no tributaries), fairly homogenous slope and sediment diameter: the mean valley slope is 1.5% and the bed material is mainly of gravel size, with pebbles: typical diameters are d_{50} of 0.04 m and d_{90} of 0.11 m.

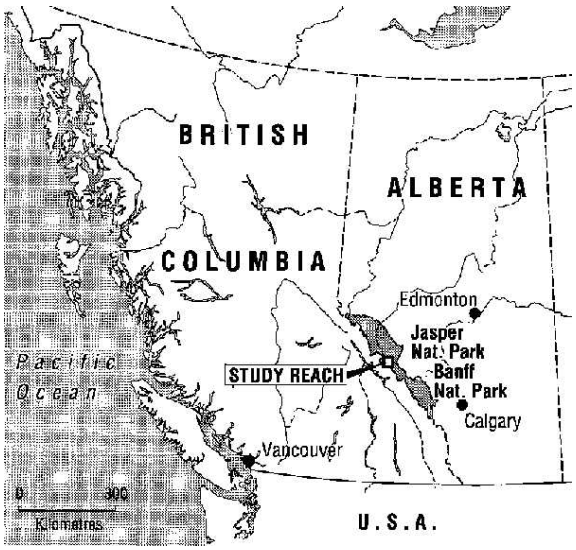

Figure 5.17: Location of the Sunwapta field study.

Figure 5.18: View of the study reach from the cliff on the right side of the river.

In the summer period the flow discharge follows a daily cycle driven by solar radiation, with similar and predictable behaviour. Low flows occur from October to May due to the quasi absence of incoming flow from the glacier upstream: in this period the free surface is often frozen. This site offers the additional advantage of being surrounded by high cliffs as well: this allows for the acquisition of digital images leading to good accuracies in the process of their orthorectification.

5.3.2 Description of the field measurements

The field measurements included both a survey of the whole braided reach and more local analysis concerning peculiar unit processes as channel bifurcations and path lengths of the sediment transport. Except for this last task, carried out by the Austrian group directed by Helmuth Habersack (Universität für Bodenkultur, Wien), the instruments employed and the monitoring techniques were very similar to that of the Ridanna field campaign. In the following a brief review of the field work is reported.

The network configuration was characterised with surveying 13 cross sections, around 12 m apart along the flow direction, with a transversal spacing of the measurements of 1 m. The survey was performed both with an automatic total station and using two levels; the measurements were repeated daily in the morning, at low flows, in the period from July 23^{rd} to August 4^{th}, 2003. In addition to the bed elevation, the free surface level was measured for each wet channel of given cross section. In this way the data provided an estimation of the free surface slope and could be

Figure 5.19: Orthoimage of the study reach taken on July 26^{th}.

Figure 5.20: The UDG station used for free surface level measurements.

used to calibrate a hydrodynamical numerical model of the network.

To characterise the planimetric configuration of the study reach, both digital and slides pictures were taken from the cliff in the right side of the river; two camera stations were placed around 120 m above the braid plane. The images were then automatically orthorectified in order to allow geometrically correct measures (an example is reported in Figure 5.19). To achieve this goal 27 photo control target were displaced throughout the study reach, consisting in 30 x 30 black and white boards, accurately surveyed with the total station. The orthorectification process was performed with the same software and methodology as reported in the previous Section.

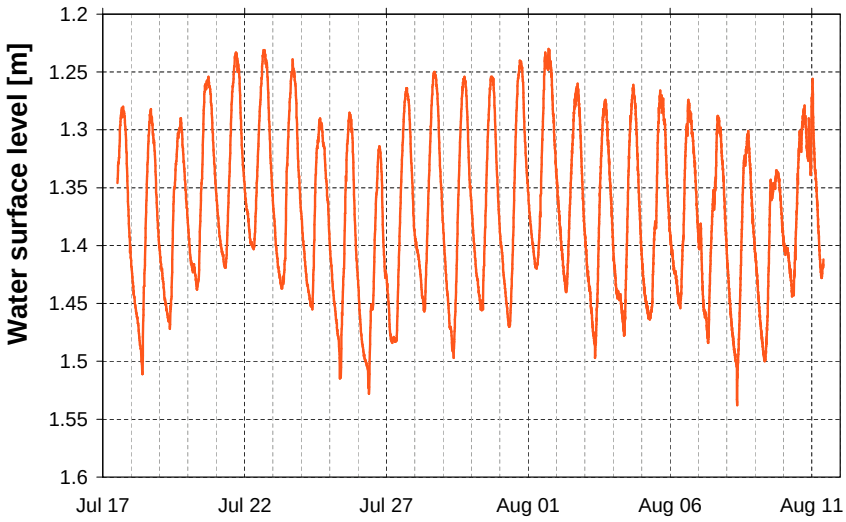

Figure 5.21: Free surface level at the UDG station during the field work.

A gauging station was established upstream of the study reach, immediately downstream of the Dome confluence, where the Sunwapta is a single thread river (Figure 5.20). The free surface elevation was measured through an Ultrasonic Distance Gauging device (UDG) and was collected every half an hour, automatically correcting the effect of air temperature. During the survey period the water level displayed a fairly regular daily cycle driven by solar radiation. Water surface daily oscillation was around 0.15 - 0.2 m, in close relationship with the air temperature. Figure 5.21 showes the water surface level as registered by the UDG station (the measure is reported as the distance between the instrument and the free surface); it is worth noticing that all the flows in the measurements period were generated by snow and ice melting, except for the last day, when a storm occurred.

In order to characterise the hydrodynamical parameters of the flow during the whole field measurements it is important to provide a continuous discharge gauging. This was obtained converting the free surface measurements by means of a stage discharge relationship. A series of velocity measurements were performed: four flow meters with 5 cm diameter propellers were used to determine transverse velocity profiles. The flow velocity was measured at an elevation of 40% the flow depth, in all the channels across a transverse section.

The above measurements were performed under different flow conditions, covering as much as possible the observed discharge range. Figure 5.22 shows the measured points, compared to the UDG data converted into discharge. The stage discharge relationship reported in Figure 5.23 displays (in the range of interest) an almost linear trend and could be fitted by the following expression:

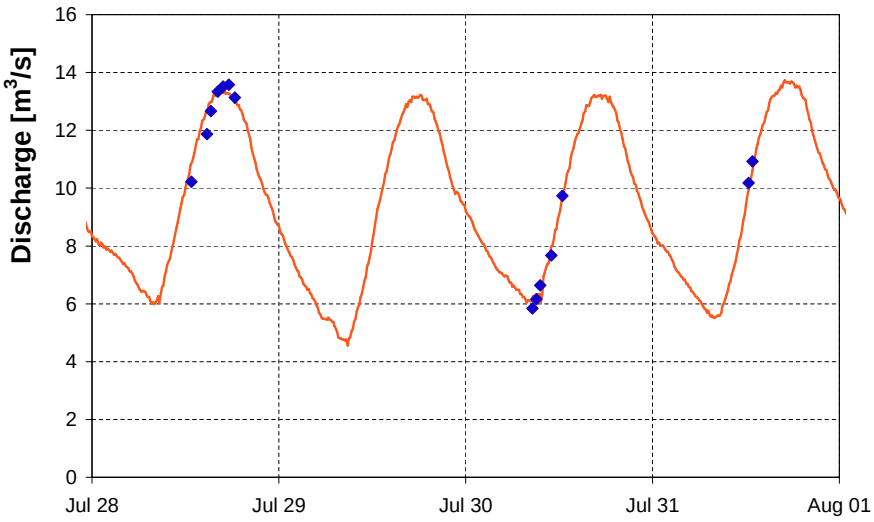

Figure 5.22: Values of discharge measured with the propellers (close symbols) compared with the UDG gauging converted into discharge (solid line).

$$Q = -35.74h + 58.07, \tag{5.2}$$

where Q is the total water discharge and h is the free surface level as measured by the UDG station.

Equation 5.2 is valid in the range between approximately 6 and 14 m^3/s. At lower flows this relationship could underestimate the water discharge, which, however fall below the threshold for sediment transport and are not relevant for the present study. In order to correctly relate the velocity measurements to the free surface level it is important to estimate the time delay between the two gauging points. Actually the UDG station was about 2.4 km upstream the study reach. The migration speed of the diurnal flood wave was determined by setting another ultrasonic device just upstream the surveyed area and comparing the two plots. The time delay was found to be approximately 25 minutes, on the average for the different discharge values.

The bed material grain size distribution was determined through random sampling of surface particles, collecting around 100 pebbles per location, in different channels along the reach. The size-by-number method proposed by Wolman (Wolman , 1954) was used, and the mean diameter of the particles was determined using a "gravelometer". The analysis revealed a fairly constant grain size distribution: no longitudinal fining was observed. Different samplings showed a mean diameter ranging from 35 to 50 mm, depending on the location in the network: finer material was generally found on bar deposits and in the left part of the network, where the channels were smaller.

Other characteristics of the network were assessed with qualitative observations, namely the

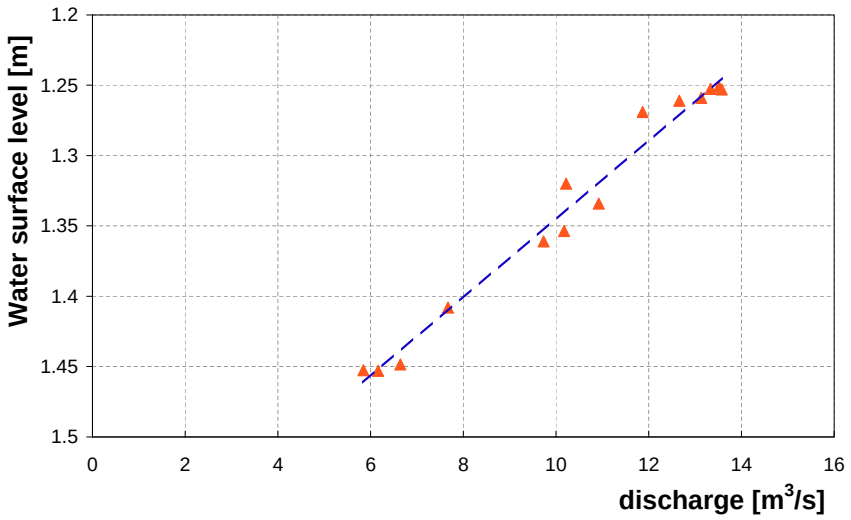

Figure 5.23: Rating curve of the Sunwapta River at the UDG station.

presence and structure of bars, channel morphodynamics activity and the intensity of sediment transport.

The data collected allow to characterise the whole network and to describe general features of a braided stream as the relationship between discharge and total wet width. It is also possible to assess how the active braiding index (defined considering only the channels transporting sediments) can be employed to describe a braided network, how it is related to discharge and whether there is some correlation between the activity of the channels and their slope and grain size, compared to the network averaged values.

Finally, more specific data were collected, with the aim to describe two main building blocks of a braided stream, as bifurcations and path lengths associated with sediment transport. The first objective was achieved through more refined topographic measurements of 4 bifurcations inside the reach and quantifying the discharge distribution in the two downstream branches. This analysis is reported in detail in the following Chapter.

The path length investigation was carried out by following a series of particles that has been modified with the insertion of a radio transmitter. The aim was to obtain information about the critical conditions for sediment transport (at which discharge pebbles start to move), the corresponding duration of particle moving and the length of each path. The detailed analysis of such processes is not object of the present work and the interested reader is referred to Habersack (2001) for further information on the survey methodologies.

6 Morphodynamics of natural bifurcations

6.1 Introduction

Detailed field analysis on bifurcation process are still lacking, in spite of the importance of this unit process in controlling the evolution of the network. The field activities carried out in the context of the present work allowed to describe morphologically and hydraulically the equilibrium configuration of a series of natural bifurcations and therefore the discharge distribution along the monitored networks together with sediment mobility of the channels. It was possible also to observe how the modification or the occurrence of a bifurcation can trigger the complete readjustment of channels and nodes. If the evolution of a single channel is quite accurately predictable, at least on a short and medium time scale, the effect of an unstable bifurcation that determine channel formation and/or obliteration of a channel is not completely understood yet. Modelling this fundamental process is a challenge for research on braided rivers: it is the main missing ingredient that can improve significantly the predictability of braided system evolution through mathematical models.

In this Chapter the results of the field investigations on 9 bifurcations observed on the Ridanna Creek and on the Sunwapta River are reported. The first section is devoted to the detailed analysis of the equilibrium configurations of bifurcations, pointing out common features and recurring elements. In Section 6.3 two events are analysed (one on the Ridanna and one on the Sunwapta) in which morphological changes of the network were observed and in each case the dynamics of bifurcation is examined. Finally, Section 6.4 describes channel adjustment of the Ridanna Creek at a wider spatial scale, investigated through the analysis of aerial images available for the latest 20 years. It is pointed out how the morphology of a braid plane can affect the occurrence of bifurcations and, vice versa, how bifurcations strictly control the evolution of the network with particular effect on the longitudinal variation of the braiding index.

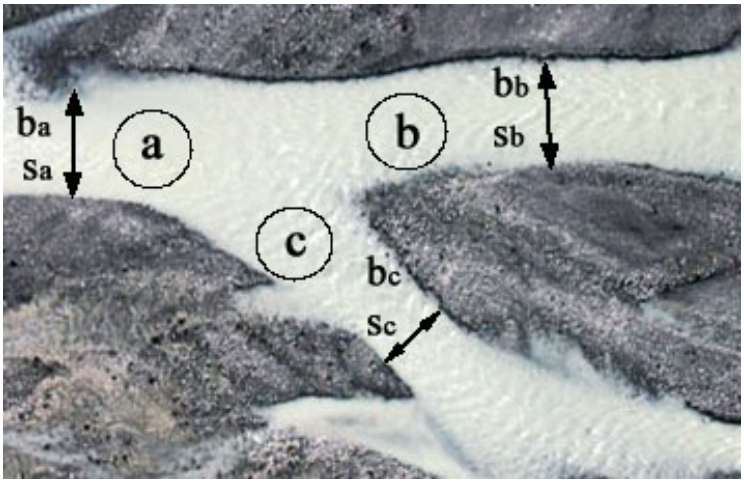

Figure 6.1: Sketch and notation of a bifurcation. *b* is the channel width, *S* the longitudinal slope.

6.2 Bifurcations morphology

Measurements on bifurcations were carried out both on the Ridanna Creek and on the Sunwapta River with the same general objective and the same monitoring techniques. The results are reported here together, pointing out the common and recurring features characterising the natural bifurcations.

A topographic survey has been employed to measure both longitudinal bed profiles and cross sections. In this case the spatial scale is the single channel width (ranging between 5 and 15 m) and therefore the cross sections spaced longitudinally 3 to 5 m. The discharge partition was also monitored through velocity measurements, thus obtaining information on the flow pattern.

In the following the same notations as in the theoretical analysis (Section 2.5) and in the experimental investigation (Chapter 4) will be used. Each bifurcation is represented by a Y-shaped configuration, where the upstream channel is marked with the letter 'a', the main of the two downstream branches with 'b' while 'c' is the third one (see Figure 6.1).

The observed bifurcations displayed several recurring elements. A first common feature is the asymmetry of discharge partition in the two downstream channels. Measurements performed at both low and high flow conditions invariably showed an unbalanced distribution of water discharge, with ratios ranging from 0.1 (in most of the Ridanna bifurcations) to 0.7 in some locations observed on the Sunwapta River. Downstream channel widths are also unequal, even if less unbalanced, with ratios ranging from 0.4 to 0.9.

Another repetitive aspect is the location of bank erosion that is always observed along the main channel downstream. In particular the outer bank (with respect to the bifurcation region) is always much steeper and higher than the others, this indicating lateral erosion in this area. The steep bank

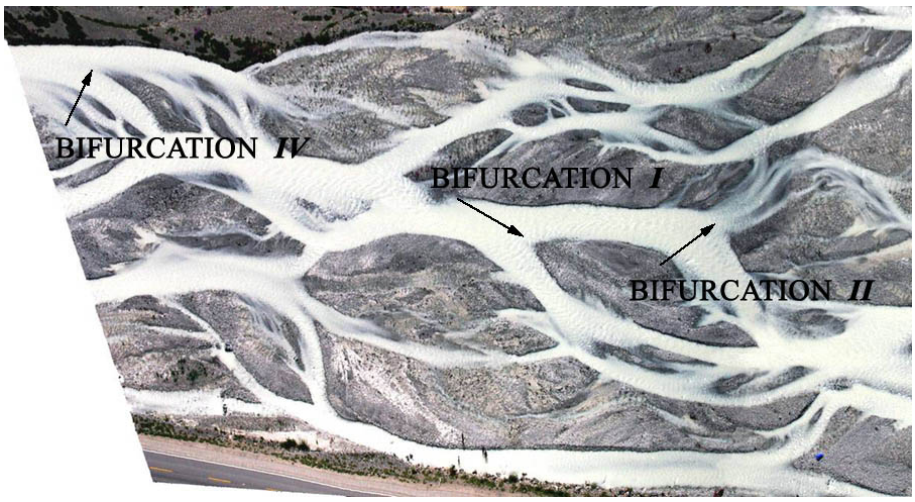

Figure 6.2: Location of the three monitored bifurcations on the Sunwapta River (orthorectified image taken on July, 26^{th}, 2003).

often extends upstream in the incoming channel over a length of some widths.

A third recurring feature is revealed by the analysis of the longitudinal profiles: the average slope of channel *a* is locally reduced in the bifurcation region, while a locally much steeper slope establishes immediately downstream in the channel where the main stream is flowing (channel *b*). As a result, the inlets of branches *b* and *c* exhibit a difference in bed elevation that is of the order of the main channel depth.

The latter observations suggest that 1D effects are likely to play a crucial role in determining bifurcation geometry, namely the longitudinal profiles of individual channels. Flow direction and partition in the downstream branches, playing a feedback effect, affect the morphodynamics of the bifurcation itself. Nevertheless, channel bifurcations can be also dominated by 2D effects, as the presence and migration of alternate bars (see Chapter 4 and Section 6.3).

A brief description of the measured bifurcations is now reported. During the field work on the Sunwapta River three bifurcations were surveyed in detail: they were named number *I*, *II* and *IV* (Figure 6.2).

Number *I* is the main bifurcation in the study reach; the upstream channel carries approximately the 65% of the overall discharge; in this channel most of the sediment transport occurred and planimetric and altimetric changes were observed to take place mostly here. Bifurcation *II* is located immediately downstream of *I* (channel *II*a is the same as channel *1*b); it is markedly unbalanced: the left channel is carrying around one quarter of the discharge in the channel *b*. Channel *II*c is very shallow and is located on the external bank of channel *II*a; it appears as the result of an overtopping of the external bank of the bend. The angle between the two downstream branches

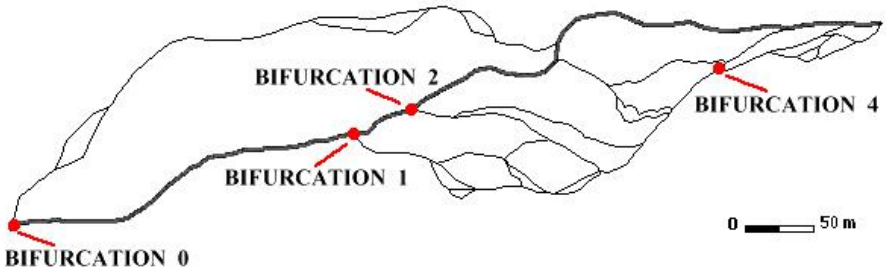

Figure 6.3: Location of the four monitored bifurcations on the Ridanna Creek.

is quite large, around 72 degrees. The third bifurcation analysed (number *IV*) is the smallest one: the discharge is around the 30% of the total; it was not included in the area covered by the daily surveyed cross sections, but it clearly displayed most of the common features observed in the other bifurcations.

Measurements on bifurcation *I* and *II* were repeated 6 times, from July 22^{nd} to August 1^{st} with different values of the total discharge flowing in the network. The aim was to assess the response of bifurcations to different flow conditions and to monitor possible planimetric and altimetric changes. It is worth noticing that channel *II*c is almost dry for low values of total discharge.

With similar aims and methodologies, four bifurcations were monitored on the Ridanna Creek. Figures 6.3 and 6.4 show the location and an image of each bifurcation.

Bifurcation 0 is located upstream and sets the beginning of the braided network. The other three belong to the central region, where the network is more active and morphological changes are likely to occur more frequently. In particular bifurcation 4 is located in a region with finer sediments and is characterised by lower values of water discharge in the incoming flow.

The analysis of morphodynamical processes relevant for the observed bifurcations requires the knowledge of the hydraulic conditions corresponding to discharges representing a good measure of *channel-forming* conditions: the mean annual flood or the five-year flood are commonly used. During the field work on the Sunwapta River the measured peak values of the discharge determined the rearrangement of the network configuration, with the formation of new bifurcations and adjustment of several channels. For this reason, we assume that the data collected well represent channel forming conditions.

On the contrary, measurements on the Ridanna Creek have been carried out with relatively low flow, not corresponding to formative conditions. During summer 2002 and 2003 the four surveyed bifurcations have not been subject to planimetric and altimetric evolution, with values of the Shields stress falling below the threshold for sediment transport. A comparison with theoretical and numerical predictive models is more problematic in this case. To fulfill this aim an extrapo-

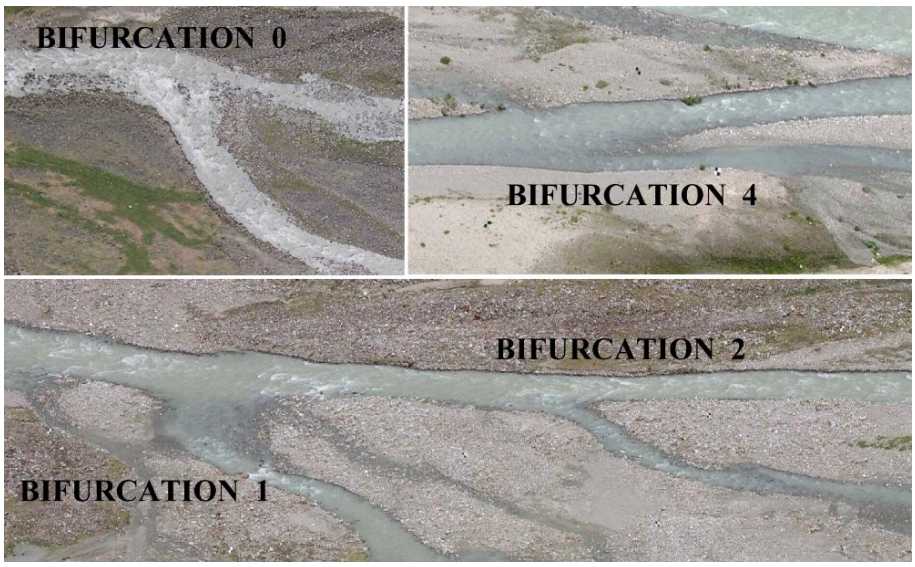

Figure 6.4: Picture of the four bifurcations monitored on the Ridanna Creek (images taken during summer 2003.

lation of the flow parameters towards formative conditions has been pursued: if this has the risk of reducing data accuracy, however it allows a gross estimate of the hydraulic and geometrical conditions of the bifurcations in the Ridanna Creek at the moment of their formation (see Chapter 7 for the comparison). Table 6.2 reports the values of discharge, averaged width and depth of each channel at the moment of survey.

In the following tables (6.1 and 6.2) all the data on the monitored bifurcations are reported: b denotes cannel width, S longitudinal slope, Q water discharge, D average flow depth, d_{50} the mean bed material size, Δ_z the difference in bed elevation, $\Delta\eta$ the same difference in bed elevation scaled with the average water depth D, rQ the discharge ratio between the two downstream channels, β_a and ϑ_a the aspect ratio and the Shields parameter of the upstream channel respectively. Bifurcation *III* included in Table 6.1 will be discussed in Section 6.3.

Bifurcation	*I*	*II*	*IV*	*III*
b_a [m]	10	8.5	8	12
b_b [m]	8.5	10	6.5	10
b_c [m]	7.5	8	6	5
S_a	0.012	0.014	0.009	0.005
S_b	0.015	0.019	0.020	0.018
S_c	0.021	0.012	0.012	0.027
Q_a [m^3/s]	9.0	5.5	4.5	4.4
Q_b [m^3/s]	5.5	4.4	2.7	2.8
Q_c [m^3/s]	3.5	1.1	1.8	1.6
D_a [m]	0.46	0.36	0.38	0.35
D_b [m]	0.37	0.23	0.27	0.21
D_c [m]	0.28	0.08	0.19	0.22
d_{50} [m]	0.04	0.04	0.04	0.04
Δz [m]	0.24	0.32	0.15	-0.15
$\Delta\eta$	0.51	0.89	0.40	-0.43
r_Q	0.64	0.25	0.66	0.56
r_b	0.88	0.80	0.92	0.50
β_a	10.9	11.8	10.7	17.2
ϑ_a	0.0836	0.0764	0.0512	0.0264

Table 6.1: Summary of the bifurcations data measured on the Sunwapta River.

Bifurcation	**0**	**1**	**2**	**4**
B_a [m]	9.8	16.7	9.6	6.5
B_b [m]	6.7	10	8.7	4.9
B_c [m]	5.4	5.5	5	2.4
S	0.029	0.022	0.017	0.011
Q_a [m^3/s]	1.00	6.0	5.4	0.86
Q_b [m^3/s]	0.95	5.4	5.1	0.80
Q_c [m^3/s]	0.05	0.6	0.3	0.06
D_a [m]	0.70	0.65	0.70	0.31
D_b [m]	0.72	0.76	0.66	0.29
D_c [m]	0.29	0.29	0.22	0.21
d_{50} [m]	0.21	0.1	0.08	0.05
Δz [m]	2.00	0.50	0.55	0.20
r_Q	0.05	0.11	0.06	0.08
r_b	0.81	0.55	0.57	0.49

Table 6.2: Summary of the bifurcations data measured on the Ridanna Creek.

A detailed description of the common features of the morphodynamics of natural bifurcations is now given.

- **Unbalanced water distribution**

  The flow distribution in the downstream branches was invariably unbalanced, with values of the discharge ratio ranging from 0.65 on the Sunwapta River to 0.1 on the Ridanna Creek. The occurrence of an asymmetrical configuration agrees with the general observation that in a braided river one or two channels carry most of the water, even if the network is fully developed and the number of channel is high. In particular, Mosley (1983) reported that the discharge of the main channel monitored on New Zealand's braided rivers ranges between 0.9 and 0.65 the total discharge. This peculiar feature affects strongly also the sediment transport and therefore the morphological activity, that is limited to few channels. As pointed out by Ashmore (2001), the braiding intensity of common networks is very low, if evaluated considering only the active channels; this would imply that the morphodynamic evolution of a braided river can be investigated carefully employing the available tools developed to model the evolution of single thread channels.

  Measurements of discharge partition were performed with different upstream conditions, i.e. with different water stages in the main channel. The analysis allowed to disclose a relationship between the discharge ratio rQ and the upstream discharge Qa, with a more unbalanced configuration when the total incoming discharge is lower (see Figure 6.5).

  It is worth noticing that the lower values of rQ were measured on the Ridanna Creek, where the measurements were performed in non-formative conditions. A laboratory test has been

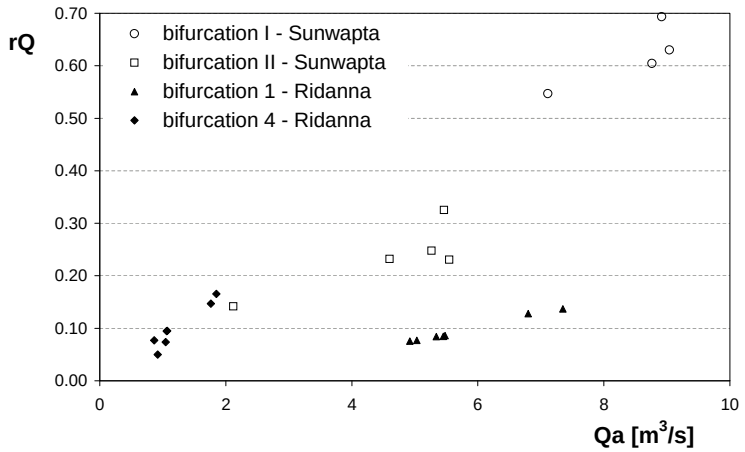

Figure 6.5: Measured values of the discharge ratio rQ in four bifurcations both on the Sunwapta River (open symbols) and on the Ridanna Creek (close symbols).

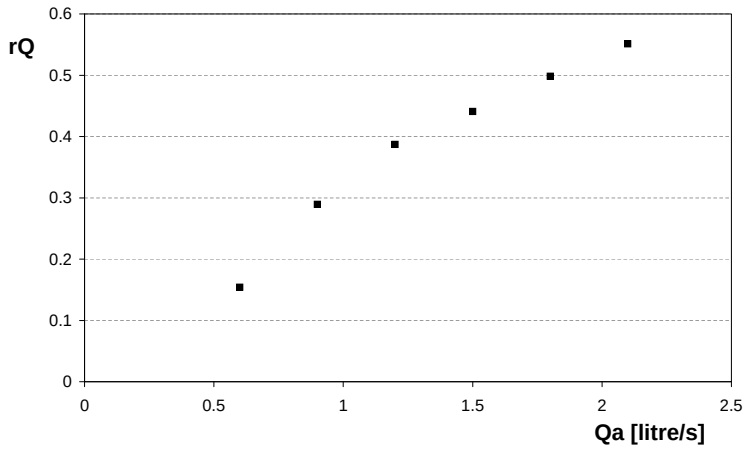

Figure 6.6: Relationship between the discharge ratio *rQ* and the total discharge *Qa* as measured in a laboratory test.

set up on the Y-shaped configuration (see Chapter 4 for the description of the laboratory setup) with the aim to verify this relationship between *rQ* and *Qa*. Starting from the unbalanced equilibrium configuration of run F3-21, with a discharge ratio equal to 0.56 (see Table 4.1), the bifurcation was subjected to a discharge cycle that reproduces the diurnal variation on a proglacial river. The discharges are such that sediment transport occur only during the peak and so topographic adjustments of the bifurcation are prevented. The result is reported in Figure 6.6. As observed in the natural bifurcations, the discharge ratio depends on the incoming flow conditions: the branch 'c', that carries a lower discharge and is characterised by a higher bed elevation, is likely to close for low water stages, as the 90% of the total discharge is flowing in branch 'b'.

- **Transverse velocity profiles**

  The analysis of the transverse velocity profiles of the downstream branches shows that the maximum velocity is generally located close to their external bank. In Figure 6.7 the velocity profiles of bifurcation *IV* on the Sunwapta River are plotted. This configuration leads to the erosion of the external bank, which is frequently steeper than the other one and implies that the flow keeps to diverge, with deposition in the central region of the channel and lateral erosion as also reported by Ashworth (1996) in an experimental investigation on central bar accretion.

- **Difference in channel bed elevation**

  In Figure 6.8 three cross sections surveyed near bifurcation *IV* are plotted: both the bed elevation and the free surface level are reported. First, it is worth noticing that the water

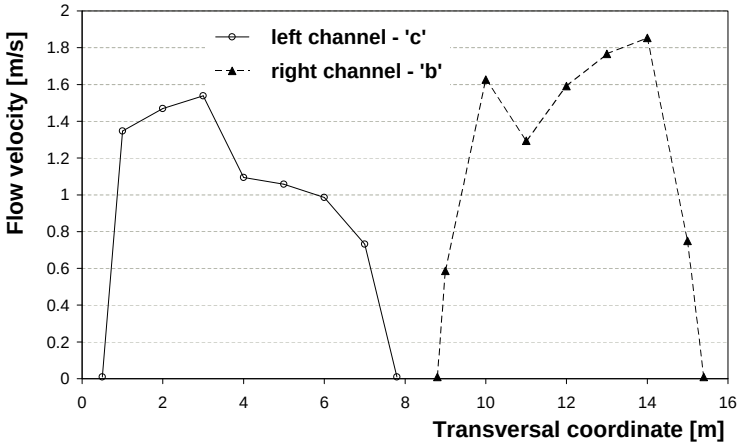

Figure 6.7: Transverse profiles of the velocity at bifurcation *IV*.

level is different in the two downstream channels, with a higher level in the smallest branch, despite almost equal values of the maximum water depth. This difference lead to a water exchange between the two channels, with a discharge flowing laterally from channel 'c' to 'b'. This effect takes place along a reach whose extension is of the order of the average width of channel 'a'.

Moreover the mean and maximum bed elevation of the two downstream branches is different and the channel with lower discharge exhibits a higher elevation. The presence of this 'step' between the two channels was invariably observed in all the monitored bifurcations. Its amplitude depends mainly on the asymmetry of the water distribution and scales with the mean upstream flow depth. The values are reported in Tables 6.1 and 6.2.

- **Longitudinal bed profiles**

  The longitudinal profiles of channels *I*a, *I*b, *IV*a and *IV*b are reported in Figure 6.9. In both cases the bed profile displays local aggradation close to the bifurcation, suggesting the tendency towards deposition due to local flow divergence. As a consequence the water surface slope decreases just upstream the bifurcation and increases downstream. This peculiar configuration could be triggered both by the bifurcation, that induces a deposit pattern or by the presence of a confluence that frequently occurs upstream. It is well known (Ashmore & Parker, 1983) that a confluence induces scour in the downstream channel, through the secondary flows associated with the formation of a deep pool.

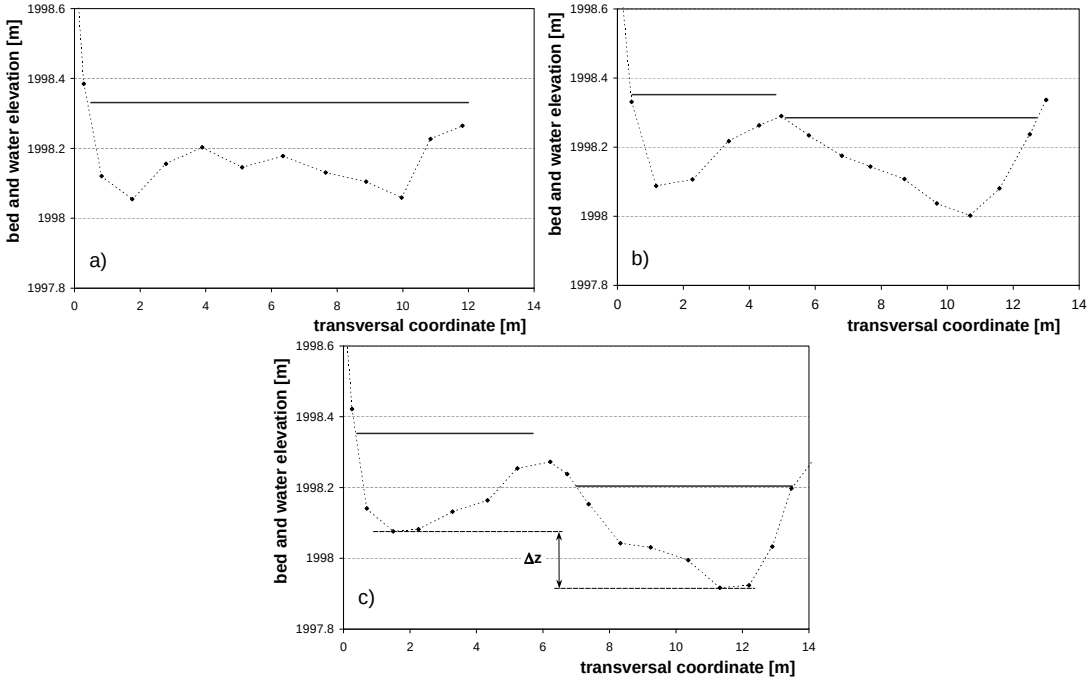

Figure 6.8: Cross sections near bifurcation *IV*. a) 3 m upstream; b) at bifurcation; c) 3 m downstream. The dashed lines with close symbols correspond to bed elevation, while straight lines denote water surface level.

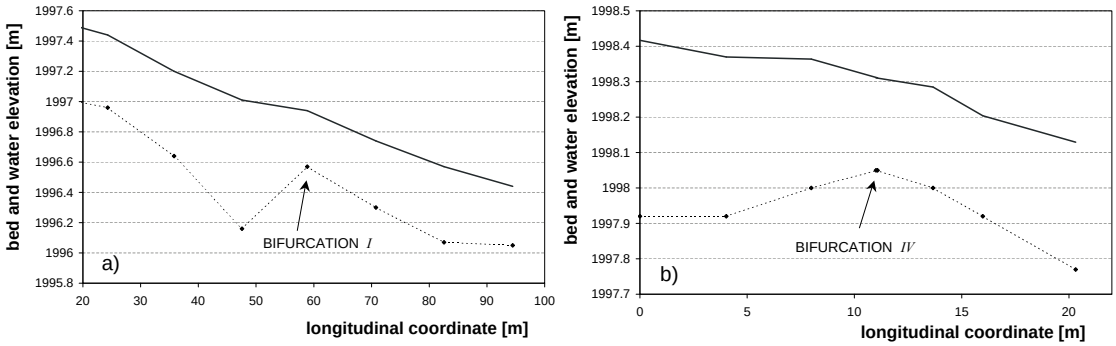

Figure 6.9: Longitudinal profiles of bifurcation *I* (a) and *IV* (b). The dashed lines with close symbols correspond to bed elevation, while straight lines denote water surface level.

6.3 Role of the bifurcations on planform changes

During summer 2003 both the Ridanna Creek and the Sunwapta River experienced morphological changes, characterised by lateral channel shift, branches creation and/or obliteration, followed by an overall rearrangement of the network. This planimetric and altimetric changes can be analysed from the viewpoint of the theoretical and predictive models proposed in Chapter 2 and regarding the evolution of bifurcations as the crucial process that triggers the rapid morphological modification often observed in the braided rivers.

Two examples are reported, that can be related to different dynamics: the first one is a chute cutoff occurred on the Ridanna Creek, with the dissection of an alternate bar (see Ashmore, 1991 and Chapter 3); the second one was observed on the Sunwapta River and was determined by the formation of a new channel that conveys more water toward the left side of the network and by a sediment wave which modified the flow partition of the main bifurcation.

- **Ridanna Creek**

  The main morphological changes occurred in the central region on July 28^{th}, 2003. The plani-altimetric adjustments are due to a channel bifurcation that can be related to the planimetric evolution of the regular, weakly meandering main stream from its displacement before the flood event (black line in Figure 6.10) to a new alignment corresponding to the white line in the same figures. The direction of the main flow has switched leftwards of approximately 40°, an angle which falls in the typical range of the observed bifurcations (see Chapter 3).

  The planimetrically true image of Figure 6.11 refers to the initial configuration and suggests a possible physical explanation of the morphological changes related to the occurrence of the bifurcation. This is likely to be related to the presence of bars in the main channel due to its progressive widening downstream of bifurcation 2; sediment mobility due to the increasing Shields stress has induced the migration of the alternate bar complex in the curved channel. This has first triggered the erosion of the right bank (see on Figure 6.10 the erosion of the vegetated area) and successively of the left upstream bank where channel avulsion then took place. Moreover bar evolution could have been affected by the forcing effects of channel curvature and width variations (Tubino & Seminara, 1990; Repetto & Tubino, 1999), that are likely to promote the process of chute cutoff (see Chapter 3).

  Unlike other bifurcations monitored in the study reach, this "switch" bifurcation (see Federici & Paola, 2003) presently displays only one open downstream branch, as the right channel has been abandoned after the formative event.

Figure 6.10: Images of the central regions of the surveyed reach in the Ridanna Creek before and after the event of July 28^{th}, 2003. Lines indicate the displacement of the main channel. Flow is from left to right.

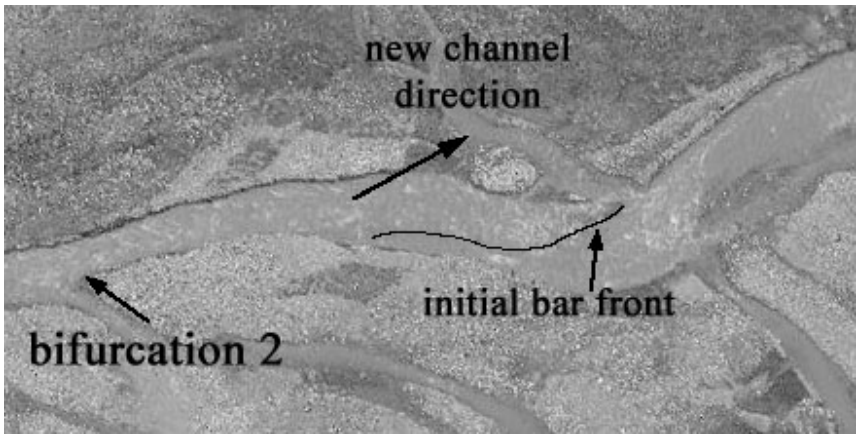

Figure 6.11: Orthoimage of the region interested to planimetric changes. The line indicates the diagonal front of the alternate bar. Flow is from left to right.

- **Sunwapta River**

  On August 1^{st}, 2003 the network was subject to morphological changes, which involved both the plane-altimetric configuration and the distribution of water in the branches. The water level measured by the UDG station (see Figure 5.21) was the highest during the field campaign, even if the peak value was similar to that registered on the previous days. Network modifications occurred after a week of high flows, during which the bed first experienced a slow rearrangement and than rapid changes, when the overall equilibrium configuration became unstable. The most interesting differences in the network topography took place in proximity to the bifurcations *I* and *II*. In Figure 6.12 are reported two orthoimages of the study reach taken on July 26^{th} and August 4^{th}. The water discharge through the reach is higher in the second picture, so they are not quantitatively comparable, but the changes could be easily recognised. Namely, the centre-left area was subject to extensive planimetric modifications, with the formation of new channels associated with scour and depositional regions of the average hight of half a meter.

  In Figure 6.13 there are three more detailed pictures of the area around bifurcation *I*; the time sequence allows to obtain a better interpretation of the evolution of the network. In particular the picture taken on August 11^{th}, with a lower water level, clearly displays the

Figure 6.12: Orthoimages of the study reach before (left) and after (right) the changes on August 1^{st}. Flow is from left to right.

Figure 6.13: Particular of the bifurcations *I*, *II* and *III*. Pictures taken on July 24^{th} (a), August 4^{th} (b) and August 11^{th} (c). Flow is from left to right.

new channel configuration, that was still changing on August 4^{th}. The main morphodynamic process that took place, was a deposition at bifurcation *I*, mainly in the channel '1b'. This determined a lower flow in bifurcation *II* and consequently the closure of the branch '2c'. Moreover channel '1b' (and '2a') migrated rightwards, eroding the central bar downstream of bifurcation *I* and depositing a new bar on the left side.

At the same time a new channel formed, starting from bifurcation *I*, that finally ended up with a more complex pattern, with one channel dividing into three branches. This new bifurcation was surveyed in detail on August 6^{th} and was named bifurcation *III* (see last column in Table 6.1). The changes in the network triggered a new equilibrium state. The water distribution in bifurcation *I* adjusted to the new configuration diminishing the water in channel 'b'; the ratio between water in channel 'b' and 'c' of the old bifurcation *I* shifting from 0.64 to approximately unity, whereas bifurcation *III* was characterised by an rQ of 0.56. This implies that the newly formed channel approximately carried the half of the old one.

A more detailed analysis of bifurcation *III* shows that the measured configuration does not represent an equilibrium state yet. In spite of a lower discharge, the smallest of the two downstream channels is characterised by a higher water surface slope, a greater mean velocity and is deeper on the average; unlike all the other surveyed bifurcations, the bed elevation of the 'c' channel is lower than the elevation of the 'b' channel. These configuration caused more and more water to be carried by channel 'c', which increased its width daily. The evolution process would probably have been continuing until the new channel would become the main branch.

6.4 Channel adjustment on the Ridanna Creek

The braided reach of the Ridanna Creek at Aglsboden was also studied through the analysis of aerial images taken from 1982, in order to describe the general features of the network and its modifications over time and to find relationships between the evolution of the main bifurcations and the displacement of the main branches with the overall geometrical and hydraulic properties of the reach.

Five images were considered, that has been taken respectively in May 1982, July 1990, September 1997, 1999 and 2000. The last three were available already in a planimetrically true format, whereas the former two had to be orthorectified, in order to allow a quantitative comparison. This operation was performed with the GRASS software.

The analysis pointed out the existence of three main regions, with different morphodynamical features (see Figure 5.3). In the upper region (A) the river displays mostly a single thread, weakly

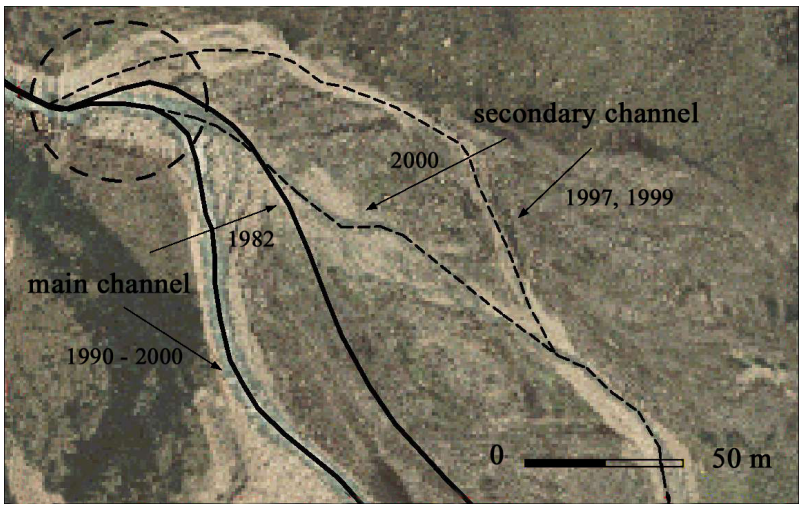

Figure 6.14: Planimetric evolution of region A, reported on the orthoimage of September 2000.

meandering pattern and is characterised by the presence of a bifurcation. The analysis of the historical images shows that this main bifurcation occurs approximately in the same location, placed in the first area, where the river is not any more laterally confined by the valley morphology (Figure 6.14). In the last twenty years this bifurcation displays invariably a high degree of asymmetry of both the discharge distribution and the morphological configuration. As a consequence, at low values of the flowing discharge the river looks like a single thread channel.

Both the branches were subject to changes: the secondary channel active in 1997 was abandoned and a similar bifurcation occurs few meters downstream, with the incision of a secondary channel recognizable on the image taken in 2000. The main channel is characterised by the same planimetric configuration since 1990. A lateral shift occurred in the period 1982 - 1990, with a rightwards migration of approximately 20 - 30 m. This modification affected strongly the network development downstream, as it shifted the main flow towards the right side of the plane. Furthermore it is possible to notice that the image taken in 1990 displays very few vegetated areas, compared with that of the other images. This suggests that the reach was subject to an intense flood event that caused the complete rearrangement of the network. This event is also recognizable from the discharge measurements taken on an automatic gauging station 25 km downstream, managed by the local fluvial authority.

Region B is more active and also more free to evolve: the glacial plane here is wider and the valley flanks do not constrain the network. This area is characterised by a higher number of channels and shows the typical features of braiding, with bifurcations and confluences, bars and small vegetated islands. Channel evolution is highly dynamic and morphological changes occur on the average every 1 - 2 years. The network configuration is strongly different in the five aerial

images, with modifications of the position and number of branches.

In spite of the strong planform modifications and of the frequent rearrangement of water distribution, the presence of a bifurcation that generally occurs in the same location was observed, representing a nodal point in which the instability of the single thread channel preferentially occurs. Figure 6.15 reported the comparison among four different images (from 1990 to 2003) pointing out the area where this first upstream bifurcation generally occurs. Here the transition between the weakly meandering pattern in region A and the fully developed braided regime is located. The downstream shifting of the first bifurcation, occurred between 1990 and 1999, affects the network development, as the downstream valley flanks limit the lateral channel evolution. As a result the braiding index is generally lower in the last years of observations.

Finally, the third region (C) is characterised by the channel convergence and the evolution is

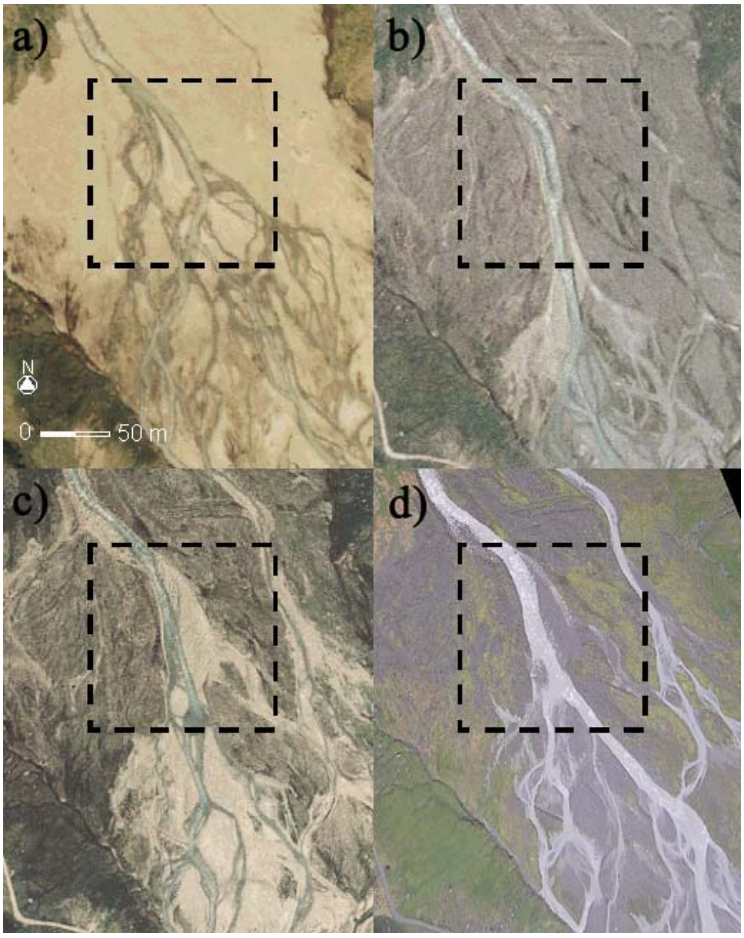

Figure 6.15: Planimetric configuration of region B in 1990 (a), 1999 (b), 2000 (c) and 2003 (d). The area where the first bifurcation occurs is pointed out.

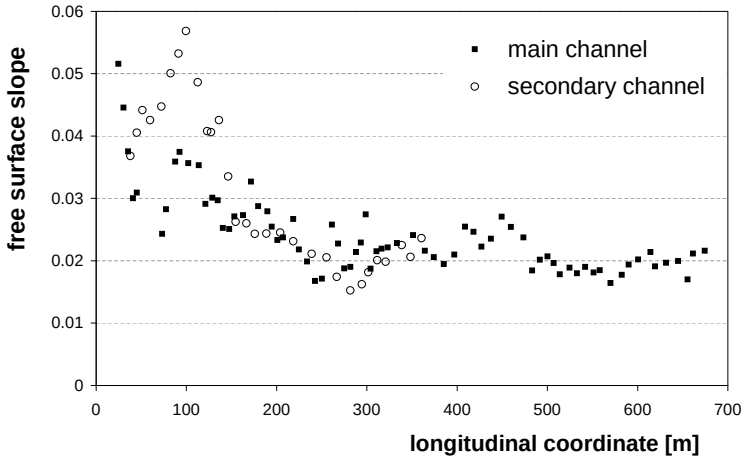

Figure 6.16: Local free surface slope for the main channel (close symbols) and for the secondary channel of region A (open symbols).

extremely dynamic, because of the lower grain size. This area was not subject to our analysis, as it is constrained by the valley morphology and it can be influenced by the presence of the dam mentioned above.

The peculiar features of the morphological evolution of the network and the differences between its behaviour in regions A and B can be better understood analysing the topographic, hydraulic and grain size data collected during the field work.

The topographic survey along the wet channels allowed to determine the free surface slope along the reach. Figure 6.16 shows the longitudinal variation of the slope of the two channels originating from bifurcation 0; the main channel displays a weakly meandering pattern and carries most of the water discharge, due to the asymmetry of bifurcations. It is worth noticing that an initial reach of approximately 200 meters is much steeper, while the central region is characterised by an almost constant slope, ranging around the value of 2%.

Similarly, the measurements of grain size distribution, obtained both with the Wolman count method and with remote sensing image analysis (see Figure 6.17 and Figure 5.16), display a gradual decrease of the sediments mean diameter; the d_{50} decreases from 0.22 m to 0.05 m. The fining effect is even more evident considering the larger diameters: d_{84} ranges about 0.6 m in the upstream region, where large boulders might be transported by the higher stream power, whereas in the central region the typical values fall between 0.1 m and 0.2 m. Changes of bed slope and grain size along a braided reach are common, even when the total discharge is constant (Chew & Ashmore, 2001). In the Ridanna Creek the sharp longitudinal variations may correspond to a non-equilibrium state of the whole reach, suggesting that an aggradation process of the glacial plane might be occurring on a larger time scale, whose quantification will require further investigations.

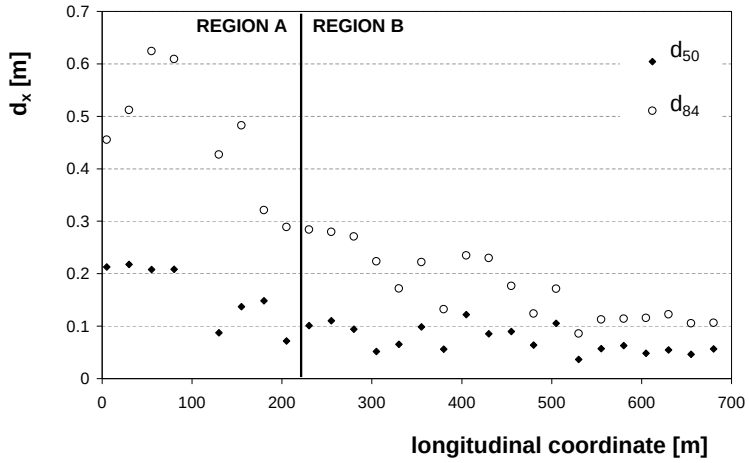

Figure 6.17: Grain size distribution along the reach. The d_{50} (close symbols) and the d_{84} (open symbols) are reported.

The separation between regions A and B is revealed also by the analysis of thermal images analysis (see Figure 5.15): the upper reach of the network is characterised by lower thermal capacities, whereas in the lower part it is fairly large. These findings indicate the low intensity of groundwater activity in the upstream reach, at least during the summer 2002, which is also confirmed by the quasi absence of active channels besides the main channel. On the contrary, the active character of the network in region B is also reflected by the presence of an intense groundwater movement.

The field measurements confirm the existence of two regions with different morphological properties along the braided reach, initially detected from the analysis of existing air photographs. In particular, free surface slope and bed material size strongly condition the development of the braided network. This effect is pointed out by theoretical (e.g. Parker, 1976) and empirical (e.g. van den Berg, 1995) regime equations that predict a threshold slope (S_t) for the occurrence of braiding as function of a characteristic discharge Q (bankfull) and of the mean grain size D_s. This relationships commonly read:

$$S_t = aQ^{-b}D_s^c, \tag{6.1}$$

with a, b, c positive coefficients. Field evidence of the influence of the grain size and of the valley slope on the onset of braiding were found also by Chew & Ashmore (2001).

In the present case the equations correctly predict the pattern of the reach being braided and also the increase of braiding intensity downstream, due to sediment fining. It is worth noticing that in the upstream region the bankfull discharge is higher, thus partially balancing the effect of the coarser grain size.

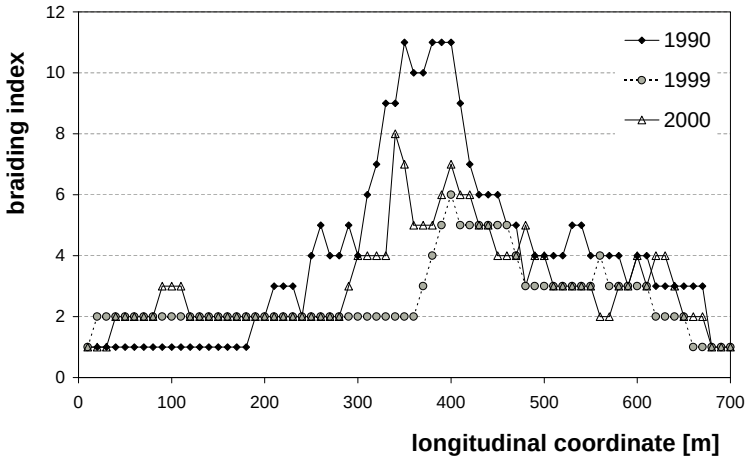

Figure 6.18: Longitudinal variation of the braiding index of the Ridanna Creek as measured from the aerial images taken in 1990, 1999, 2000.

Finally, the braiding index on the Ridanna Creek has been measured from the aerial photographs taken in 1990, 1999 and 2000; the anabranches were counted along cross sections approximately 10 m apart, minimizing possible sources of uncertainty due to the different image quality (Figure 6.18).

The analysis confirms the presence of three regions, with different values of the braiding index. In the central region the average number of channels ranges between 6 and 11, with a peak in 1990. This variation can be related to a different network configuration induced by the activity of the main bifurcation in the upstream region, but also depends on the value of the total discharge flowing when the images were taken. The relationship between braiding index and discharge is not completely clear: Mosley (1983) found a weak positive relation of this two parameters in New Zealand braided rivers and the issue needs further exploration.

The continuous discharge measurements and the automatic digital image acquisition allowed to determine how braiding index is related to the total discharge in this reach. Essentially it was possible to observe the activation of branches for different stages (Figure 6.19). In Figure 6.20 the longitudinal variation of the braiding index is reported, as a function of the total discharge. Note that for values lower than $2m^3/s$ the reach shows a single thread meandering pattern, whereas with higher discharges more branches become wet. In the central region the braiding index increases until 8 - 9 for the higher discharges observed during summer 2003. It is worth noticing that the increase of the total discharge does not invariably produce an increase in braiding intensity: bankfull conditions can determine the flooding of bars that at lower stage splits one channel in different branches.

This observation points out the limitation of the past aerial images analysis, when the total

discharge at the moment of photograph is unknown, although it has the advantage to confirm the weak correlation of braiding index with discharge, particularly for near-bankfull conditions. Moreover note that, if the exact determination of the time variation of the braiding index time can be somewhat limited, its longitudinal variation and therefore the determination of the three different morphological regions is not significantly affected by the discharge.

Figure 6.19: Planimetric configuration of the Ridanna Creek during summer 2003: arrows indicate subsequent activation of the branches.

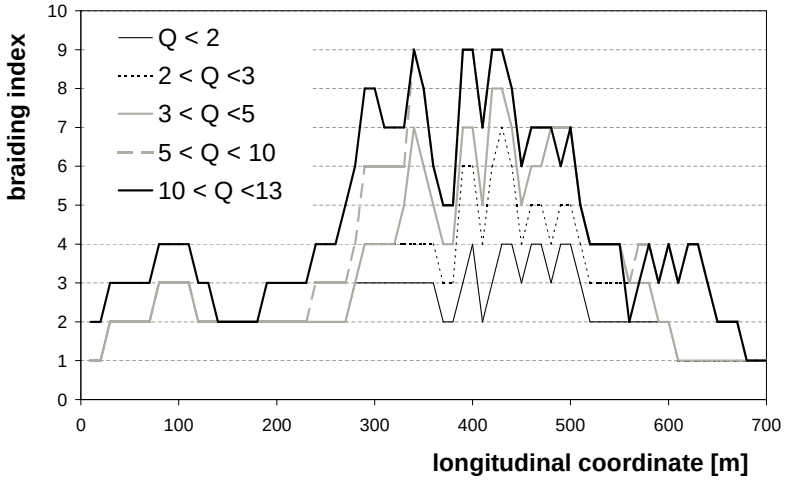

Figure 6.20: Longitudinal variation of the braiding index of the Ridanna Creek as a function of the total discharge (m^3/s).

7 Comparison and discussion

7.1 Prediction of bifurcation configuration

Field and laboratory observations show that the equilibrium configuration of channel bifurcations is often unbalanced. In particular, this behaviour is enhanced in gravel bed braided rivers, due to the relatively small values of the Shields stress and the high values of the width to depth ratio. Natural diffluences frequently concentrate most of the flow in a main channel downstream, which is deeper and wider than the other branch. This analysis confirms the detailed field observations of Mosley (1983) who pointed out that in braided rivers the main channel carries generally a high percentage of the total discharge, ranging from 65% to 85%.

Also the dynamics of bed topography analysed by Stojic et al. (1998) and the remarks of Ashmore (2001) on the *active* braided index are in close agreement with experimental and field observations reported in Chapters 4 and 6, and with the theoretical predictions of Bolla Pittaluga et al. (2003): equilibrium configurations are such that often only one of the downstream branches is active. Furthermore, the inverse relationship between the Shields stress and the discharge ratio in the downstream channels (e.g. Figure 4.6a) suggests that higher values of water discharge could lead to a greater number of active channels and to higher values of the braiding index, as empirically shown by several authors and reported by Ashmore (2001).

The influence of bar migration on the discharge distribution and on the bed topography of the bifurcations (preliminarily investigated by Hirose et al. (2003) and intensively explored in Section 4.4.2) can play a crucial role in the planimetric evolution of a braided network, determining the shift of the main flow either inside a single branch or from one side of the plane to the other, inducing bifurcations through the mechanism of chute cutoff. This interaction between bar migration and the bifurcation configuration was also observed by Ferguson et al. (1992), who measured the evolution of a chute and lobe unit.

The one-dimensional theoretical model proposed by Bolla Pittaluga et al. (2003) catches the main features of the equilibrium configurations of a bifurcation, correctly predicting the existence of an unbalanced water distribution. If reported on a β/ϑ plane (Figure 7.1), the experimental runs performed on a Y-shaped bifurcation (see Chapter 4) show a trend similar to that predicted by the

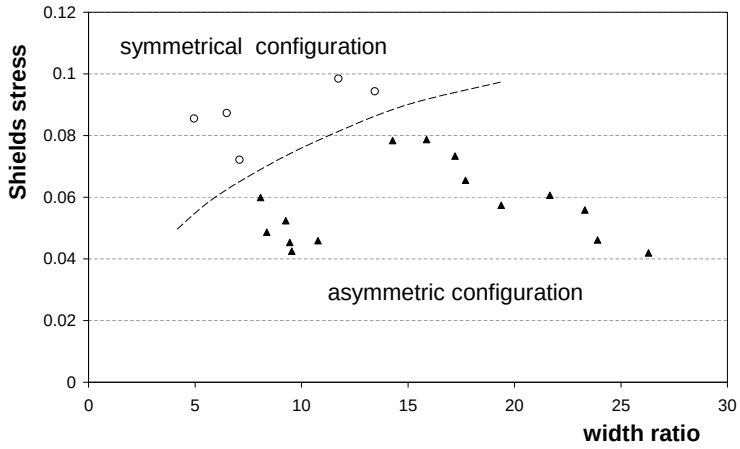

Figure 7.1: Observed bifurcation configurations on the width ratio / Shields stress plane.

model (see Figure 2.19b). A direct comparison is more problematic: in particular the coefficient α, related to the length of the upstream region affected by the bifurcation, needs to be calibrated in the model. A promising hint is given by the observed dependence of the bifurcation configuration on the distance from resonant conditions, suggesting a relationship between α and the width to depth ratio. In Figure 7.2 the comparison between measured and computed values of the inlet step ($\Delta\eta$) is reported. In this case values of α ranging about 3 seems to better fit the experimental observations. Note that the one-dimensional model of Bolla Pittaluga et al. (2003) generally predicts a weaker variation of the inlet step, as revealed by Figure 7.2 where $\Delta\eta$ is overestimated under sub-resonant conditions and underestimated when β exceeds β_R. It is worth recalling that the one-dimensional scheme of this theoretical model does not consider neither two-dimensional effects, associated with bar formation and propagation, the angle between two downstream channels, nor three-dimensional features, like those inducted by secondary circulations.

The comparison with field observations preliminarily requires to face the problem of defining formative condition. For bifurcation on the Sunwapta River it has been assumed that measurements were done in formative conditions, due to the rearrangement of the network occurred during the field campaign. This can not be applied in the case of the Ridanna Creek, where a suitable value of the total discharge has been determined extrapolating a *bankfull* value from the cross sectional topography. This has implied the impossibility to compare every measured and computed flow parameters as the discharge ratio rQ, but only the altimetric configurations.

In Table 7.1 the comparison referring to bifurcations *I* and *IV* of the Sunwapta River and bifurcations 1, 2 and 4 on the Ridanna Creek are reported.

Predicted and measured inlet steps in the field are also compared in Figure 7.3, for different values of α: smaller value of this parameter seem to lead to a better reproduction.

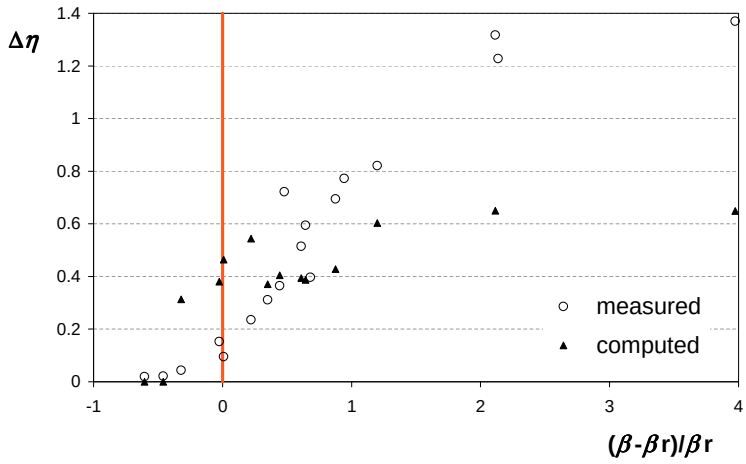

Figure 7.2: Comparison between experimental and computed values of the inlet step ($\alpha = 3$).

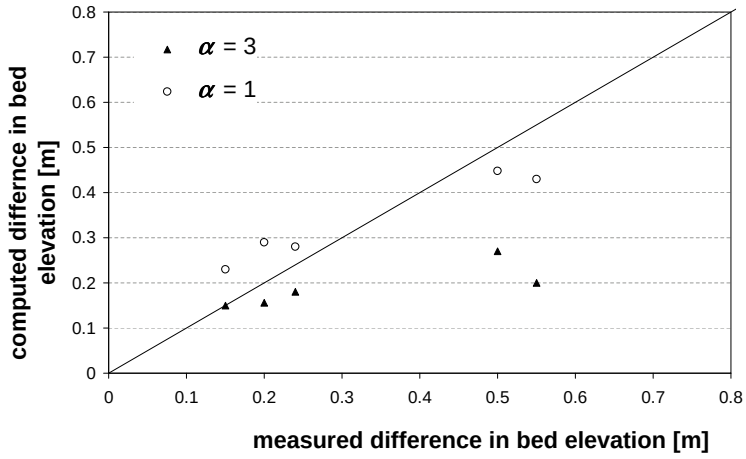

Figure 7.3: Comparison between the measured and the computed values of the inlet step of natural bifurcations.

Bifurcation	*I*	*IV*	*1*	*2*	*4*
	Sunwapta		Ridanna		
rQ measured	0.64	0.66	0.14	0.06	0.16
rQ calculated	0.36	0.39	0.29	0.26	0.31
Δz [m] measured	0.24	0.15	0.50	0.55	0.20
Δz [m] calculated	0.18	0.15	0.27	0.20	0.16

Table 7.1: Comparison between observed configurations and theoretical predictions for five bifurcations on the Sunwapta River and the Ridanna Creek.

7.2 Ingredients for a predictive model of braided rivers evolution

The complexities arising in the numerical solution of the governing equations for sediments and water motion and continuity, together with the poor effectiveness in the long term prediction of the evolution of a braided network has suggested to explore research alternatives offered by different approaches, namely 'object-oriented' models. In this context braiding is viewed as the result of the interaction between channels and nodes, treated as separated objects. The morphodynamics of single channels then becomes a relevant issue for braiding, as highlighted in recent reviews on braided systems by Ashmore (2001) and Paola (2001). The experimental investigation presented in Chapter 3 shows that planimetric forcings due to channel curvature and width variations play a crucial role in determining the onset of flow bifurcation, especially driving the mechanism of chute cutoff. Such planimetric non uniformities promote the development of steady bed topography, dominated by the transition from alternate to mid channel bars which rapidly leads to bifurcation. In order to exploit these experimental findings and to obtain suitable rules to be implemented in predictive object-oriented models of braiding a new theoretical framework is required, able to consider the coupled effect of channel curvature and width variations on channel morphology.

The weakly meandering planform typical of individual channels within braided networks is generally maintained by a relatively high frequency of chute cutoffs: low sinuosity often determines that bed deformation may be controlled by the interaction of free migrating forms with steady patterns (Figure 7.4). Moreover, the migration of alternate bars has been shown to be relevant also for the subsequent evolution of a bifurcation (see Figures 6.10 and 6.11) and for

Figure 7.4: The weakly meandering main channel of the Ridanna Creek, with a complex bar system. (flow is toward the camera)

Figure 7.5: The Mydal Ssandur, Iceland.

the discharge partition in the downstream branches. Also in this case, a theoretical model which consider the free-forced interactions with both planimetric forcing effects is needed.

In order to extend the time span of sound morphological predictions in braided streams, a branches model like that proposed by Jagers (2003) or a multi-layer model like that suggested by Paola (2001) require a physical description of the conditions that lead to the occurrence of bifurcation and need suitable rules that quantify its further evolution. The bifurcation process is of fundamental relevance in determining flow distribution, hence controlling the activity of the network. Until now, this process is one of the most difficult to predict; it can be viewed as the element adding most uncertainty to a braiding system which can cause the complete rearrangement of the plane- and altimetric configuration (Figure 7.5). The experimental and field observations and the data analysis presented in this work offer a detailed explanation of the main physical processes, integrating field observations and laboratory measures with existing and underdevelopment theories, allowing a quantitative description and improving the opportunities to predict the main morphodynamical features of river bifurcations.

References

Andreatta, R., Zolezzi, G., Tubino, M., *Parametrizzazione di circolazioni secondarie lungo le linee di corrente nei corsi d'acqua naturali.* Submitted to the XXIX Convegno di Idraulica e Costruzioni Idrauliche, Trento, September 2004, (in Italian).

Ashmore, P.E., *Laboratory modelling of gravel braided stream morphology.* Earth Surface Processes and Landforms 7, 201-225, 1982.

Ashmore, P.E., *Bed load transport in braided gravel-bed stream models.* Earth Surface Processes and Landforms 13, 677-695, 1988.

Ashmore, P.E., *How do gravel-bed rivers braid?* Canadian Journal of Earth Sciences 28, 326-341, 1991.

Ashmore, P.E., *Braiding Phenomena: statics and kinetics.* In: Mosley M.P. (eds) Gravel bed rivers V, New Zealand Hydrologic Society, Wellington, 95-121 ,2001.

Ashmore, P.E., Parker, G., *Confluence scour in coarse braided stream.* Water Resources Research 19 (2), 392-402 ,1983.

Ashworth, P.J., *Mid-channel bar growth and its relationship to local flow strength and direction.* Earth Surface Processes and Landforms 21, 103-123, 1996.

Ashworth, P.J., Ferguson, R.I., *Interrelationships of channel processes, changes and sediment in a proglacial river.* Geografiska Annaler 68A: 361-371, 1986.

Bartholdy, J., Billi, P., *Morphodynamics of a pseudomeandering gravel bar reach.* Geomorphology 42, 293- 310, 2002.

Blondeaux, P., Seminara, G., *A unified bar-bend theory of river meanders.* Journal of Fluid Mechanics 112, 363-377, 1985.

Bolla Pittaluga, M., Federici, B., Repetto, R., Paola, C., Seminara, G., Tubino, M., *The morphodynamics of braiding rivers: experimental and theoretical results on unit processes.* In: Mosley M.P. (eds) Gravel-bed Rivers V, New Zealand Hydrological Society, Wellington, 143-181, 2001.

Bolla Pittaluga, M., Repetto, R., Tubino, M., *Channel bifurcation in braided rivers: equilibrium configurations and stability*, Water Resources Research 39 (3), 1046-1059, 2003.

Bridge, J.S., *The interaction between channel geometry, water flow, sediment transport and deposition in braided rivers.* In: J.L. Best and C. Bristows (Eds.), Braided Rivers: form, process and economic applications, Geological Society Special Publication 75, 13-71, 1993.

Chandler, J.H., *Effective application of automated digital photogrammetry for geomorphological research.* Earth Surface Processes and Landforms (24): 51-63, 1999.

Chandler, J.H., Ashmore, P., Paola, C., Gooch, M., Varkaris, F., *Monitoring river channel change using terrestrial oblique digital imagery and automated digital photogrammetry.* Annals of the Association of American Geographers 92(4): 631-644 (14), 2002.

Chandler, J.H., Buffin-Bélanger, T., Rice, S., Reid, I., Graham, D.J., *The accuracy of a river bed moulding/casting system and the effectiveness of low-cost digital camera for recording river bed fabric.* Photogrammetric record 18 (103), 209-223, 2003.

Chew, L.C., Ashmore, P.E., *Channel adjustment and a test of rational regime theory in a proglacial braided stream.* Geomorphology 37, 43-63, 2001.

Colombini, M., Seminara, G., Tubino, M., *Finite amplitude alternate bars.* Journal of Fluid Mechanics 181, 213-232, 1987.

Colombini, M., Tubino, M., *Finite-amplitude free bars: a fully nonlinear spectral solution.* In: R. Soulsby and R. Bettes (eds), Sand Transport in rivers, estuaries and the sea. Proceedings of Euromech. 262 Colloquium, Wallingford, UK, 26-29 June, 163-169, Balkema.

de Heer, A., Mosselman, E., *Flow structure and bedload distribution at alluvial diversions*, Proceedings of RiverFlow2004, Napoli, June 2004, 2004.

de Vriend, H.J., *Model-based morphological prediction: from art to science.* Proceedings of RiverFlow 2002, Lovain la Neuve, Belgium 4-6 September 2002, 3-12, 2002.

Enggrob, H., Tjerry, S., *Simulation of Morphological Characteristics of a Braided River.* 1° IAHR-RCEM Symposium, Genova, 6-11 September 1999, 585-594, 1999.

Federici, B., Paola, C., *Dynamics of bifurcations in noncohesive sediments.* Water Resources Research 39 (6) 1162/3-1 3-15, 2003.

Ferguson, R.I., *The missing dimension: effects of lateral variation on 1-D calculations of fluvial bedload transport.* Geomorphology 56, 1-14, 2003.

Ferguson, R.I., Ashmore, P.E., Ashworth, P.J., Paola, C., Prestegaard, K.L., *Measurements in a braided river chute and lobe. 1. Flow pattern, sediment transport and channel change.* Water Resources Research 28(7), 1877-1886, 1992.

Fredsøe, J., *Meandering and braiding of rivers.* Journal of Fluid Mechanics 84, 607-624, 1978.

Fujita, Y., Muramoto, Y., *Studies on the process of development of alternate bars.* Disaster Prevention Research Institute Bulletin, Kyoto University, 35, Part 3, 314 55-86, 1985.

Fujita, Y., Muramoto, Y., *Multiple bar and stream braiding.* In: W.R. White (Eds.) International Conference on river regime, Wallingford, 289-300, 1988.

Garcia, M.H., Niño, Y., *Dynamics of sediment bars in straight and meandering channels: experiments on the resonance phenomenon.* Journal of Hydraulic Research 31(6), 739-761, 1993.

Gay, G.R., Gay, H.H., Gay, W.H., Martinson, H.A., Meadem, R.H., Moody, J.A., *Evolution of cutoffs across meander necks in Powder River, Montana, USA.* Earth Surface Processes and Landforms 23 (7), 651-662, 1998.

Gilvear, D.J., *Fluvial geomorphology and river engineering: future roles utilizing a fluvial hydrosystems framework.* Geomorphology 31, 229-245, 1999.

Goff, J.R., Ashmore, P.E., *Gravel transport and morphological change in braided Sunwapta river, Alberta, Canada.* Earth Surface Processes and Landforms 19, 195-212, 1994.

Griffiths, G.A., *Stable-channel design in gravel-bed rivers.* Journal of Hydrology 52, 291-305, 1981.

Habersack, H.M., *Radio-tracking gravel particles in a large braided river in New Zealand: a field test of the stochastic theory of bed load transport proposed by Einstein.* Earth Surface Processes and Landforms 15(3), 377-391, 2001.

Hirose, K., Hasegawa, K., Meguro, H., *Experiments and analysis on mainstream alternation in a bifurcated channel in mountain rivers.* Proceedings 3° International Conference on River, Costal and Estuarine Morphodynamics, Barcelona, Spain, 1-5 September 2003, 571-583, 2003.

Hoey, T.B., *Temporal variations in bedload transport rates and sediment storage in gravel-bed rivers.* Progress in Physical Geography 16 (3), 319-338, 1992.

Hoey, T.B., Sutherland, A.J., *Channel morphology and bedload pulses in braided rivers: a laboratory study.* Earth Surface Processes and Landforms 16, 447-462, 1991.

Howard, A.D., *Modelling channel evolution and floodplain morphology.* In M.G. Anderson, D.E. Walling and P.D. Bates, eds., Floodplain processes, 15-62, John Wiley & Sons, 1996.

Howard, A.D., Keetch, M.E., Vincent, C.L., *Topological and geometrical properties of braided streams.* Water Resources Research 6, 1674-1688, 1970.

Ikeda, S., Parker, G., Sawai, K., *Bend theory of river meanders. Part 1 - Linear development.* Journal of Fluid Mechanics 112, 363-377, 1981.

Jaeggi, M., *Formation and effects of alternate bars.* Journal of Hydraulic Division ASCE 110, 1103-1122, 1984.

Jagers, H.R.A., *A comparison of prediction methods for medium-term planform changes in braided rivers.* 2° IAHR-RCEM Symposium, Obihiro, September 10-14, 713-722, 2001.

Jagers, H.R.A., *Modelling planform changes of braided rivers.* University of Twente, The Netherlands, Ph.D. thesis, 2003.

Johannesson, J., Parker, G., *Linear theory of rivers meanders.* In: River Meandering, Ikeda S. and Parker G. (eds), Washington DC, Water Res. Monograph 12, 181-214, 1989.

Kalkwijk, J.P.Th., De Vriend, H.J., *Computation of the flow in shallow river bends.* Journal of Hydraulic Research 18 (4), 327-342, 1980.

Kinoshita, R., Miwa, H., *River channel formation which prevents downstream translation of transverse bar.* Shinsabo 94, 12-17, 1974 (in Japanese).

Klaassen, G.J., van Zanten, B.H.J., *On cutoff ratios of curved channels.* In 23^{rd} Congress of the International Association on Hydrological Research, 21-25 August 1989, Ottawa, B 121-130, 1989.

Klaassen, G.J., Douben, K., van der Waal, M., *Novel approaches in river engineering.* Proceedings of RiverFlow 2002, Lovain la Neuve, Belgium 4-6 September 2002: 27-43, 2002.

Kuroki, M., Kishi, T., *Regime criteria on bars and braids.* Hydr. Paper, Hokkaido University, 1985.

Lanzoni, S., *Experiments on bar formation in a straight flume 2. Graded sediment.* Water Resources Research 36(11), 3351-3363, 2000.

Lanzoni, S., Tubino, M., *Grain sorting and bar instability.* Journal of Fluid Mechanics 393, 149-174, 1999.

Lanzoni, S., Tubino, M., *Experimental observations on bar development in cohesionless channels.* Excerpta 14, 119-152, 2000.

Larson, P., *Restoration of river corridors: German experiences.* In: Petts, G.E., Calow, P. (Eds.), River Restoration, Blackwell, 124-143, 1996.

Leopold, L.B., Wolman, G., *River channel patterns: braiding, meandering and straight.* Phisical and Hydraulic Studies of Rivers 14, 283-300, 1957.

Makaske, B., *Anastomosing rivers: forms, processes and sedimnets.* University of Utrecht, The Netherlands, Ph.D. thesis, 1998.

McArdell, B.W., Faeh, R., *A computational investigation of river braiding.* In: Mosley M.P. (eds) Gravel bed rivers V, New Zealand Hydrologic Society, Wellington, 2001.

Miori, S., Repetto, R., Tubino, M., *Configurazioni di equilibrio di biforcazioni in canali a fondo mobile e sponde erodibili.* Submitted to the XXIX Convegno di Idraulica e Costruzioni Idrauliche, Trento, September 2004, (in Italian).

Mosley, M.P., *Response of braided rivers to changing discharge.* Journal of Hydrology NZ 22 (1), 18-67, 1983.

Murray, B., Paola, C., *A cellular model of braided rivers.* Nature 371, 54-57, 1994.

Paola, C., *Modelling stream braiding over a range of scales.* In: Mosley M.P. (eds) Gravel bed rivers V, New Zealand Hydrologic Society, Wellington, 11-46, 2001.

Paola, C., Foufoula-Georgiou, E., *Statistical geometry and dynamics of braided rivers* . In: Mosley M.P. (eds) Gravel bed rivers V, New Zealand Hydrologic Society, Wellington, 47-69, 2001.

Parker, G., *On the cause and characteristic scales of meandering and braiding in rivers.* Journal of Fluid Mechanics 70, 457-480, 1976.

Parker, G., *Self-formed straight rivers wuth equilibrium banks and mobile bed. Part 2. The gravel river.* Journal of Fluid Mechanics 89, 127-146, 1978.

Parker, G., *Surface-based bedload transport relation for gravel rivers.* Journal of Hydraulic Research 28, 417-436, 1990.

Repetto, R., Tubino, M., *Transition from migrating alternate bars to steady central bars in channels with variable width.* International Symposium on River, Coastal and Estuarine Morphodynamics, Genova, Italy, September 6-10, 1999.

Repetto, R., Tubino, M., Paola, C., *Planimetric instability of channels with variable width.* Journal of Fluid Mechanics 457, 79-109, 2002.

Richardson, W.R., Thorne, C.R., *Multiple thread flow and channel bifurcation in a braided river: Brahmaputra-Jamuna River, Bangladesh.* Geomorphology 38, 185-196, 2001.

Sapozhnikov, V.B., Foufoula-Georgiou, E., *Self-affinity in braided rivers.* Water Resources Research 32(11), 1429-1439, 1996.

Schielen, R., Doelman, A., de Swart, H.E., *On the nonlinear dynamics of free bars in straight channels.* Journal of Fluid Mechanics 252, 325-356, 1993.

Seminara, G., *Invitation to river morphodynamics.* Pitman Research Notes in Mathematincs 335, A. Doelman and A. van Harten (eds), 269-294, Longman, 1995.

Seminara, G., Tubino, M., *Alterante bars and meandering: free, forced and mixed interactions.* In: River Meandering, Ikeda S. and Parker G. (eds), AGU Water Resources Monograph 12, 267-320, 1989.

Seminara, G., Tubino, M., *Weakly nonlinear theory of regular meanders.* Journal of Fluid Mechanics 244, 257-288, 1992.

Seminara, G., Zolezzi, G., Tubino, M., Zardi, D., *Downstream and upstream influence in river meandering. Part two: planimetric development.* Journal of Fluid Mechanics 438, 213-230, 2001.

Shimizu, Y., Tubino, M., Watanabe, Y., *Numerical calculation of bed deformation in a range of resonant wavenumber of meandering channel.* Proc. of Hydraulic Engineering JSCE 36, 15-22, 1992.

Slingerland, R., Smith, N.D., *Necessary conditions for a meandering-river avulsion.* Geology 26 (5), 435-438, 1998.

Stojic, M., Chandler, J., Ashmore, P., Luce, J., *The assessment of sediment transport rates by automated digital photogrammetry.* Photogrammetric Engineering and Remote Sensing 64 (5), 387-395, 1998.

Surian, N., Rinaldi, M., *Morphological response to river engineering and management in alluvial channels in Italy.* Geomorphology 50, 307-326, 2003.

Talmon, A., van Mierlo, M.C.L.M., Struiksma, N., *Laboratory measurements of direction of sediment transport on transverse alluvial bed slopes.* Journal of Hydraulic Research 33 (4), 519-534, 1995.

Thomas, R., Nicholas, A.P., *Simulation of braided river flow using a new cellular routing scheme.* Geomorphology 43, 179-195, 2002.

Tubino, M., Repetto, R., Zolezzi, G., *Free bars in rivers.* Journal of Hydraulic Research 37 (6), 759-775, 1999.

Tubino, M., Seminara, G., *Free-forced interactions in developing meanders and suppression of free bars.* Journal of Fluid Mechanics 214, 131-159, 1990.

van den Berg, J.H., *Prediction of alluvial channel pattern of perennial rivers.* Geomorphology 12, 259-279, 1995.

Wang, Z.B., Fokkink, R.J., De Vries, M., Langerak, A., *Stability of river bifurcations in 1D morphodynamics models.* Journal of Hydraulic Research 33 (6), 739-750, 1995.

Warburton, J., *Channel change in relation to meltwater flooding, Bas Glacier d'Arolla, Switzerland.* Geomorphology 11, 141-149, 1994.

Warburton, J., *Active braidplain width, bed load transport and channel morphology in a model braided river.* Journal of Hydrology NZ 35 (2), 259-286, 1996.

Warburton, J., Davies, T., *Variability of bedload transport and channel morphology in a braided river hydraulic model.* Earth Surface Processes and Landforms 19, 403-421, 1994.

Wilcock, P.R., *Critical shear stress of natural sediments.* Journal of Hydraulic Engineering 119, 491-505, 1993.

Wolman, M.G., *A method of sampling coarse river-bed material.* Trans. Am. Geophys. Union 35, 951-956, 1954.

Yalin, M.S., *Theory of Hydraulic Models.* MacMillan, London, 1971.

Young, W.J., Warburton, J., *Principles and practice of hydraulic modelling of braided gravel-bed rivers.* Journal of Hydrology NZ 35 (2), 157-174, 1996.

Zolezzi, G., Seminara, G., *Downstream and upstream influence in river meandering. Part one: general theory and application of overdeepening.* Journal of Fluid Mechanics 438, 183-211, 2001.

Zolezzi, G., Guala, M., Termini, D., Seminara, G., *Experimental observation of upstream overdeepening.* Accepted for publication in Journal of Fluid Mechanics, 2004.